



# Phylogenetic analysis, taxonomic revision, and dental ontogeny of the Cretaceous Zhelestidae (Mammalia: Eutheria)

J. DAVID ARCHIBALD<sup>1\*</sup> and ALEXANDER AVERIANOV<sup>2</sup>

<sup>1</sup>Department of Biology, San Diego State University, San Diego, CA 92182-4614, USA

<sup>2</sup>Zoological Institute, Russian Academy of Sciences, Universitetskaya nab. 1, 199034, Saint Petersburg, Russia

Received 25 October 2010; revised 11 May 2011; accepted for publication 5 July 2011

The eutherian, family-level clade Zhelestidae is consistently although weakly supported in five phylogenetic analyses that we performed on all Cretaceous eutherians. Additionally in the fifth analysis, which included some placentals, Zhelestidae is placed as a stem eutherian clade rather than grouping within the crown clade Placentalia as argued in some previous studies but not others. The subfamily Zhelestinae, Dzharakuduk (Turonian –?Coniacian ages), Kyzylkum Desert, Uzbekistan includes *Zhelestes temirkayzk*, *Aspanlestes aptap*, *Parazhelestes mynbulakensis* (= *Sorlestes budan*), *Parazhelestes robustus*, *Eoungulatum kudukensis*. Additional taxa for the time being recognized as Zhelestidae *incertae sedis* are: *Sheikhdzheilia rezvyii* (Cenomanian, Uzbekistan), ***Borisodon kara* gen. nov.** (= ‘*Sorlestes*’ *kara*) (Turonian, Kazakhstan), *Lainodon orueetxebarriai* (Campanian or Maastrichtian, Spain), *Labes quintanillensis* (Maastrichtian, Spain), *Labes garimondi* (Campanian, France), *Gallolestes pachymandibularis* (Campanian, Mexico), *Gallolestes agujaensis* (Campanian, USA), and *Avitotherium utahensis* (Campanian, USA). *Eozhelestes mangit* (Cenomanian, Uzbekistan) is a questionable zhelestid (?Zhelestidae), possibly stem to Zhelestidae. *Paranyctoides* (Asia and North America) is often linked to Zhelestidae. *Alostera*, previously referred to Zhelestidae, is a eutherian of unknown affinities. Associated skull fragments permitted the first reconstruction of a zhelestid (*Aspanlestes*) skull. Abundant dentulous and edentulous dentaries allowed examination of dental replacement from the canine posteriorly in Dzharakuduk zhelestids as follows: [dc, p1, dp2, p3, dp4, dp5] → m1 → p2 → c, p4, m2 → p5 → m3.

© 2012 The Linnean Society of London, *Zoological Journal of the Linnean Society*, 2012, 164, 361–426.  
doi: 10.1111/j.1096-3642.2011.00771.x

**ADDITIONAL KEYWORDS:** biogeography – dental replacement – Late Cretaceous – phylogeny – Placentalia – taxonomy – Uzbekistan.

## INTRODUCTION

In the first monographic treatment of Zhelestidae, Nesov, Archibald & Kielan-Jaworowska (1998) described what was then known of this relatively new taxon of Late Cretaceous eutherians, as well as providing the first phylogenetic analysis including zhelestid taxa. In earlier papers in which Nesov named and described zhelestids (Nesov, 1987, 1997; Nesov *et al.*, 1994), he noted the great dental resemblance between zhelestids and the early Cenozoic archaic ungulates

(condylarths). In 1996 and 1998, Archibald (also Archibald, Averianov & Ekdale, 2001) presented this relation more formally, placing zhelestids as sister to all later ungulates. This placed zhelestids within the crown group Placentalia. Using more fossil as well as recent placentals, Wible *et al.* (2007) argued that Zhelestidae was a more basal eutherian clade, and accordingly that zhelestids were not placentals and had no close relationship to ungulates. We accept this assessment as the currently best-supported placement of Zhelestidae. Further, recent work on ear regions (Ekdale, Archibald & Averianov, 2004) and postcrania (Szalay & Sargis, 2006; Chester *et al.*, 2010) that can confidently be assigned to Zhelestidae do not show any

\*Corresponding author. E-mail:  
darchibald@sunstroke.sdsu.edu

clearly placental attributes but rather possess features usual for other basal eutherians.

Between 1997 and 2006, eight URBAC expeditions, mostly to the Dzharakuduk sites in the Kyzylkum Desert, Uzbekistan, greatly increased the number and in some cases quality of specimens referable to Zhelestidae. Archibald & Averianov (2005) discussed faunal succession in the Kyzylkum Desert, Uzbekistan, as known as of 2005. Here we provide a detailed description of this new dental, maxillary, and dentary material and show how it has allowed us to synonymize taxa that previously had been referred to taxa known either by upper or lower dentitions, but not both. Additionally, although fragmentary, the remains of the skull of the smallest Dzharakuduk zhelestid, *Aspanlestes aptap*, are described. The extensive new dental material and edentulous dentaries have allowed the most comprehensive examination of the lower tooth eruption sequence for any Cretaceous eutherian. The phylogenetic analyses of eutherians presented here support the family-level clade Zhelestidae although weakly and suggest, as did Wible *et al.* (2007, 2009), that zhelestids are basal eutherians not belonging to the crown Placentalia. In fact, as was found by Wible *et al.* (2007, 2009), no Cretaceous eutherians were found to belong to Placentalia in our analyses. Intrafamilial relationships are not well established; thus for the time being, we recognize the following: four genera of zhelestine zhelestids from Dzharakuduk (*Zhelestes*, *Aspanlestes*, *Parazhelestes*, and *Eoungulatum*); additional taxa as Zhelestidae *incertae sedis* from Uzbekistan (*Sheikhdzheilia*), Kazakhstan (*Borisodon*, gen. nov.), Japan (*Sorlestes*), Spain (*Lainodon* and *Labes*), France (*Labes*), the USA (*Avitotherium*, *Gallolestes*), and Mexico (*Gallolestes*), and the genus *Eozhelestes* as ?Zhelestidae. *Alostera*, based primarily on worn isolated teeth, was referred to Zhelestidae by Nesov *et al.* (1998). We here regard it as a eutherian of unknown affinities. The taxon *Paranyctoides* known from both Asia and North America is often linked to Zhelestidae. It will be treated in another publication.

## MATERIAL AND METHODS

### DENTAL TERMINOLOGY, MEASUREMENTS, AND PHOTOGRAPHY

We use the dental terminology in Nesov *et al.* (1998: fig. 1). Measurements were taken according to the method illustrated by Archibald (1982: fig. 1). Dental abbreviations are: I, C, P, and M for upper permanent incisor, canine, premolar, and molar, respectively; i, c, p, and m for permanent lower incisor, canine, premolar, molar, respectively; d refers to deciduous teeth. When shown in sequence with arrows, relative position of teeth refers to sequence of eruption of the teeth. Premolars are identified as upper or lower 1, 2, 3, 4,

and 5, based on information that position 3 is lost in some early eutherians and placentals (Novacek, 1986; Sigogneau-Russell, Dashzeveg & Russell, 1992; Archibald, 1996; Nesov *et al.*, 1998; Cifelli, 2000). Premolars 4 and 5 correspond to numbers 3 and 4 in most other traditional descriptions. Teeth were projected on a computer screen using a video camera mounted on a binocular microscope and measured to the nearest 0.01 mm using NIH Image 1.61 software. Teeth were photographed with a Nikon CoolPix 4500 digital camera mounted on a Meiji binocular microscope. Specimens were placed on a 'tilt table' to produce stereopairs.

### INSTITUTIONAL ABBREVIATIONS

CCMGE, Chernyshev's Central Museum of Geological Exploration, Saint Petersburg, Russia; IZANUZ, Institute of Zoology, National Academy of Sciences of Uzbekistan, Tashkent, Uzbekistan; LACM, Natural History Museum of Los Angeles County, Los Angeles, USA; LIAT, Museo de Ciencias Naturales de Álava, Vitoria-Gasteiz, Spain; MNA, Museum of Northern Arizona, Flagstaff, USA; OMNH, Oklahoma Museum of Natural History, Norman, USA; UCMP, Museum of Paleontology, University of California, Berkeley, USA; URBAC, Uzbek/Russian/British/American/Canadian Joint Paleontological Expedition specimens currently in the National Museum of Natural History, Smithsonian Institution, Washington, DC, USA; ZIN, Zoological Institute, Russian Academy of Sciences, Saint Petersburg, Russia.

### SYSTEMATIC PALAEOLOGY

MAMMALIA LINNAEUS, 1758

THERIA PARKER & HASWELL, 1897

EUTHERIA GILL, 1872

ZHELESTIDAE NESOV, 1985A

Zhelestinae: Nesov, 1985a: 15.

Zhelestidae: Nesov, 1990: 59.

*Type genus: Zhelestes* Nesov, 1985a.

*Included taxa:* The subfamily, Zhelestinae Nesov, 1985a; six zhelestid genera *incertae sedis*, *Sheikhdzheilia* Averianov & Archibald, 2005, *Borisodon* gen. nov., *Lainodon* Gheerbrant & Astibia, 1994, *Labes* Sigé in Pol *et al.*, 1992, *Gallolestes* Lillegraven, 1976, and *Avitotherium* Cifelli, 1990; and questionably *Eozhelestes* Nesov, 1997.

*Revised diagnosis:* Differs from other Cretaceous eutherians by a unique combination of derived states: upper molar styler shelf width less than 25% of molar

length; ectoflexus shallow to absent (reversed in *Sheikhdzheilina*); conular region width more than 51% of the total molar width; paracone prominent and midway or closer to paracone; protocone similar in height to paracone and metacone; p5 with incipient basin lingual to talonid ridge; protoconid subequal in height to paraconid and or metaconid.

*Distribution*: Asia, Europe, North America, and Madagascar; Late Cretaceous (Cenomanian – Maastriichtian).

*Comments*: A possible distinct taxon of Zhelestidae is represented by edentulous dentary fragments in the Cenomanian Khodzshakul Formation of Uzbekistan ('Zhelestidae' indet., unnamed large sp. A in Averianov & Archibald, 2005). An isolated axis from this locality, the holotype of *Oxlestes grandis* Nesov, 1982, may be referable to this taxon (see Averianov & Archibald, 2005 for description and discussion).

'*Sorlestes*' *mifunensis* Setoguchi *et al.*, 1999 from the Upper Mifune Formation of Japan is referable to Zhelestidae. The age of this stratigraphical unit was originally identified as Cenomanian–Turonian (Setoguchi *et al.*, 1999) and later changed to the Coniacian–Campanian (Kusuhashi, Ikegami & Matsuka, 2008), but the cited radiometric data  $86.4 \pm 7.8$  Mya is at the Coniacian–Santonian boundary (Gradstein, Ogg & Smith, 2004). This taxon is represented by fragmentary dentaries and lower dentition. Its generic attribution is not clear. *Sorlestes* Nesov, 1985a is considered here a junior subjective synonym of *Zhelestes* Nesov, 1985a (see below).

#### ZHELESTINAE NESOV, 1985A

Zhelestinae: Nesov, 1985a: 15.

*Type genus*: *Zhelestes* Nesov, 1985a.

*Included taxa*: Type genus, *Aspanlestes* Nesov, 1985a, *Parazhelestes* Nesov, 1993, and *Eoungulatum* Nesov *et al.*, 1998.

*Revised diagnosis*: The monophyly of Zhelestinae is supported by the following unambiguous synapomorphies: M1 parastylar lobe anterior to paracone; M2 metastylar lobe more labial than parastylar lobe; mandibular symphysis extends to p3 or more posteriorly (reversed in *Parazhelestes*); Meckelian groove absent (unknown for *Aspanlestes*); p5 metaconid separate (unknown for *Eoungulatum*); p5 lingual cingulid is absent.

*Distribution*: Asia; Late Cretaceous (Turonian – ?Coniacian).

#### ASPANLESTES NESOV, 1985A

*Aspanlestes*: Nesov, 1985a: 14.

*Ortalestes*: Nesov, 1997: 170.

*Type species*: *Aspanlestes aptap* Nesov, 1985a.

*Included species*: Type species and *Aspanlestes* sp.

*Diagnosis*: As for the type species.

*Distribution*: Uzbekistan; Late Cretaceous (Turonian – ?Coniacian).

*Comments*: A lower molar fragment from the Campanian Darbasa Formation of southern Kazakhstan identified by Averianov (1997: fig. 5) as ?*Aspanlestes* sp. is best classified as Zhelestidae indet.

#### ASPANLESTES APTAP NESOV, 1985A

##### FIGURES 1–10

(See Appendix 4 for synonymies, referred illustrations, and referred specimens.)

*Holotype*: CCMGE 4/12176, right dentary fragment with p4–5, m1–2 and alveoli for p2–3.

*Type locality and horizon*: CDZH-17a, Dzharakuduk, Kyzylkum Desert, Uzbekistan. Bissekty Formation, Upper Cretaceous (middle–upper Turonian).

*Revised diagnosis*: Differs from *Zhelestes* by P3 double-rooted; mandibular condyle positioned at or slightly above alveolar level; p5 paraconid is trigonid cusp rather than part of cingulum. Differs from *Zhelestes* and *Eoungulatum* by upper and lower canine double-rooted. Differs from *Parazhelestes* and *Eoungulatum* by P1 single-rooted; protocone labial shift absent. Differs from *Eoungulatum* by P5 protocone smaller, lower than paracone; P5 metacone swelling small; upper molars metacone slightly smaller than paracone; 'coronoid' facet absent; masseteric fossa bordered ventrally by well-defined crest connected to condyle. Differs from *Parazhelestes* by trigonid angle between 36–49°.

*Description*: Skull. Fragments of a skull were recovered in 2003 from CBI-14. These consisted of most of the frontal, much of the presphenoid, much of the basisphenoid, the left pars cochlearis of the petrosal, the pars cochlearis and pars canicularis of the right petrosal, the right exoccipital, and the right maxillary fragment with M2 and alveoli for M1 and M3. Although no fragments were in direct contact with each other, they almost certainly belong to the same individual based on the similarity of preservation and

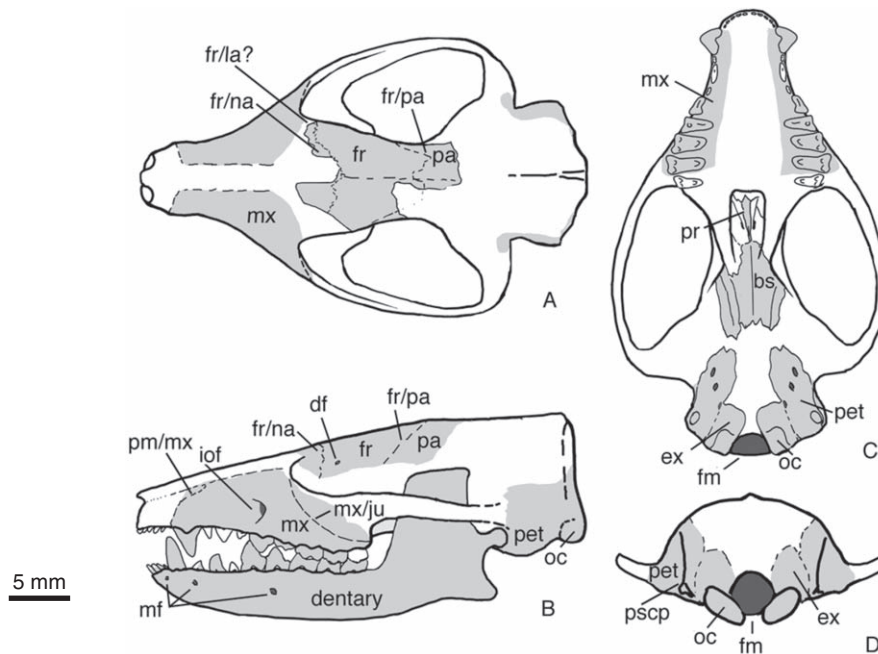


**Figure 1.** *Aspanlestes aptap*, reconstruction of the skull and dentary based on URBAC 03–93 and 02–45 as well as various dentary and dental remains referred to this species. A, dorsal; B, lateral; C, ventral; D, posterior views. Light grey areas represent known parts or mirror images of known parts. Scale bar = 5 mm. See Appendix 1 for abbreviations.

because they were the only mammalian cranial remains from a particular bag of screen washing concentrate. Additionally, the pars cochlearis and pars canicularis of the right petrosal and the right exoccipital fit well together, and the presphenoid and basisphenoid slightly less so. All cranial remains were given the same number, URBAC 03–93, except for the right maxillary fragment, which was given the number URBAC 03–188 because of a slight doubt that it was from the same individual. All fragments, including the maxilla, are of the correct, smaller size to be assignable to *Aspanlestes aptap*, the smallest of the Dzharakuduk zhelestids. Further, the two damaged petrosals accord well with the smallest petrosals described elsewhere for zhelestids (Ekdale *et al.*, 2004) and are probably referable to *Aspanlestes*.

Each of the bones is described below in more detail as well as being figured. Here, we describe and compare broadly our reconstruction of the skull relative to other Asian (Mongolia and Uzbekistan) Cretaceous eutherians (Fig. 1). For comparison we use the reconstructions of Wible, Novacek & Rougier (2004: fig. 51), Wible *et al.* (2009: fig. 35) of the zalambdalestids *Kulbeckia*, *Barunlestes*, and *Zalambdalestes*, as well as the asioryctitheres *Kennalestes*, *Asioryctes*, and *Daulestes*, and the cimolestan *Maelestes*. Identifications of anatomical features extensively used the following sources: Crouch, 1969; Wible 1990, 2003,

2008; Ekdale *et al.* 2004; Wible *et al.* 2004, 2009; Mead & Fordyce 2009.

Although much of the skull is unknown, what is preserved provides some limits on the proportions of the skull and dentary. In overall size, the skull was probably some 5 mm longer than skulls of both *Barunlestes* and *Kulbeckia*, but almost 10 mm shorter than *Zalambdalestes*. Recall that *Aspanlestes* is the smallest Dzharakuduk zhelestid, so the largest taxon, *Eoungulatium* would probably have exceeded the length of *Zalambdalestes*. Relative to the zalambdalestids and the asioryctitheres, *Aspanlestes*, and almost certainly other Dzharakuduk zhelestids, were built somewhat more robustly. The preorbital region was wider and shorter, and probably deeper compared to these other taxa. The snout was definitely less laterally constricted than in zalambdalestids and possibly also than in asioryctitheres. As the premaxillary region is unknown we do not know the anatomy of this region, but the dentary probably extended nearly as far anteriorly as the premaxilla. This slightly greater robustness continues in the dentary, notably in the depth, which is similar to that in *Barunlestes*. The ascending ramus of the dentary, and most especially of the dorsal part of the mandibular condyle, is quite large and rectangular in outline. This most resembles *Asioryctes* although the flat, dorsal margin of the ascending ramus is probably longer in *Aspanlestes*.

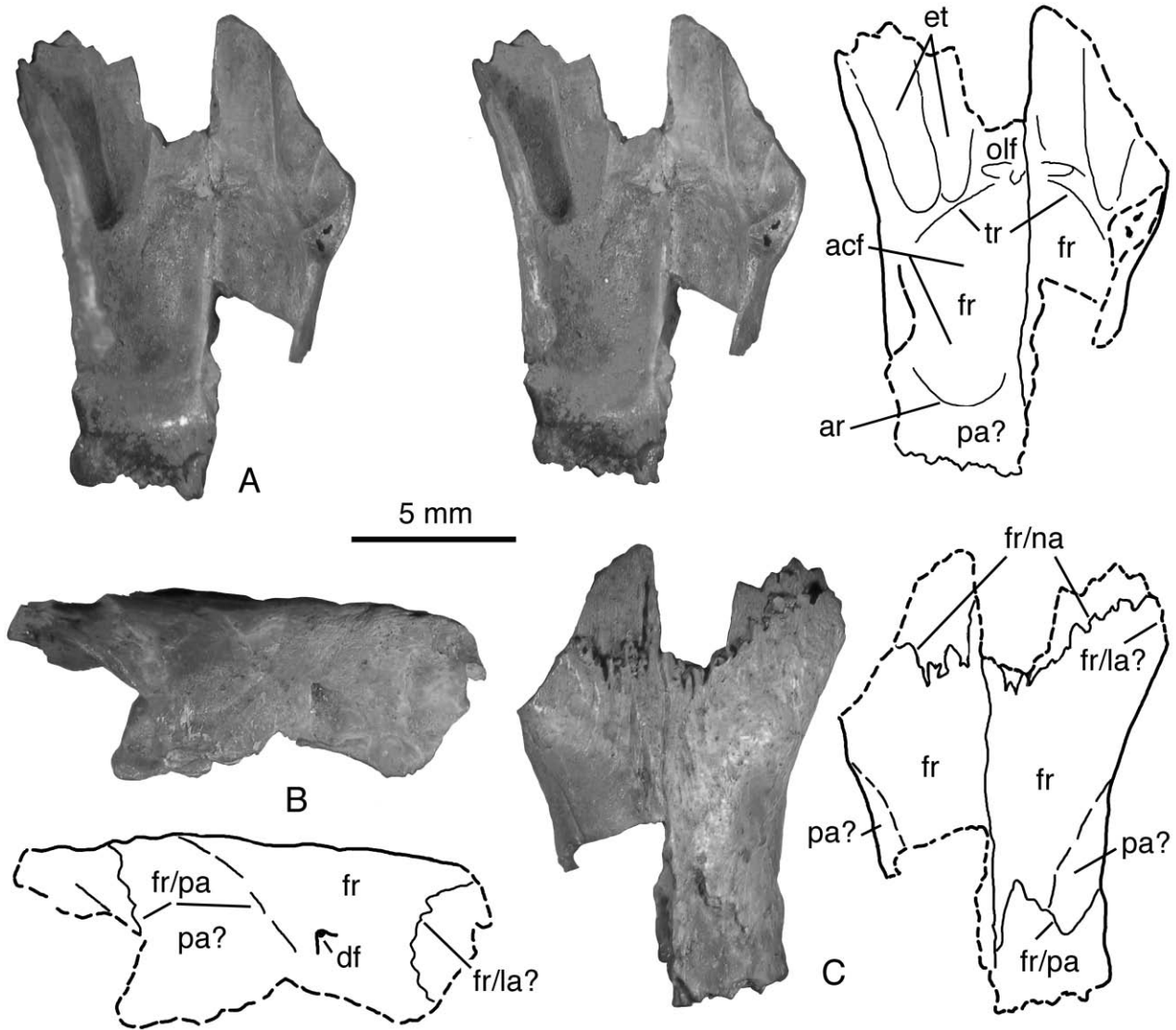


**Figure 2.** *Aspanlestes aptap*, URBAC 03–93, frontals and possibly parts of parietals. A, ventral stereophotograph (intracranial) and line drawing. Photographs and line drawings, B, lateral; C, dorsal views. See Appendix 1 for abbreviations.

Frontal and parietal(?). Much of both frontals are preserved (Fig. 2). There is considerable constriction laterally through the frontals, slightly more so than in the placental *Erinaceus* but less than in the marsupial *Didelphis*. On the dorsal surface at the anterior and posterior margins of the preserved portions of the frontals, denticulated sutures are present for the nasals (fr/na) and parietals (fr/pa), respectively. The nasals and parietals clearly formed lappets of bone overlying the frontals dorsally. The nasals were expanded at least posteriorly at their contact with the frontals. The better-preserved right frontal has a facet at its anterolateral margin that was probably for the lacrimal (fr/la?), which in turn probably contacted

the right nasal. What are probably small lappets of the parietals can be seen near the posterolateral margins of both frontals (pa?). This would place the narrowest part of the cranial vault near the frontal/parietal suture as in many smaller-brained mammals. In lateral view there is a small foramen that has no endocranial aperture. This is most likely to be the frontal diploic vein foramen (df). Intracranially (ventral), elongate semicircular depressions and ridges are present at the anterior end of the frontals and housed ethmoturbinals (et). Medially is the olfactory fossa (olf). Posteriorly a transverse ridge (tr) separates the olfactory fossa from the anterior cranial fossa (acf). This fossa is delimited posteriorly

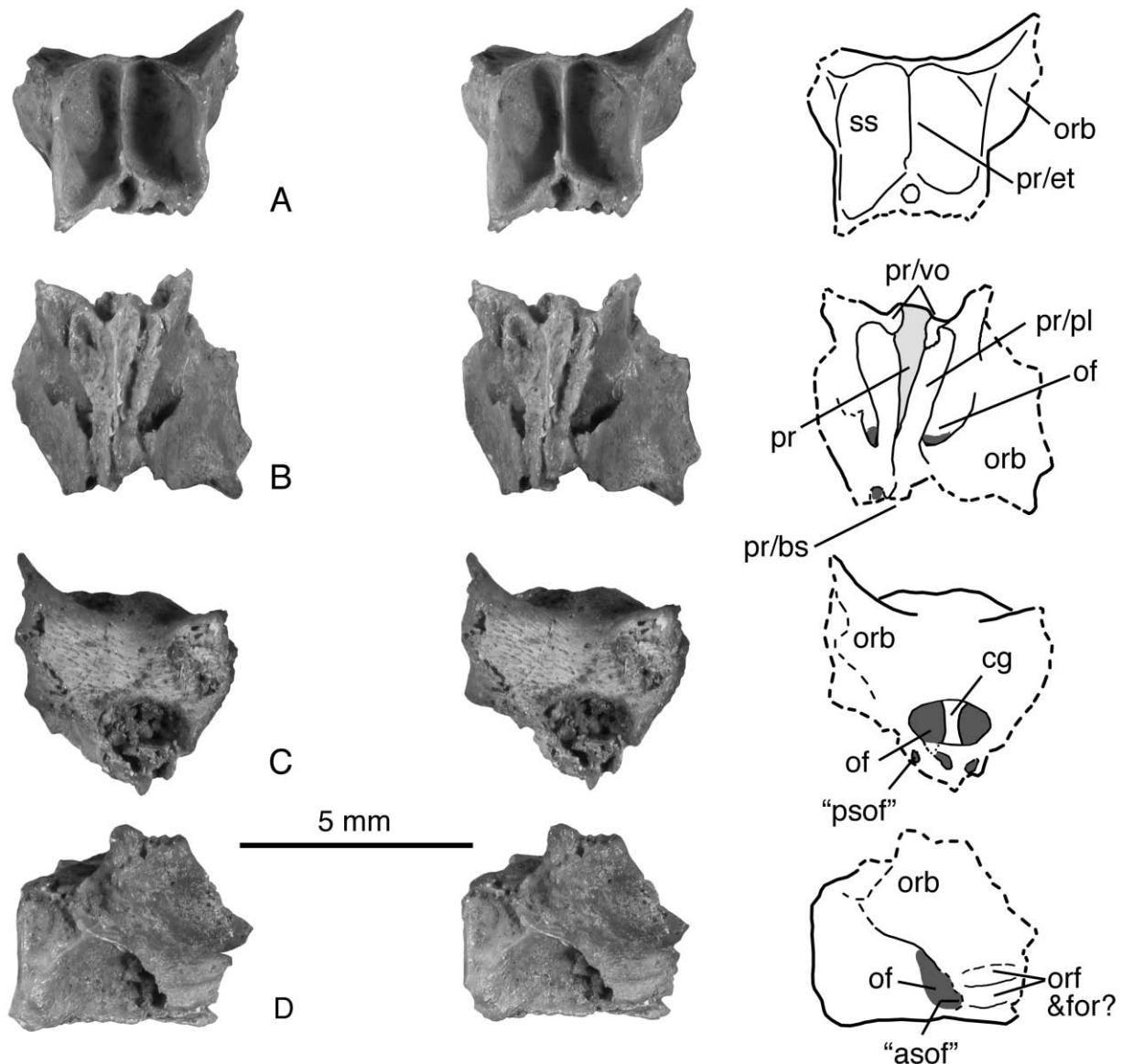


**Figure 3.** *Aspanlestes aptap*, URBAC 03–93, stereophotographs and line drawings of presphenoid. A, anterior; B, ventral; C, posterior (intracranial) views; D, left lateral. Light grey area is portion exposed ventrally in articulated skull. See Appendix 1 for abbreviations.

by a broad, low annular ridge (ar) between the anterior and middle cranial fossae. The parietals certainly overlaid this region dorsally as lappets of bone covering the frontals, but it cannot be determined if the parietals are also exposed internally on the preserved portion of the bone.

**Presphenoid.** Most of the body of the presphenoid (pr) and part of the orbitosphenoid wings (orb) are preserved (Fig. 3). Ventrally, articulation surfaces are recognizable for the basisphenoid (pr/bs), the palatines (pr/pl), and the vomer (pr/vo). In the articulated skull, the only part of the presphenoid that would have been exposed ventrally would have been a

long, narrow dagger-shaped surface (light grey in Fig. 3B). The lateral sides of the orbitosphenoid wings would have been exposed in the orbital region. The floor of each large optic foramen (of) is traversed by a small canal, the function of which is not known. The anterior aperture is labelled the ‘anterior small optic foramen’ (‘asof’) and the ‘posterior small optic foramen’ (‘psof’) (Fig. 3C, D). Two similarly sized canals (‘smf’) on the anteromedial margin of the preserved part of the basisphenoid (Fig. 4A) may have been a continuation of these small canals. A small area of bone-to-bone contact may be preserved between the presphenoid and basisphenoid (pr/bs).

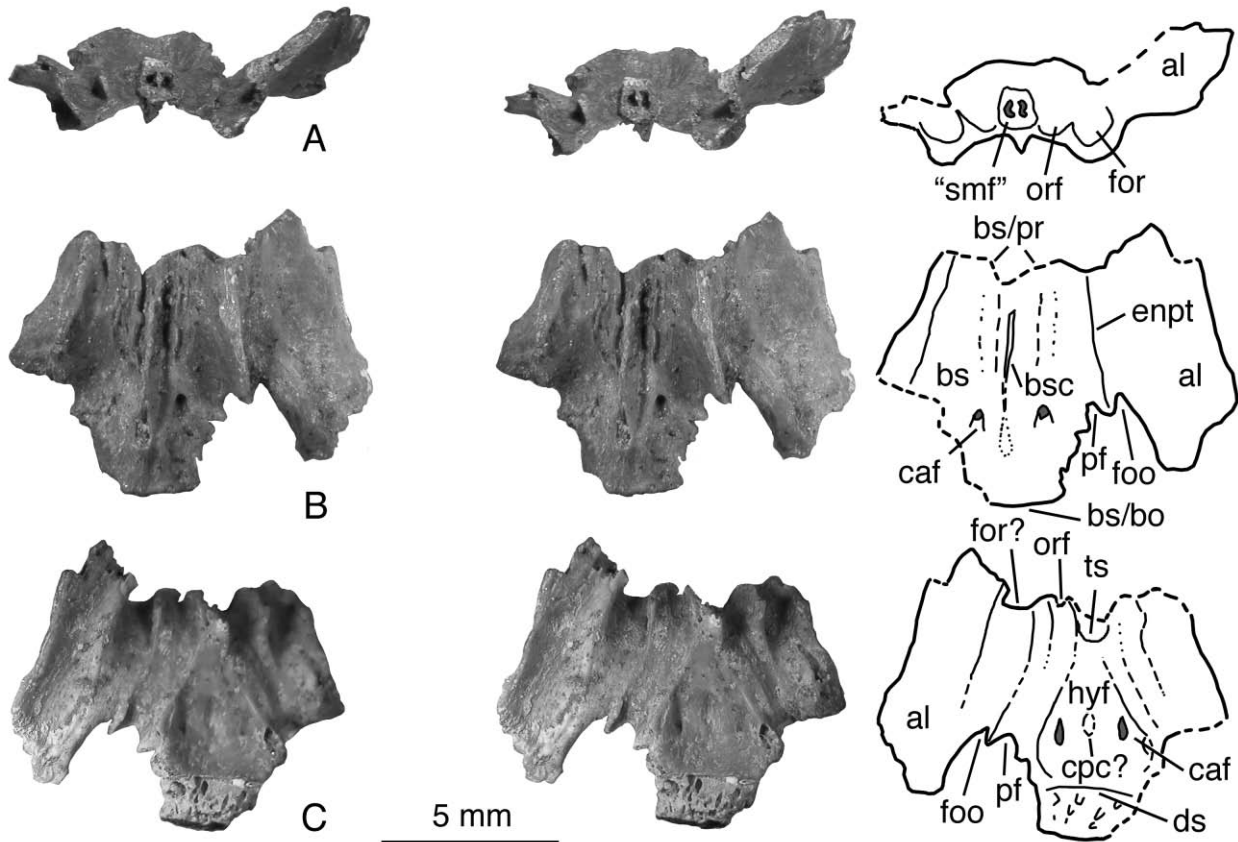


**Figure 4.** *Aspanlestes aptap*, URBAC 03–93, stereophotographs and line drawings of basisphenoid. A, anterior; B, ventral; C, dorsal (intracranial) views. See Appendix 1 for abbreviations.

There is not enough of the contact present to determine if the presphenoid and basisphenoid were fused or separate bones. Medially there is a small depression or foramen between the two posterior small optic foramina. Dorsal to these openings is a much larger oval opening, the chiasmatic groove (cg), into which the two optic foramina (of) empty intracranially. Anteriorly, the presphenoid is well preserved with a pair of deep sphenoidal sinuses (ss) and a median, vertical ridge for the ethmoid lamina (pr/et). On the better-preserved left side, posterolateral to the optic foramen, there are two shallow depressions that formed the medial wall of the orbital fissure (orf) and possibly the medial wall of the foramen rotundum or an alisphenoid canal (for?).

**Basisphenoid.** Much of the body of the basisphenoid (bs) and part of the left alisphenoid wing (al) are preserved (Fig. 4). Viewed anteriorly, and moving medially to laterally on each side, there are small foramina ('smf'), and ventrolateral margins of the orbital fissure (orf), and questionably the foramen rotundum (for?) or alisphenoid canal. The small foramina may have been confluent with the posterior small optic foramen on the posterior margin of the

presphenoid. Their function is unknown. In ventral view there is a prominent midline basisphenoid crest (bsc) flanked by two crests. The bone is distinctly crenulated on either side of this medial crest. This appears to be natural rather than caused by weathering. No remnants of the pterygoid bones are discernible. The two lateral crests are possibly the broken bases of the entopterygoid processes (enpt). On the better-preserved left side, at the posterior margin where the alisphenoid and basisphenoid meet there is a finished edge with two curved surfaces that are tentatively identified as the anterior margins of the piriform fenestra (pf) and foramen ovale (foo). A carotid foramen (caf) is found on either side near the posterior extent of the basisphenoid crest. The right foramen is occluded with sediment but the left foramen opens dorsally (intracranially) into the lateral margin of the hypophyseal fossa of the sella turcica, where it continues for a short distance anteriorly as a shallow groove to the margin of the sella turcica. Anteriorly the sella turcica is bounded by the remains of a rounded, laterally narrow tuberculum sellae (ts), and posteriorly by the remains of a laterally broader dorsum sellae (ds). The intervening

teardrop-shaped hypophyseal fossa is shallow but distinct. In its centre is a small fossa that may have housed a craniopharyngeal canal (cpc?).

Petrosal and exoccipital. Both petrosals are preserved but the ventral surfaces of both promontoria are damaged, more so the left side. The right side is more complete in preserving both the pars cochlearis (pco) and pars canicularis (pca). The right exoccipital (ex) is also preserved and can be articulated with the right petrosal (pet) (Fig. 5). It is this side that is referred to in the following description. Zhelestid petrosals have been described in detail elsewhere (Ekdale *et al.*, 2004) and some comparisons are made here.

The dominant aspect of the ventral part of the pars cochlearis is the ovoid-shaped and slightly bulbous promontorium (prm) that houses the cochlea of the inner ear. Although the fenestrae cochleae (fc) and vestibuli (fv) are somewhat damaged (light grey region in Fig. 5A), their original outlines can be reconstructed. The fenestra vestibuli, which receives the footplate of the stapes, had a length to width ratio of about 2 or 2.5 to 1. A similarly high ratio is common in many extant eutherians. Anterolaterally of the promontorium is the ridge-like remnant of the tegmen tympani (tt). Between the tegmen tympani and the promontorium is the tympanic aperture of the facial canal (ta). This communicates with the fenestra semilunaris (fse) on the anteromedial margin of the intracranial surface of the pars cochlearis. Running anteromedially from the facial canal is the groove of a partially covered hiatus Fallopii (hfa). Ekdale *et al.* (2004) noted a distinct, broad sulcus for the inferior ramus of the stapedia artery running anteriorly just lateral to the promontorium, but that there was no indication of a transpromontorial sulcus for the internal carotid artery in any of the zhelestid petrosals. The *Aspanlestes* petrosal described here similarly has no indication of the latter sulcus, and although there is no clear indication of the former sulcus, the shallow groove roofing the hiatus Fallopii could have held an inferior ramus of the stapedia artery. On the medial side of the promontorium is a shallow, broad depression interpreted as the sulcus for the internal carotid artery (sica). Although the petrosal and basisphenoid are not in direct contact, the identification of this sulcus is likely because just anteromedial to the sulcus there is a carotid foramen near the posterior margin of the basisphenoid described in the previous section. Posterolateral to the promontorium is a distinct, deep fossa here identified as the fossa for the stapedia muscle (fs). Ekdale *et al.* (2004) figured and discussed this fossa in *Kulbeckia*, which they termed the fossa musculus minor, but did not indicate its presence in zhelestids. They figured a zhelestid petrosal in their figure 2 (URBAC 99–41) that is at least

a third larger than the petrosal here described. Although not visible in their figure because of a bony overhang of the pars canicularis, we observed the fossa for the stapedia muscle in URBAC 99–41, although it is smaller and occurs in a more trough-shaped depression rather than as distinct, deep fossa as in *Aspanlestes*. Using the terminology of Wible *et al.* (2004), the mastoid contribution to the paroccipital process (ppr) is preserved on the posterolateral margin of the pars canicularis. The jugular foramen is found on the ventral surface near the anterior end of the petrosal/exoccipital suture. Just anterior to this a portion of the sulcus for the inferior petrosal sinus (ips) can be discerned in ventral view. On the ventral, anterolateral margin of the exoccipital is an elongate fossa that bears a hypoglossal foramen (hf) at either end. The right occipital condyle (oc) is shaped like a squat half-barrel and is visible in all views except the lateral (squamosal) view.

In posterior view, the preserved portion of the skull is quite flat with only a slight medial to lateral concavity. It is dominated by the occipital condyle and what Wible *et al.* (2004) termed the posterior semicircular canal prominence (pscp) on the pars canicularis (pca). The posterior surface of the pars canicularis was completely exposed as the mastoid exposure of the petrosal. Dorsal to the paraoccipital process (ppr) is the medial margin of the post-temporal foramen (ptf). There is not enough of the exoccipital preserved to determine whether or not it was united with the supraoccipital and basioccipital to form an occipital bone. The right margin of the foramen magnum (fm) is preserved.

The anterodorsal (intracranial) surface of the petrosal is dominated by the more posterodorsal subarcuate fossa (sf) and the more anteroventral internal auditory meatus (iam). The sulcus for the sigmoid sinus (sss) is identified dorsomedially of the subarcuate fossa. A sulcus running the vertical length of the intracranial petrosal/exoccipital suture ending ventrally at the jugular foramen is questionably identified (indicated by the dashed line in Fig. 5C) as part of the sulcus for the sigmoid sinus. Part of the quite large prootic canal (pc) is preserved dorsolaterally of the subarcuate fossa. Anteroventral to this is the opening into the cavum supracochleare referred to as the fenestra semilunaris (fse; Wible *et al.*, 2001), which communicates with the tympanic aperture of the facial canal (ta) on the ventrolateral surface of the petrosal. In intracranial view, one hypoglossal foramen (hf) is visible in the exoccipital.

Laterally, the rugous surface of the pars canicularis (pca) bears two shallow sulci. The post-temporal canal (ptc) horizontally traverses the length of the pars canicularis from the posteriorly placed post-temporal foramen (ptf) to the margin of the pars

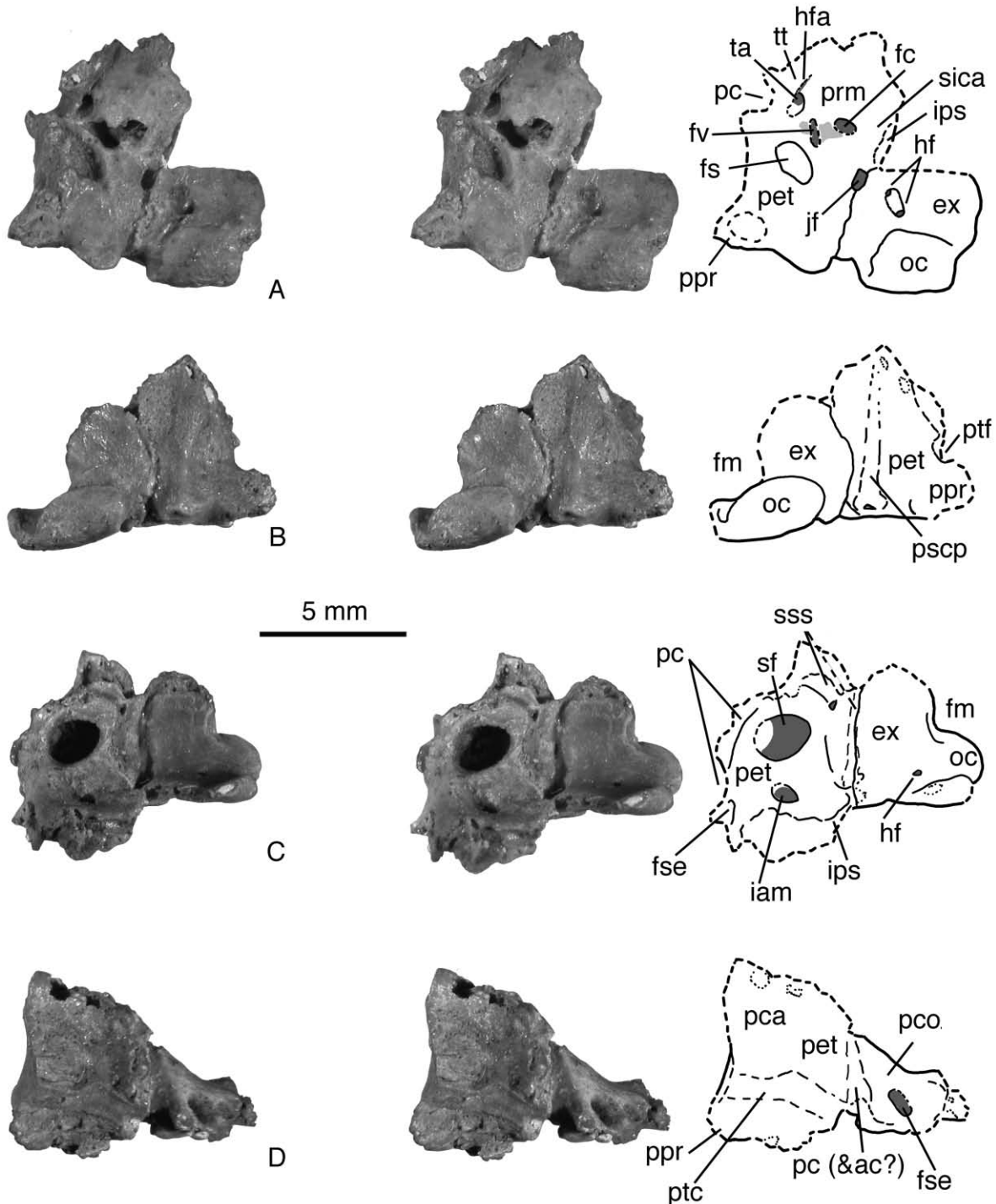


**Figure 5.** *Aspanlestes aptap*, URBAC 03–93, stereophotographs and line drawings of right petrosal and exoccipital. A, ventral; B, posterior; C, anterodorsal (intracranial); D, lateral views. Light grey area in A is damaged section. See Appendix 1 for abbreviations.

canicularis anteriorly. The absent squamosal formed the lateral wall of this sulcus as well as covering all of the lateral side of the pars canicularis except for probably near the posteroventral

margin of the paraoccipital process. Immediately anterior to the post-temporal canal is the vertically orientated continuation of the medial wall of the prootic canal. There are some unresolved differences

in structure and interpretation between the zhelestid petrosals (notably URBAC 99–41) described by Ekdale *et al.* (2004) and the petrosal of *Aspanlestes* described here. On URBAC 99–41 the prootic canal is complete whereas in the *Aspanlestes* petrosal it is not (compare fig. 2a in Ekdale *et al.*, 2004 with Fig. 5C). Ekdale *et al.* (2004) labelled a second sulcus in this region as the ascending canal of the superior ramus of the stapedia artery. No separate sulcus can be identified for this vessel in the *Aspanlestes* petrosal, possibly because of the damage noted above. Thus the sulcus identified on the lateral (squamosal) side as the prootic canal (pc) may have in part housed the ascending ramus (ac?).

**Maxilla.** The best-preserved maxillary fragment is URBAC 02–45 (Fig. 6), with completely preserved facial and zygomatic processes, but an incomplete palatal process. The facial process is a thin, vertical plate with a convex dorsal border. It is highest above the alveoli for P2. On the lateral side at the anterior end of the facial process, above the mesial root for the upper canine, there is a short strap-like facet for the premaxilla (pmf) or possibly part of the bone is preserved. On the medial side along the anterodorsal border of the facial process there is another premaxillary facet. Approximately halfway between this facet and the palatal process there are two very faint horizontal ridges, a longer dorsal ridge and a shorter ventral ridge. These are the attachment areas for the maxilloturbinals (mtc). On the lateral surface the large oval infraorbital foramen (iof) is positioned close to the alveolar margin dorsal to the roots of P4. The zygomatic process of the maxilla extends from dorsal of P5 posteriorly to the alveolar margin of M2. Much of the maxillary process of the jugal is preserved (mpj). The maxilla–jugal contact is high above P5 but sharply descends to the alveolar margin above M2. The dorsal surface of the palatal process of maxilla is subdivided into three portions separated by two oblique ridges: the longer and smooth anterior portion is the ventral floor of the nasal cavity, the shortest middle portion of rhomboid shape possibly housed part of the maxilloturbinals, and the posterior portion sculptured by numerous pits forms the ventral floor of the orbit. The orbital floor is an anteriorly pointed triangular area bordered laterally by the zygomatic process and medially by an oblique ridge making the contact line with the palatine. The palatine facet (paf) extends anteriorly into a wedge-like pocket posterior to the maxilloturbinal area. In the anterior corner of the orbital floor there is the posterior opening of the infraorbital canal.

**Jugal.** As noted there is a maxillary process of the jugal laterally overlapping the zygomatic process of the maxilla in URBAC 02–45 (Fig. 6A). It extends anteriorly to dorsal of the roots of P5. On the anterodorsal margin of the jugal–maxillary contact there is

a wedge-shaped facet for the facial process of the lacrimal (not visible in Fig. 6). The facet extends posteriorly to above the contact of M1 and M2.

**Upper dentition.** The upper canine is represented by an isolated specimen (ZIN 88983) and an in situ although worn specimen (URBAC 02–45; Fig. 6). It is a large double-rooted tooth slightly larger in length than P4. The crown is low and conical, subdivided by a vertical groove on both lingual and labial sides. The mesial and distal crown halves continue dorsally forming robust and widely separated roots.

Anterior upper premolars are not known for *Aspanlestes*. In URBAC 02–45 (Fig. 6) there are five alveoli between the upper canine and P4 that are interpreted as alveoli for a single-rooted P1 and for double-rooted P2 and P3. The alveoli for P1 and P2 are approximately of the same size, whereas the alveoli for P3 are half this size. There are no diastemata between these teeth, but there is a small diastema between P3 and P4. The latter diastema is lacking in a presumably younger specimen (URBAC 00–15).

There are two specimens of P4, one of which is preserved worn but in situ (Fig. 6). The tooth is double-rooted with a crown somewhat longer than that of P5. The crown is conical with a large main cusp and a short distal heel. On URBAC 04–100 there is also a small mesial accessory cusp. The distal half of the crown is expanded lingually forming a protocone bulge. On URBAC 04–100 there is a lingual cingulum along the protocone bulge, as well as the distal cingulum, with a minute cuspule labial to the distal accessory cusp. The distal root of P4 is twice wider labiolingually than the mesial root (URBAC 04–100 and the edentulous maxilla URBAC 00–15). In URBAC 04–100 the distal root is subdivided on the distal side by a vertical groove.

The P5 is known from several specimens, including two specimens in maxillary fragments with the molars (Figs 6, 7). The P5 is a submolariform tooth with a paracone, an incipient metacone, and a large protocone reaching lingually as far as the lingual margin of M1–2. The labial side is gently concave without a styler shelf but with a narrow ectocingulum. About half of the crown is occupied by a large paracone. Anteriorly is a large parastylar lobe with a prominent parastyle. The parastyle and paracone are widely separated. The mesial side of the paracone is conical whereas the distal side is connected by a salient crest to the metastyle. On this crest there is a variably developed incipient metacone. It can be cusp-like, separated by a notch from the paracone (URBAC 04–274), a swelling on the crest (most specimens), or nearly lacking (CCMGE 19/12953). The protocone is large but distinctly lower than the paracone. The shallow trigon basin is facing distoventrally and is bordered by an almost perpendicular preprotocrista

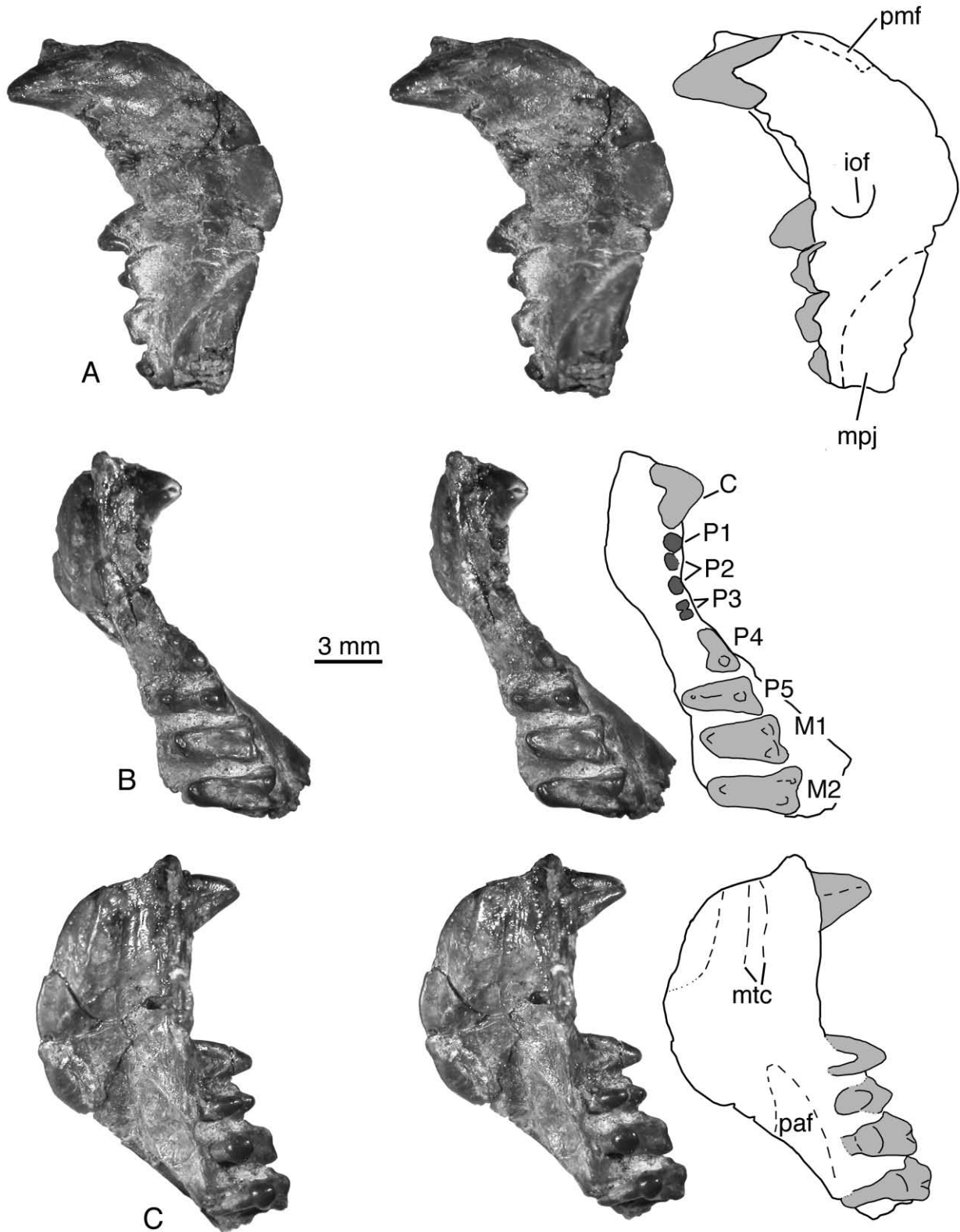


**Figure 6.** *Aspanlestes aptap*, URBAC 02–45, stereophotographs and line drawings of left maxillary fragment with heavily worn canine, P4–5, M1–2 (in grey in drawing) and alveoli for P1–3 (in black in drawing). A, labial; B, occlusal; C, lingual views. See Appendix 1 for abbreviations.

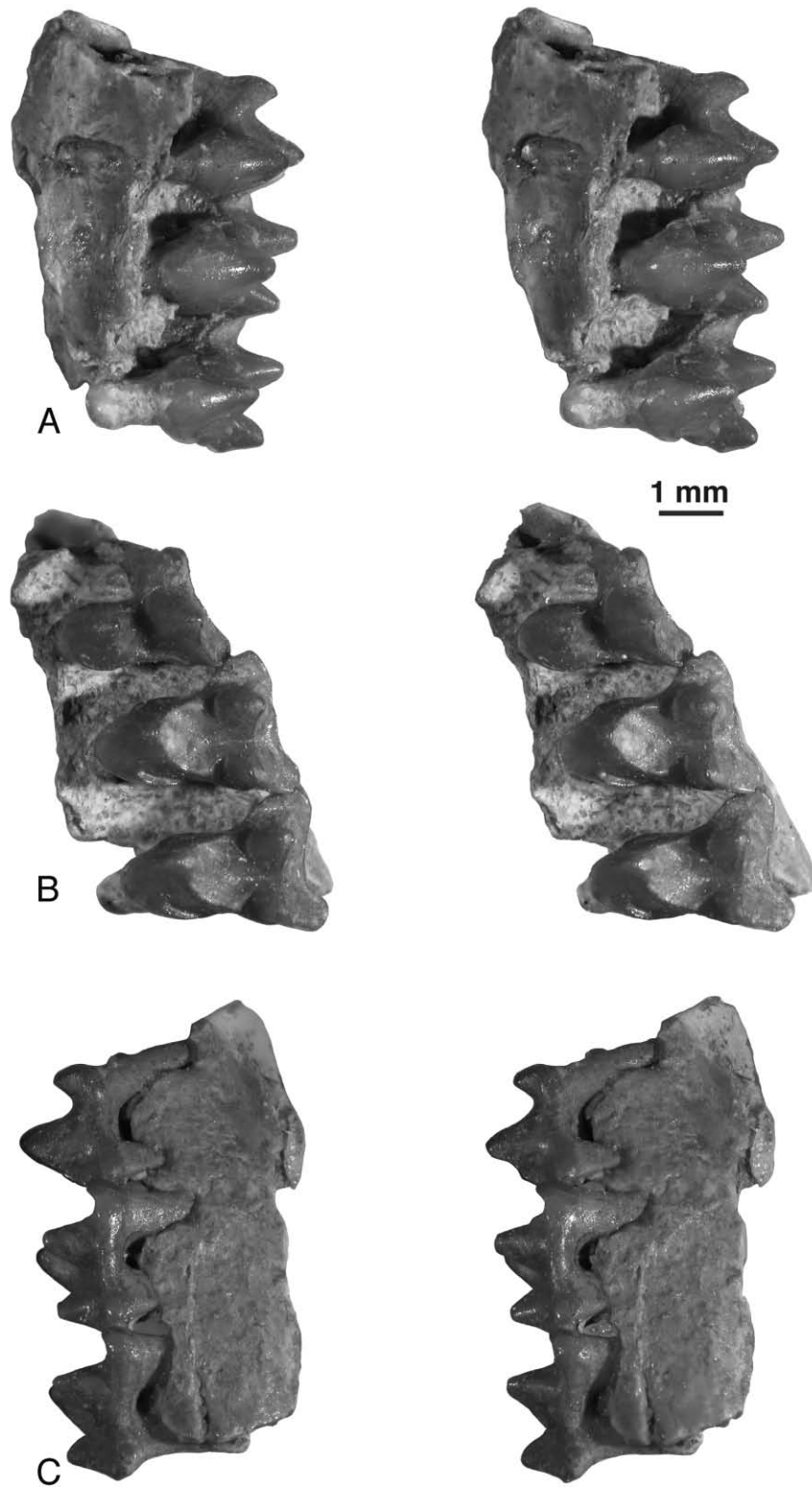


**Figure 7.** *Aspanlestes aptap*, CCMGE 1/12455, stereophotographs of left maxillary fragment with P5, M1–2. A, lingual; B, occlusal; C, labial views.

and a slightly distally convex postprotocrista. In unworn specimens, such as CCMGE 1/12455 (Fig. 7), there is a short postparaconule and a longer preparaconule crista defining the paraconule. It is not elevated above the level of the preprotocrista. In one specimen there is a distinct ridge between the paracone and protocone and there is no paraconule (Nesov, 1997: pl. 52, fig. 5). The preparaconule crista extends mesially towards the base of the parastyle and the postprotocrista extends distally towards the base of the metastyle. There are very faint precingulum and postcingulum at the base of the protocone. The length of these cingula varies between specimens. The P5 is three-rooted, with the smaller labial roots nearly equal in size and the lingual root much larger.

The DP5 is known from a single worn specimen (Nesov, 1987: pl. 1, fig. 4; Nesov, Sigogneau-Russell & Russell, 1994: pl. 7, fig. 6; Nesov, 1997: pl. 48, fig. 8). The crown is triangular, with a well-developed parastylar lobe. The labial side of the crown is almost straight, with a very shallow ectoflexus. The stylar shelf is absent labial to the paracone and is very narrow labial to the metacone. On the ectocingulum there are two cusp-like crenulations labial to the paracone. The paracone is a tall, conical cusp directed somewhat mesially. The metacone (now missing) is slightly smaller and lower than the paracone. The centrocrista is a sharp, straight crest. The protocone is large but distinctly lower than the paracone. Its apex is closer to the mesial side of the crown. The conules have well-developed wings and are placed near the bases of the labial cusps; the paraconule is somewhat closer to the protocone than is the metaconule. The preparaconule and postmetaconule cristae are short and do not extend labially beyond the bases of the paracone and metacone, respectively. There are very faint, short pre- and postcingula; the latter is slightly longer. On the parastylar lobe there are a parastyle and smaller preparastyle; the latter is obscured by the wear.

The upper molars M1–2 are known from several dentulous maxillae and isolated specimens. These teeth are quite similar in structure, differing mostly in proportions (Figs 6–8). The proportions of M1 are similar to DP5: the labial margin of the crown is nearly straight with only a slight ectoflexus. This is because the parastylar lobe is projecting mostly mesially to the paracone and the metastylar lobe is distolabial to the metacone. In M2 the ectoflexus is deeper because the parastylar lobe is projecting mesiolabially to the paracone and the metastylar lobe is mostly labial to the metacone. Also in M1 the trigon is slightly more expanded mesiodistally compared to M2. In both molars there is a distinct ectocingulum and narrow stylar shelf. Usually there are no cusps on the ectocingulum, but some M1s show inflation of the ectocingu-

lum in the position of the stylar cusp E and in one M2 (URBAC 04–252; Fig. 8C) this cusp is well developed. In one M2 (URBAC 99–30; Fig. 8D, E) there are crenulations on the ectocingulum in positions of the stylar cusps B (stylocone), C, and E. In M1 and M2 the stylar shelf, a flat area between the ectocingulum and the bases of the labial cusps, is widest between the paracone and metacone, narrower labial to the metacone, and very narrow or almost absent labial to the paracone. The metacone is distinctly smaller than the paracone (it is relatively smaller in M2 compared with M1). The centrocrista is straight. In less worn M1s the preparacrista is directed labially towards the parastyle (URBAC 03–10, 04–126, 04–392; Fig. 8A). In worn specimens the preparacrista is gone. The preparastylar groove excavates the mesial side of the paracone and its margin could be mistaken for the preparacrista, which contacts the area of stylocone. In less worn M2s the preparacrista extends mesially towards an area between the parastyle and preparastyle (URBAC 04–252, 06–67, 06–117; Fig. 8C). The stylocone is not a distinct cusp in most M1s and M2s, except for one M1 (URBAC 04–165; Fig. 8B). On M1 and M2 the postmetacrista extends from the apex of the metacone toward the metastyle, which is usually not a distinct cusp. The trigon forms two-thirds of the crown width in M1 and M2. The protocone is large and is as tall as the metacone but lower than the paracone. Its apex is situated mesial of the centrocrista notch, in some cases almost opposite the paracone. The conules are well developed and winged, located about twice as close to the labial cusps compared to the protocone (the paraconule is a slightly closer to the protocone than is the metaconule). These conules project well above the pre- and postprotocristae. The internal conular cristae are well separated and extend labially towards the bases of their respective labial cusps. These cristae and the centrocrista border the deepest part of the trigon basin. The preparaconule crista extends labially towards the preparastyle. The paracingulum quickly becomes obliterated by wear forming part of the expanded preparastylar groove. The postmetaconule crista extends labially dorsal to the metacone apex but does not reach the metastyle. The precingulum and postcingulum are narrow but well developed (more prominent on M1 than M2). They extend labially towards the area dorsal to the conules. On the parastylar lobe there are labial parastyle and lingual, smaller preparastyle; these cusps are easily obliterated by wear and not recognizable on worn specimens.

The M3 is not known for *Aspanlestes*. Judging from its alveoli, best preserved in CCMGE 68/12455 [Nesov, 1993: fig. 2(3), 1997: pl. 52, fig. 4] its lingual margin was aligned with other molars suggesting that it was not reduced in width relative to M1 and M2.

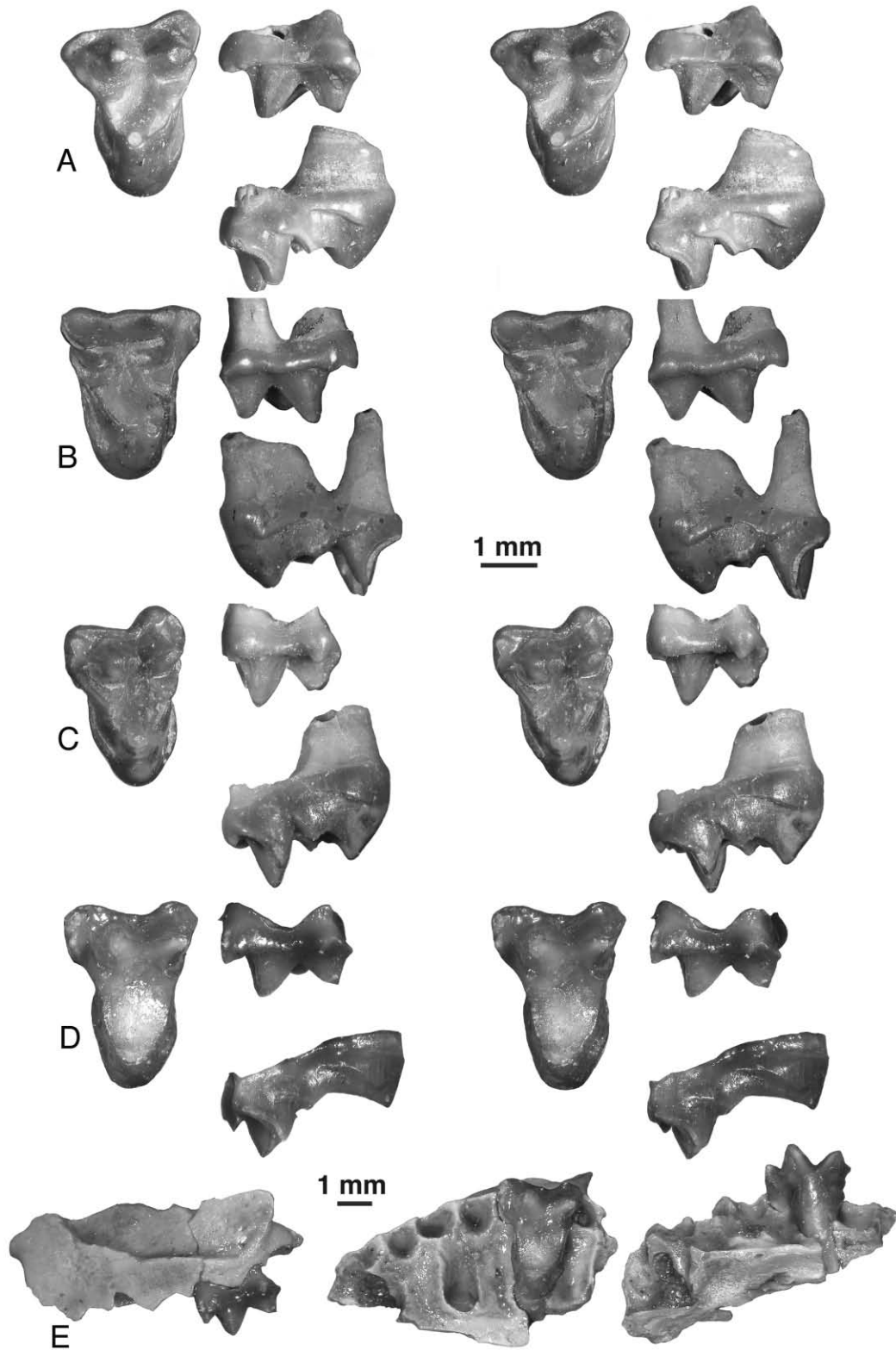


**Figure 8.** *Aspanlestes aptap*, stereophotographs of isolated upper molars and photographs of a maxillary fragment. A, URBAC 04–126, left M1; B, URBAC 04–165, right M1; C, URBAC 04–252, left M2; D, URBAC 99–30, left M2 in maxillary fragment. Views for A to D are occlusal, labial, and distal. E, URBAC 99–30, maxillary fragment with M2, labial, occlusal, and lingual views.

Dentary. The dentary is known from several fragments, but the anterior portion is preserved only in URBAC 04–395 (Fig. 9A). Here the dentary is quite shallow, suggesting a juvenile or subadult. The mandibular symphysis occupies the ventral half of the entire length of the preserved fragment. A prominent horizontal ridge borders the symphysis dorsally. The alveolar border parallels this ridge in the region of canine and premolars. On the labial side there are two anterior mental foramina: a small one below i3 and another, much larger, below the mesial root of p1. The ventral border of the dentary is convex except the concavity immediately posterior to the i3.

The posterior mental foramen is between p4 and p5 (URBAC 02–66), under mesial root of p5 (ZIN 88475), or under the distal root of p5 (holotype, CCMGE 4/12176, Fig. 9D). The posterior end of the mandibular symphysis extends to the level of p4 in an old individual (ZIN 88488) in which p3 was probably lost and the alveoli filled by bone.

The ascending dentary ramus is best preserved in URBAC 02–77 (Fig. 9E). The posterior edge is complete whereas the anterior edge is not. The horizontal ramus continues in a gentle arc on to the ascending ramus. The ascending ramus is about 2.5 times higher than the horizontal ramus, with a steep, distinct anterior border of the coronoid process, sloping at an angle of about 40° relative to the alveolar margin. The coronoid process is almost complete in URBAC 02–77, missing only a small triangular anterior piece. Accounting for the missing piece, the coronoid process is trapezoidal in form, with an almost straight anterior margin and a concave posterior margin. The masseteric fossa is very large and deep, extending posteriorly to the mandibular condyle, and bordered anteriorly by a very prominent coronoid crest. It is deepest along the ventral portion of the coronoid crest. There are two large labial mandibular foramina in most specimens. In CCMGE 69/12455 there is a single large lateral mandibular foramen that continues dorsally into a short groove. The ventral shelf of the masseteric fossa continues on to the mandibular condyle. This shelf is more prominent posteriorly than anteriorly. The medial side of the coronoid process is flat. The mandibular foramen is relatively large, oval-shaped, and facing posteriorly. It opens above the anterior portion of the angular process. On URBAC 03–31 there is a bump-like eminence in the position of the ‘coronoid facet’, which is not as developed in other specimens. Half of the mandibular condyle is above and the other half below the alveolar margin. The condyle is convex, oval in posterior and dorsal views, and at an angle of about 30° from the horizontal with the lateral end higher. The mandibular angle is a thin triangulate plate with very little medial deflection. Its anteroventral margin

is convex and the posterior margin is concave, forming part of the round incisura between the mandibular angle and condyle.

Lower dentition. Lower incisors, canine, and anterior premolars are known from a single specimen referable to *Aspanlestes* (URBAC 04–395; Fig. 9A). It is an anterior dentary fragment with the roots of i1–3, alveolus for i4, subdivided root of c, posterior portion of p1, and mesial alveolus for p2. The i1–3 are basically similar in size, but i4, judging from the alveolus, was much smaller. The i1–3 are inclined anteriorly, with the angle of inclination decreasing from i1 to i3. The alveolus for i4 is located mesiolabial to the mesial root of the canine. The roots of the canine are subdivided by vertical grooves on both lingual and labial sides, with the distal root being more than three times larger than the mesial root, but both roots are set in a single alveolus. The worn distal portion of p1 is preserved, with a distinct distal accessory cusp. The p1 is small, with the mesial root shorter than the distal root. The p2, judging from its mesial alveolus, was distinctly larger than p1.

Judging from the alveoli in the holotype (CCMGE 4/12176) and ZIN 88475, p3 was double-rooted and more than twice smaller than p2 or p4. In ZIN 88488 p3 is absent probably having been lost during life with a resulting diastema between p2 and p4.

The p4 is known only from the holotype dentary fragment (Fig. 9B–D). The tooth is distinctly smaller than p5. The main cusp occupies most of the crown and has a strong distal crest, but no mesial crest. The mesial margin of the cusp is almost vertical. The distal half of the crown is distinctly wider than the mesial half and bears a distal heel that can be considered a distal accessory cusp. At the widest point of the crown there is a bulge-like swelling in the position of the metaconid. The distal side of the p4 crown – with a flat area between the distal crest of the main cusp, the metaconid swelling, and the distolingual cingulid – is reminiscent of the p5, although the talonid basin is more elaborated in the latter. There are no mesial accessory cusps or cingulids, except for the distal accessory cusp.

The p5 is known from two dentary fragments, including the holotype (CCMGE 4/12176, Fig. 9B–D), and several isolated specimens (Fig. 10A, B). This tooth is longer than p4 and shorter than m1. The tooth is submolariform with a three-cusped trigonid and a unicuspid talonid with an incipient talonid basin. The crown morphology is quite variable. The protoconid is high and occupies the anterior two thirds of the crown. The metaconid is distinctly lower than the protoconid and variably developed: it can be just a swelling on the lingual side of the protoconid, with apices of two cusps connected by a vertical ridge (ZIN 88473, URBAC 04–288; Fig. 10A), or fully

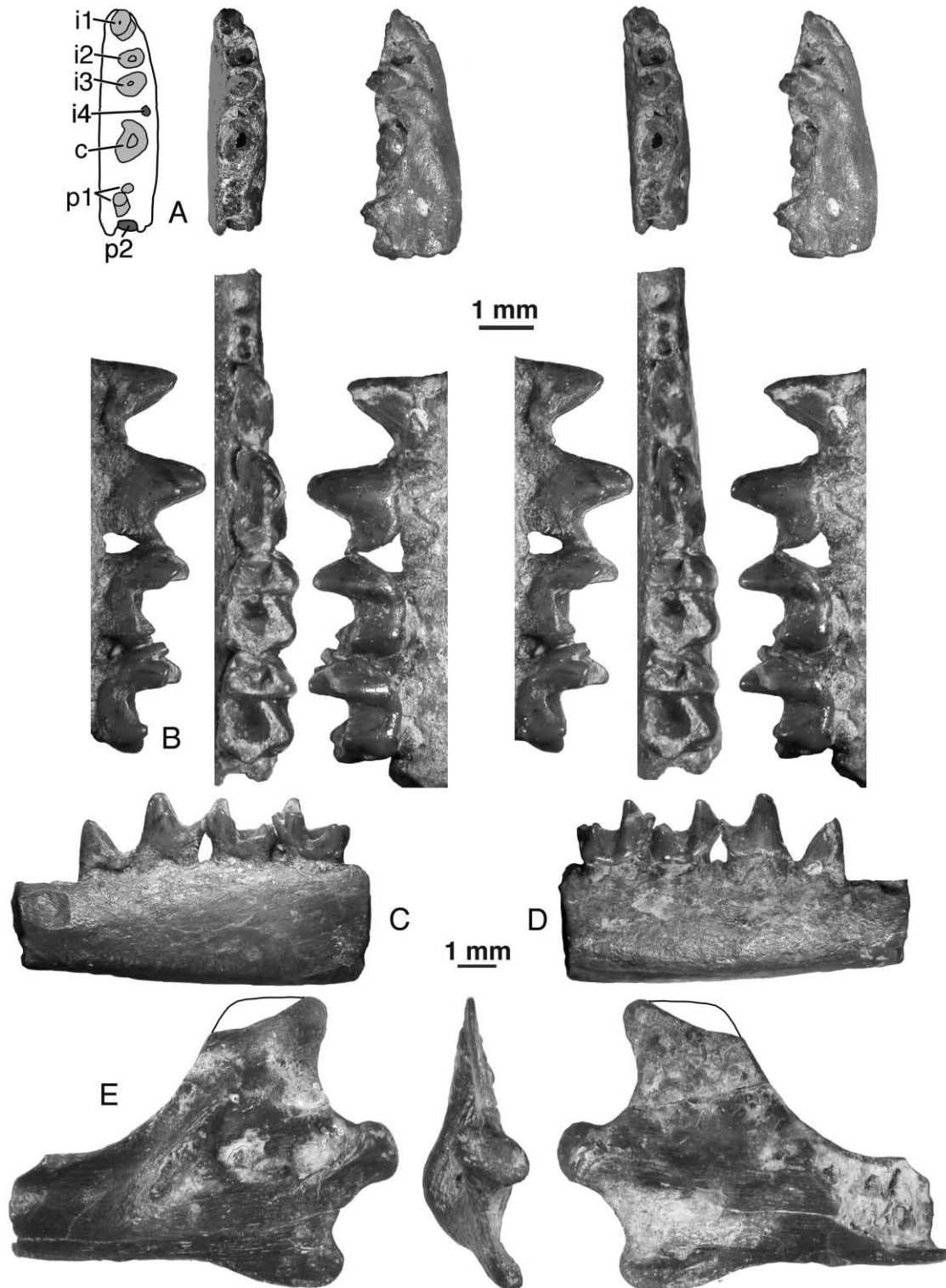


**Figure 9.** *Aspanlestes aptap*, stereophotographs and photographs of dentary fragments. A, URBAC 04-395, right dentary fragment with roots of i1-i3, alveolus for i4, roots of canine, worn partial crown of p1, and alveolus for p2, occlusal and labial views (roots or crown in grey and alveoli in black in line drawing); B-D, CCMGE 4/12176 (holotype), right dentary fragment with posterior alveolus for p2, roots of p3, p4-5, m1-2, B, stereophotographs of dentition in lingual, occlusal, and labial views; C and D, photographs of the whole specimen in lingual and labial views; E, URBAC 02-77, left edentulous dentary fragment in labial, posterior, and lingual views.

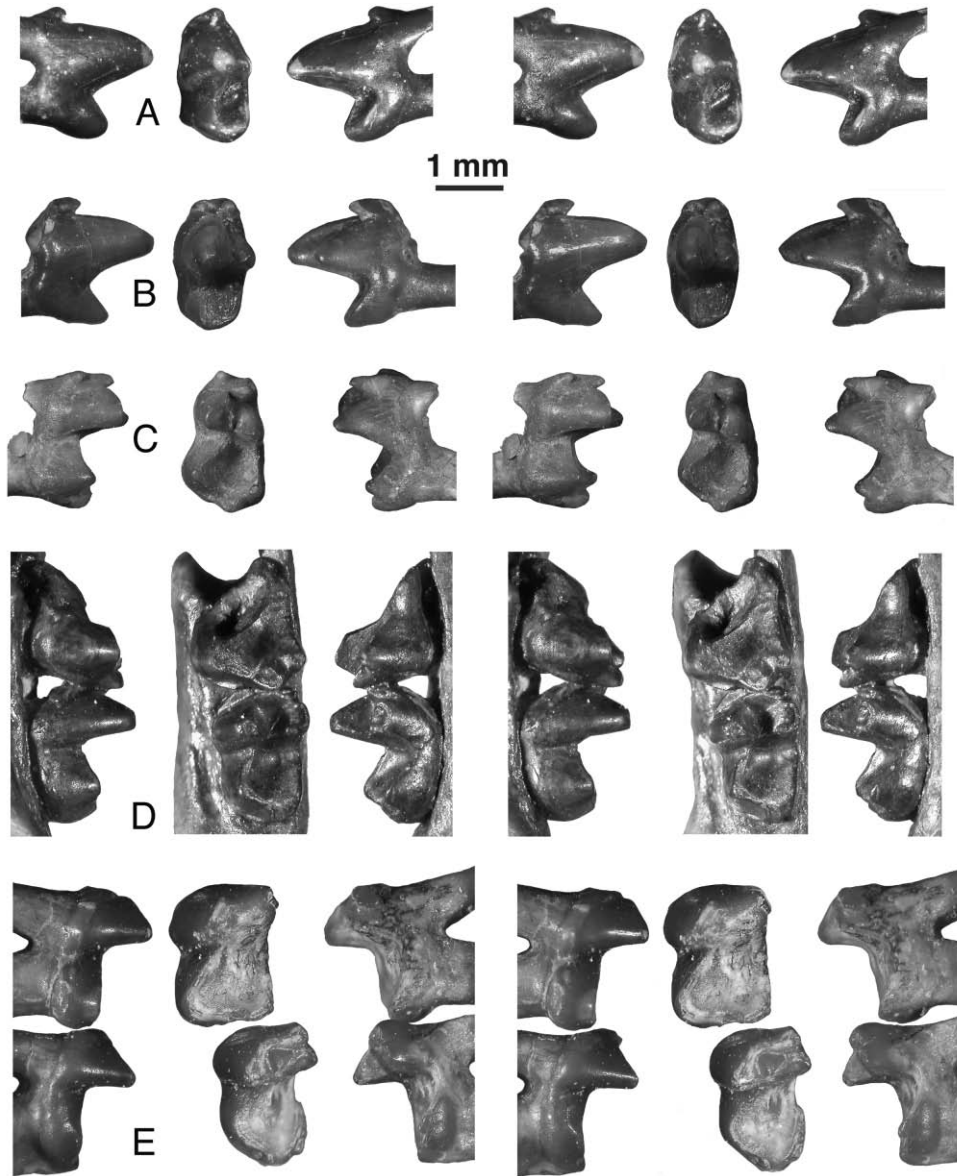


**Figure 10.** *Aspanlestes aptap*, stereophotographs of URBAC 04-288, left p5, A; URBAC 98-7, left p5, B; URBAC 97-8, left dp5, C; CCMGE 6/12176, left dentary fragment with m2 talonid and m3, D; CCMGE 69/12455, left dentary fragment with worn m2-3, E. For all specimens, views are labial (left), occlusal (middle), and lingual (right).

separated from the protoconid by the protocristid notch (URBAC 98-7; Fig. 10B). The p5 metaconid in the holotype dentary is intermediate in morphology between these variants. The development of the paraconid is highly variable: it can be totally absent (holotype), a small cingulid cusp mesially (URBAC 04-288) or mesiolingually (URBAC 99-77, 04-320) of the protoconid, or more elevated above the cingulid but still very small (URBAC 98-7). On URBAC 04-288 there is a strong paracristid, a vertical ridge extending between the protoconid apex and the paraconid base. This crest is not as well developed in other specimens.

There is no trigonid basin, except that in URBAC 04-288 a shallow area is delimited by the paracristid and a more lingual cristid between the bases of the paraconid and the metaconid. The talonid cusp is only slightly lower than the metaconid. The talonid basin varies in depth. It is bordered by the cristid obliqua, postcristid, and entocristid, and is confluent with the depressed area on the distal trigonid wall that is bordered by vertical ridges from the protoconid and metaconid. The lingual of these ridges (the entocristid and the metaconid ridge) are more basal in position, so the talonid basin and the depression on the distal

trigonid wall are well exposed on the lingual side. In most specimens only a mesial cingulid is present, which connects lingually with the paraconid. In URBAC 99–77 there is a very faint lingual cingulid and in ZIN 88473 there is a distinct labial cingulid at the base of the talonid extending vertically towards the apex of the talonid cusp.

The dp5 is known from several isolated specimens, amongst which URBAC 97–8 (Fig. 10C) is the most complete and unworn. Another specimen is preserved in a dentary fragment (URBAC 02–68). The trigonid angle is considerable (i.e. the trigonid basin is quite open lingually). The protoconid is distinctly higher than the metaconid, but on worn teeth the height of these cusps might be equal. The metaconid is set somewhat distal to the protoconid, resulting in an oblique position of the protocristid relative to the dentary longitudinal axis. The paraconid varies in size, but is usually much smaller than the metaconid. There is a well-developed cusp-like precingulid on the mesial side of the crown below the paracristid notch. The talonid is longer and about 1.5 times wider than the trigonid. The hypoconid is the largest talonid cusp and the hypoconulid is the smallest. The hypoconulid projects distally and is closer to the entoconid, but is not twinned with the latter. The cristid obliqua extends to below the protocristid notch. On the distal side of the hypoconid there is a faint postcingulid, extending lingually towards the hypoconulid apex.

The lower molars are known from several isolated specimens and dentulous dentary fragments. All lower molars can be easily distinguished: in m1 the trigonid angle is greater than in m2 and the paraconid is smaller and placed more labially compared with m2; in m3 the trigonid is the same as in m2 but the talonid is distinctly longer and narrower than the trigonid and the hypoconulid is more distally projecting (Figs 9B–D, 10D, E). In m1–2 the talonid is wider than the trigonid. The metaconid is only slightly lower than the protoconid. Lingually the bases of the paraconid and metaconid are separated by a variably developed groove. The trigonid basin is the largest on m2 and smallest on m3. The protocristid is transverse to the longitudinal axis of the dentary in all molars. The precingulid is well developed and is below the protoconid. All talonid cusps are well developed; the hypoconid is the largest and the entoconid the smallest. The hypoconulid occupies the most posterior position on the talonid; it is closer to the entoconid than to the hypoconid. With the wear, which removes part of the hypoconulid from the labial side, the hypoconulid appears to be even closer to the entoconid. The cristid obliqua extends to below or slightly labial to the protocristid notch. There is a short postcingulid on all molars below the hypoconid. In one m1 (CCMGE 13/12953), there is a distinct labial cingulid

around the base of the protoconid between the precingulid and hypoflexid and in one m2 (URBAC 00–63) there is a short labial cingulid within the hypoflexid (ectostylid).

*Measurements:* See Appendices 2 and 3.

#### ASPANLESTES SP.

(See Appendix 4 for synonymies, referred illustrations, and referred specimens.)

*Locality and horizon:* CDZH-117, Dzharakuduk, Kyzylkum Desert, Uzbekistan. Aitym Formation, Upper Cretaceous (upper Turonian – Coniacian?).

*Description:* P4 (Averianov & Archibald, 2003: fig. 10a, b), if correctly attributed to *Aspanlestes* sp., differs from *Aspanlestes aptap* in lacking a protocone bulge (only a distolingual cingulum is present), by having a larger anterior accessory cusp, and by having a more prominent distolabial cingulum.

The fragmented and heavily worn P5 is somewhat smaller than that in *A. aptap*, but apparently does not differ in the structure from what is preserved.

For description of DP5 see Archibald & Averianov (2001: 542; misidentified there as M1 of *Paranyc-toides*). In morphology it is very close, if not identical, to DP5 of *A. aptap* (CCMGE 4/12455).

The upper molars (for M2 see Averianov & Archibald, 2003: fig. 10c) are the same as that in *A. aptap*.

The fragment of a worn lower molar (Averianov & Archibald, 2003: fig. 10d, e), originally identified as m1 or m2, is most certainly identified here as m2. It shows no differences from m2s of *A. aptap*, except its somewhat smaller size.

*Measurements:* See Averianov & Archibald (2003: 179, 181) and Appendix 2.

*Comments:* The sample of *Aspanlestes* sp. from the Aitym local fauna is very close to *A. aptap* from the Bissekty local fauna. It may belong to the same species but more material is needed to verify this.

#### PARAZHELESTES NESOV, 1993

*Parazhelestes:* Nesov, 1993: 123.

*Type species:* *Parazhelestes robustus* Nesov, 1993.

*Included species:* Type species, *Parazhelestes mynbulakensis* (Nesov, 1985b) comb. nov., and *Parazhelestes* sp.

*Revised diagnosis:* Differs from *Zhelestes* by diastema between upper canine and premolars absent; diastema posterior to P1 absent; P3 double-rooted (unknown for *P. robustus*). Differs from *Zhelestes* and *Eoungulatum* by double-rooted upper and lower canine. Differs from *Aspanlestes* and *Zhelestes* by P1 double-rooted; protocone labially shifted more than 21%. Differs from *Aspanlestes*, *Zhelestes*, and *Eoungulatum* by mandibular symphysis at p2 or more anterior; trigonid angle less than 35°. Differs from *Eoungulatum* by P5 protocone smaller than paracone; P5 metacone swelling; P5 para- and metastylar lobes subequal; upper molars preparastyle present; metacone slightly smaller than paracone; 'coronoid' facet absent; masseteric fossa bordered ventrally by well-defined crest connected to condyle; m3 subequal to larger than m2.

*Distribution:* Uzbekistan; Late Cretaceous (Turonian–?Coniacian).

*PARAZHELESTES MYNBULAKENSIS*  
(NESOV, 1985B) **COMB. NOV.**

FIGURES 11–17

(See Appendix 4 for synonymies, referred illustrations, and referred specimens.)

*Holotype:* CCMGE 36/12000, left dentary with m2 and alveoli for m3.

*Type locality and horizon:* CBI-4b, Dzharakuduk, Kyzylkum Desert, Uzbekistan. Bissekty Formation, Upper Cretaceous (middle–upper Turonian). Found in 1980.

*Diagnosis:* Differs from *P. robustus* in lower teeth averaging 13% smaller (range equals 4 to 21%) and upper teeth averaging 10% smaller (range equals 7 to 13%) and width of M3 subequal to M2 [37(0)].

*Description:* Maxilla. The known portions of the maxilla for *P. mynbulakensis* are similar to that bone in *Aspanlestes*, but some structural differences do exist. In *P. mynbulakensis* the jugal facet is closer to the alveolar margin above all molars (above the distal root of M1 to M2–3 in *Aspanlestes*). The infraorbital foramen is placed above the distal root of P4 or between the roots in *P. mynbulakensis* (URBAC 00–24, 02–59, 04–162) (but above the mesial root of P4 in *Aspanlestes*). In the most complete maxillary fragment (URBAC 04–162) there is not a wedge-like palatine facet anterior to the medial opening of the

infraorbital foramen, and no detectable facets for maxilloturbinals.

*Palatine.* In ZIN 88468 there is a partial horizontal (palatal) process of the palatine attached to the maxillary fragment (Fig. 11). The anterior portion of the process overlaps the maxilla ventrally and the maxilla–palatine suture is located close to the lingual border of the upper molars. There may be a postpalatine torus. Medial and posterior to M3 there is a longitudinally elongated complex depression bordered by elevated bone walls. This depression may correspond to the postpalatine foramen or minor palatine foramen in *Zalambdalestes* (Wible *et al.*, 2004).

*Upper dentition.* The upper incisors, canine, and anterior premolars are not known for *P. mynbulakensis*. Judging from alveoli in URBAC 04–162 (Fig. 12), P2 and probably P1 were double-rooted and relatively unreduced. P3 was also double-rooted, but much smaller than P2 (CCMGE 11/12176, URBAC 04–162). In URBAC 02–59 the P3 was lost and its alveoli were filled by bone, leaving a diastema between P2 and P4. As in *Aspanlestes*, the distal root of P4 is labiolingually wider than the mesial root (CCMGE 11/12176, URBAC 02–59), suggesting that P4 had a well-developed protocone swelling.

The P5 is known from several maxillary fragments and isolated specimens. The structure of P5 is essentially the same as in *A. aptap*. The development of the metacone is highly variable. In CCMGE 11/12176 (Fig. 13) and URBAC 02–83, 04–109 the metacone swelling is almost indistinguishable. It is slightly more pronounced in URBAC 00–42, 02–1, and 02–59. In an unworn (unerupted) P5, URBAC 98–20, the metacone is a distinct trenchant cusp separated by a deep notch from the paracone; but with wear this cusp is easily eliminated leaving only a swelling distal to the paracone. A relatively worn CCMGE 21/12953 is unique in having the metacone as a distinct cusp widely separated from the paracone (Nesov *et al.*, 1998: fig. 12F–H). Some specimens (URBAC 98–20, 02–59) show a well-developed meta-style distolabial to the metacone. The paraconule is present in all specimens and the metaconule is absent. The precingulum is usually shorter than the postcingulum. URBAC 02–59 is unique in having the precingulum but not the postcingulum.

The DP5 is known from five isolated specimens. It is somewhat larger than DP5 of *A. aptap*, but similar in structure. The specimens vary in development of the preparastyle, which can be smaller than the parastyle or almost the same size. The biggest discrepancy between the size of the preparastyle and parastyle is in URBAC 04–168. In URBAC 04–151, 04–168, 04–206, and 04–397 there is a distinct cingular cusp C connected by a transverse ridge to the centrocrista.

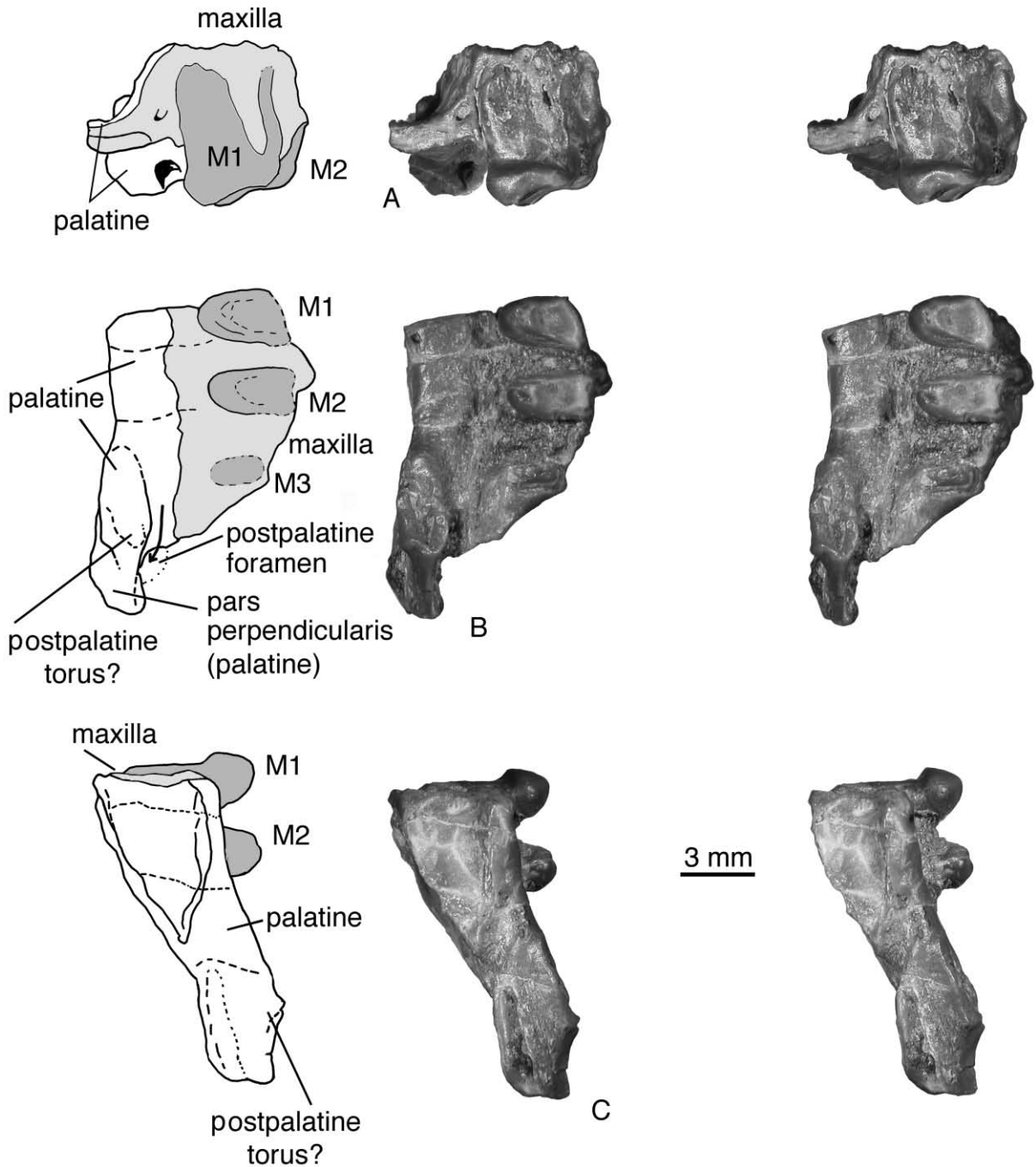


**Figure 11.** *Parazhelestes mynbulakensis*, ZIN 88468, stereophotographs and line drawings left palatine and maxilla with worn M1–2 and M3 fragment. A, anterior; B, occlusal; C, lingual views.

In URBAC 04–213 the cusp C is much less developed, not more than a crenulation on the ectocingulum. In URBAC 04–151 and 04–397 there is a smaller additional cingular cusp immediately mesial to the cusp C. A small cingular cusp E is present in four specimens (in URBAC 04–213 this area of ectocingulum is missing). The lingual cingula vary in development.

The precingulum is shortest in URBAC 04–151 and longest in URBAC 04–168.

The upper molars M1–2 are known from several maxillary fragments and numerous isolated specimens. The structure of these teeth is basically the same as in *A. aptap*. The most variable part of the crown is the ectocingulum. A majority of M1s have no

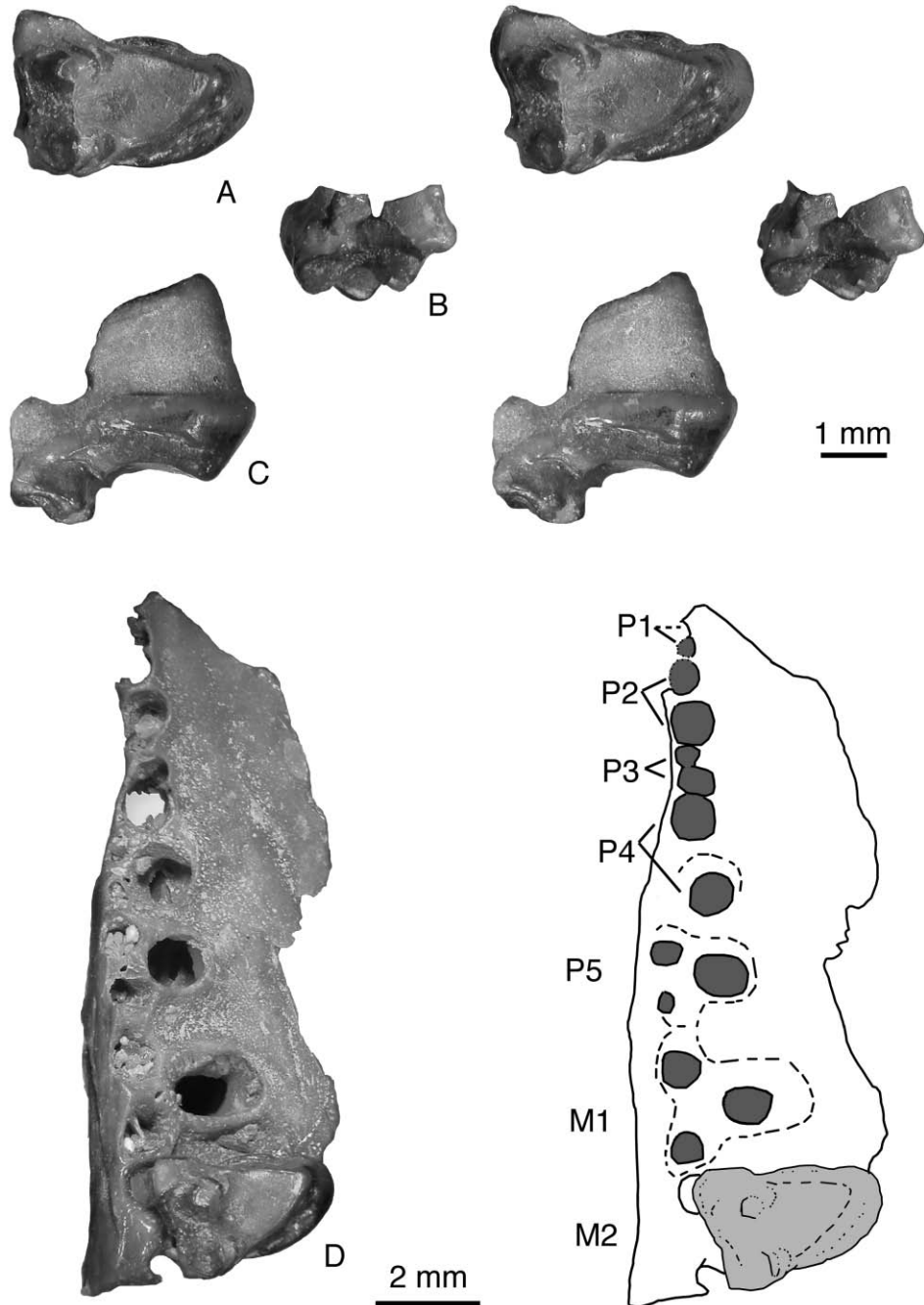


**Figure 12.** *Parazhelestes mynbulakensis*, URBAC 04–162, right maxillary fragment with M2 and alveoli for P1–P5, and M1. Stereophotographs of M2, A, occlusal; B, labial; C, distal views. D, photograph and line drawing of occlusal view of maxillary fragment.

styler cusps. In some M1s there is a small, but distinct stylocone (URBAC 98–18, 98–108, 02–8), crenulations in C and E cusp positions (CCMGE 11/12176, URBAC 98–19), or in C position (URBAC 02–8), or distinct cusp in E position (URBAC 98–18, 02–8, 04–99). The M1s of CCMGE 11/12953 and URBAC 02–27 have a distinct cusp C connected by a

transverse ridge with the centrocrista, as in DP5s. The M2 appears to be less variable. No M2 has a stylocone or cusp C and only two M2s have a distinct styler cusp E (URBAC 04–121 and 04–192). Two quite worn M2s (URBAC 02–28 and 06–93) still have a strong preparacrista extending mesially between the parastyle and preparastyle.

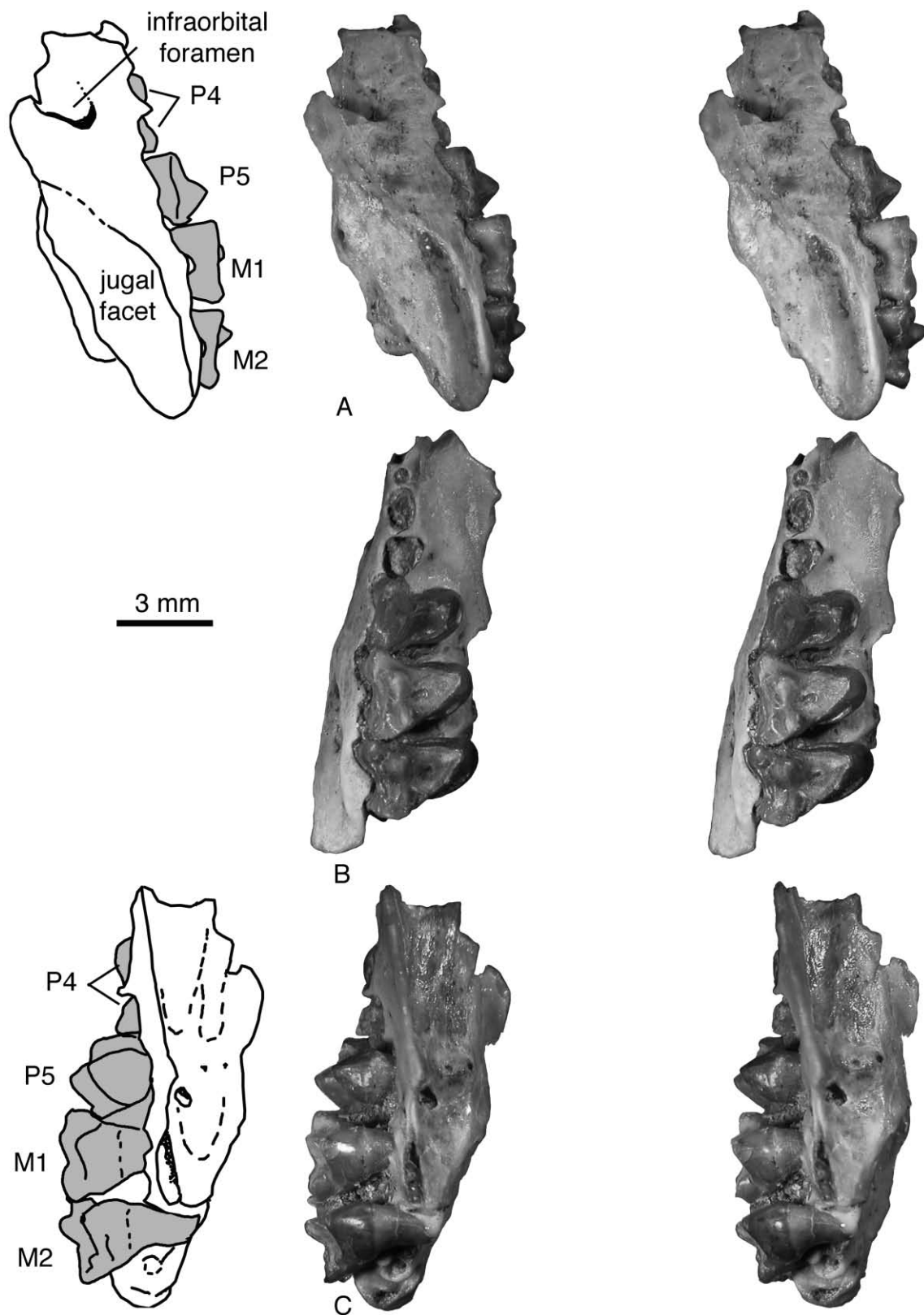


**Figure 13.** *Parazhelestes mynbulakensis*, CCMGE 11/12176, stereophotographs and line drawings of right maxillary fragment with P3 alveoli, P4 roots, P5, M1–2. A, labial; B, occlusal; C, lingual views.

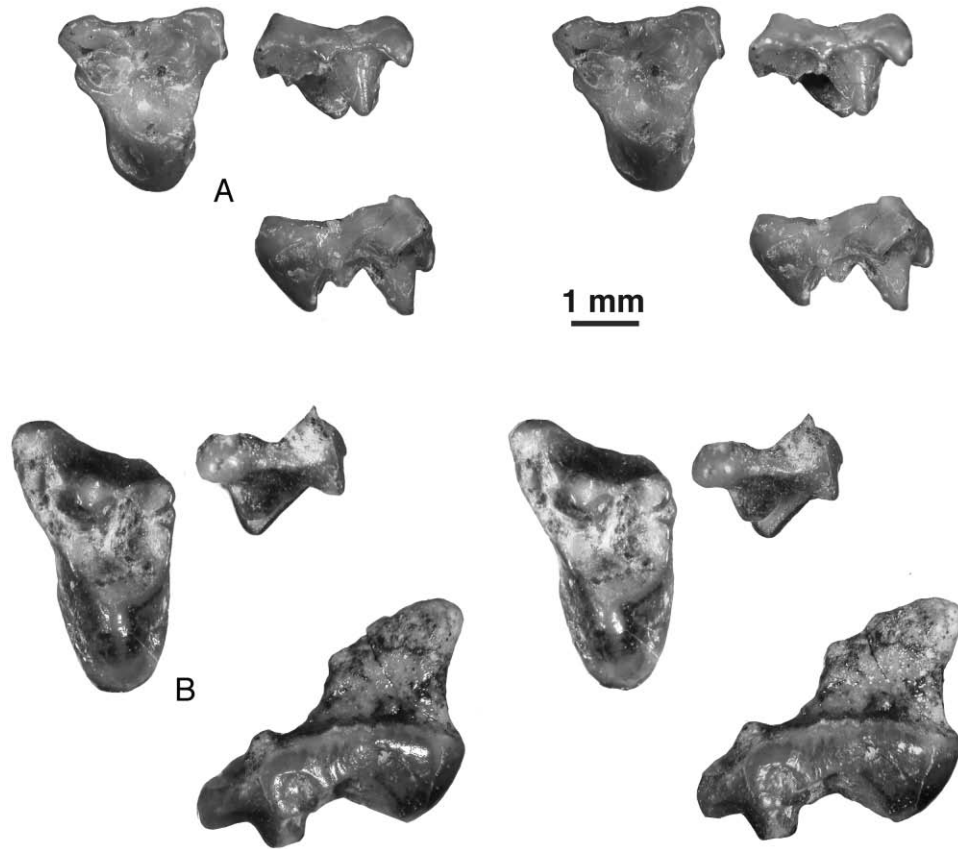


**Figure 14.** *Parazhelestes mynbulakensis*, stereophotographs of URBAC 04–168, right DP5, A, occlusal, labial, and distal views, and URBAC 03–179, left M3, B, occlusal, labial, and distal views.

The M3 is known from a single isolated and quite worn specimen (URBAC 03–179; Fig. 14). Compared to M2, it has a larger and more labially projecting parastylar lobe, very reduced metastylar lobe, and a more mesiolabially positioned protocone. The metacone and the metaconule are relatively unreduced. In contrast to the M1–2, the postcingulum is much shorter than the precingulum. The M3 lingual root preserved in a maxillary fragment ZIN 88468 (Fig. 11) shows that the lingual side of this tooth is aligned with other molars.

**Dentary.** The structure of the dentary in preserved fragments is the same as in *Aspanlestes* (the coronoid processes are not known for *P. mynbulakensis*). The posterior end of the mandibular symphysis is between the roots of p2 (ZIN 88470), the distal root of p2 (six specimens), between p2 and p3 (URBAC 98–24), the mesial root of p3 (URBAC 00–11, 06–92), or between the roots of p4 (URBAC 02–104). The posterior shift of the mandibular symphysis is probably ontogenetically correlated. In URBAC 06–113 there are two small anterior mental foramina under i2 and one larger under the mesial root of canine. Two other

specimens also preserve an anterior mental foramen under i3 (URBAC 04–193) or under the distal root of the canine (ZIN 88481). In other specimens the distal-most of the anterior mental foramina is under the mesial root of p1 (eight specimens), distal root of p1 (five specimens), or mesial root of p3 (URBAC 03–40). In ZIN 88482 and URBAC 98–24 this foramen is very large and extends for the whole length of p1. In URBAC 02–104 there is a lateral groove from below p1 to the mesial root of p3, which houses two large mental foramina at its ends. The posterior mental foramen is under the mesial root of p5 (seven specimens), between the roots of p5 (two specimens), or under the distal root of p5 (five specimens). The labial mandibular foramen is usually represented by three to six relatively large irregular openings.

The condylar and angular processes are preserved only in IZANUZ P2155-M-1 (Nesov *et al.*, 1998: fig. 17). The shape and configuration of these processes and the mandibular foramen are essentially the same as in URBAC 02–77 of *Aspanlestes*. The medial end of the condylar process is completely preserved (abraded in

URBAC 02–77) and pointed, giving a tear-like shape of the condyle in posterior view.

Lower dentition. In URBAC 06–113 (Fig. 15), i2–3 are incompletely preserved, with most of the crowns eliminated by wear or breakage. Numerous edentulous anterior dentary fragments provide information about the lower incisors and canine. Most specimens had three lower incisors, with large i1–3 (i1 is somewhat smaller than i2–3) and a minute i4 wedged on the labial side between the alveoli for i3 and the canine. The root of i4 can be seen in URBAC 99–109 (Fig. 16). The i4 position can be absent in some specimens, such as URBAC 98–13 (Fig. 17).

The lower canine was a large, double-rooted tooth; its mesial root was shorter (URBAC 98–13, 06–113; Figs 15, 17) or as large as the distal root (URBAC 99–109; Fig. 16). In ZIN 88470 the tip of the erupting lower canine crown is preserved with the remainder of crown in its crypt. It has a flattened lingual side with the apex deflected somewhat distally. In the deciduous canine the distal root was relatively smaller than in the permanent canine.

The p1, judging from its alveoli, was a small, double-rooted tooth set obliquely (the smaller mesial root was more labial than the distal root) in the dentary between the larger canine and p2.

The p2 is known from dentary fragments URBAC 97–3 and 02–13 (Fig. 15). It is a relatively large, double-rooted tooth with a high main cusp and a small distal accessory cusp (there is no mesial accessory cusp). The mesial side of the main cusp is almost vertical; its apex is deflected somewhat distally. There is a very faint lingual cingulid above the mesial root. An unerupted p2 is also preserved in URBAC 00–68 and 06–111.

The p3, judging from the alveoli, was smaller than p2 and p4, but slightly larger than p1. It is aligned with other premolars in most specimens, but in URBAC 02–13 it is set obliquely to the longitudinal axis of the dentary, with the mesial root placed more labially than the distal root (Fig. 15). The latter specimen is also unique in having the mesial root distinctly larger than the distal root, whereas in other specimens the distal root is somewhat larger than the mesial root. In some specimens p3 is absent and may have been lost during ontogeny (e.g. ZIN 88482, URBAC 99–109). In URBAC 99–109 there is a short diastema between the p2 and p4 with a little hole attached to the mesial alveolus of p4, possibly representing the distal alveolus for p3 (Fig. 16). In ZIN 88482 there are no traces of p3 in the diastema between p2 and p4.

The p4 is known from three dentary fragments (ZIN 88477, 88485, URBAC 99–109; Fig. 15). The p4 is a simple double-rooted tooth like p2, with a high main cusp having an almost vertical mesial side. The posterior accessory cusp is larger than in p2. There is

a very small anterior accessory cusp (URBAC 99–109), or a short, faint mesial cingulid in its place (ZIN 88477).

The p5 is known from three dentary fragments and three isolated specimens (Figs 16, 17). This tooth is close in structure to p5 in *Aspanlestes* and is as variable as in the latter taxon. The paraconid is absent in CCMGE 1/12953 (there is a very short mesial cingulid in its place), a minute cingular cusp in ZIN 82580 (the mesial cingulid on this specimen is much longer than in CCMGE 1/12953), a distinct, but still very small cusp at the base of the protoconid, closer to the lingual side of the latter (URBAC 98–16, 99–109, 04–226), or a larger and more elevated cusp, approximating the position of the paraconid in m1 (URBAC 98–13). In URBAC 98–13 and 99–109 there is a prominent mesial cingulid extending from the paraconid to around the labial base of the protoconid. The metaconid is represented by a metaconid swelling on the lingual side of the protoconid in most specimens, but in URBAC 98–13 it is a distinct cusp separated from the protoconid by a wide protocristid groove (Fig. 17).

The dp5 is known from one dentary fragment and two isolated specimens. This tooth is almost identical in morphology and only slightly larger than dp5 in *Aspanlestes*. One structural difference does exist: the precingulid in the dp5 of *P. mynbulakensis* is much reduced and ridge-like compared with the prominent cusp-like precingulid in this tooth in *Aspanlestes*.

The lower molars are known from several dentary fragments [amongst which URBAC 98–13 and 99–109 are most complete (Figs 16, 17)] and a number of isolated specimens. The structure of the molars is identical to that in *Aspanlestes*. In m1 the variation concerns the postcingulid, which can be faint (URBAC 00–80, 04–399) or strong (other specimens). One m1 is unique in having an almost complete labial cingulid (URBAC 04–398). In another m1 there is a labial cingulid around the talonid and hypoflexid (URBAC 04–227). Other m1s totally lack the labial cingulid. In m2, as in m1, the most variable structure is the postcingulid. The postcingulid is absent in URBAC 06–65, faint in URBAC 03–170, 04–6, 04–123, and stronger in other specimens. In one m2 (URBAC 98–112) there is an almost complete labial cingulid connected with the postcingulid. The known sample of m3s shows no variation.

*Measurements:* See Appendices 2 and 3.

#### *PARAZHELESTES ROBUSTUS* NESOV, 1993

##### FIGURES 18–20

(See Appendix 4 for synonymies, referred illustrations, and referred specimens.)

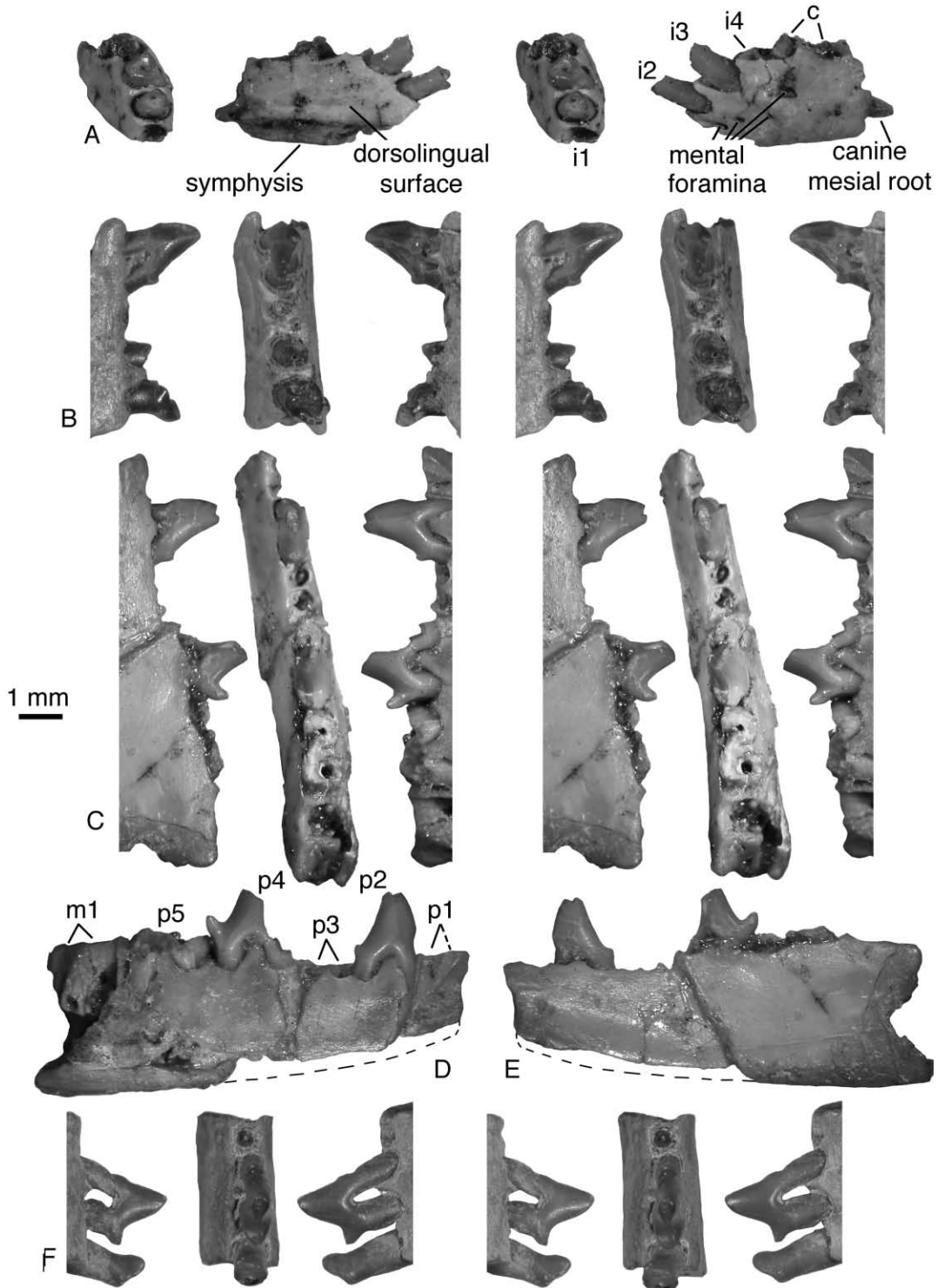


**Figure 15.** *Parazhelestes mynbulakensis*, dentary fragments, stereophotographs of URBAC 06–113, left dentary fragment with i1 alveolus, i2–4 fragments, i4 alveolus, and canine roots, A, anterior and labial views; stereophotographs of URBAC 02–13, left dentary fragment with p2, p3 roots, and p4 anterior root and talonid; B, labial, occlusal, and lingual views; stereophotographs of URBAC 97–03, right dentary fragment with p1 alveoli, p2, p3 alveoli, p4 lacking anterior, p5 roots, and m1 alveoli, C, lingual, occlusal, and labial views; photographs of URBAC 97–03 showing ventral margin of dentary, D, labial and E, lingual (dashed line shows missing anteroventral margin); stereophotographs of ZIN 88477, left dentary fragment with p4, anterior root of p5, and alveoli for p3, F, lingual, occlusal, and labial views.

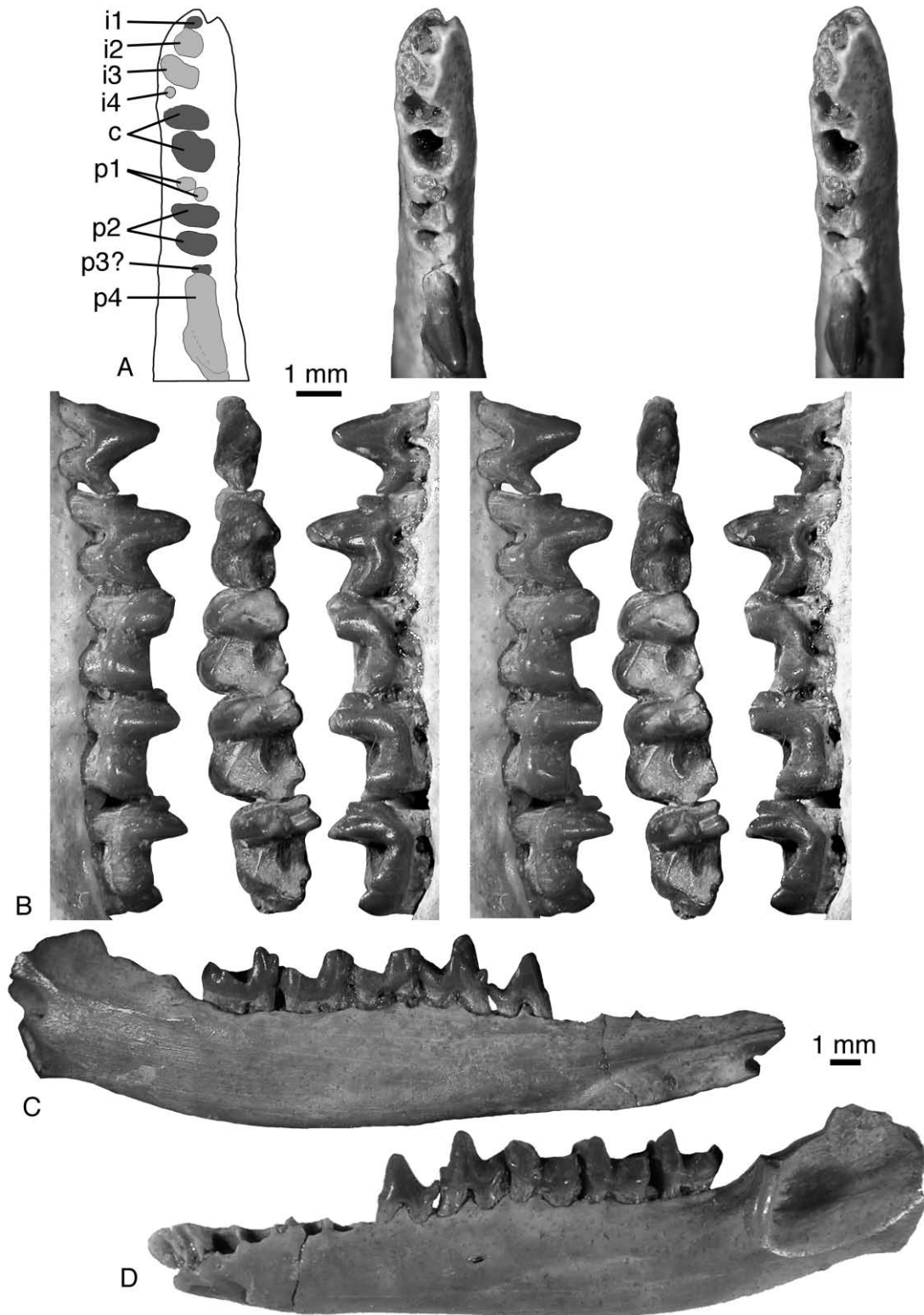


**Figure 16.** *Parazhelestes mynbulakensis*, stereophotographs URBAC 99–109, left dentary with i1–4, c, p1–3(?) roots or alveoli, and p4–5, m1–3. A, stereophotograph and line drawing of anterior end. Light grey indicates roots teeth and dark grey indicates alveoli. B, stereophotograph of teeth in labial, occlusal, and lingual views. Photographs showing entire dentary, C, lingual view and D, labial view.

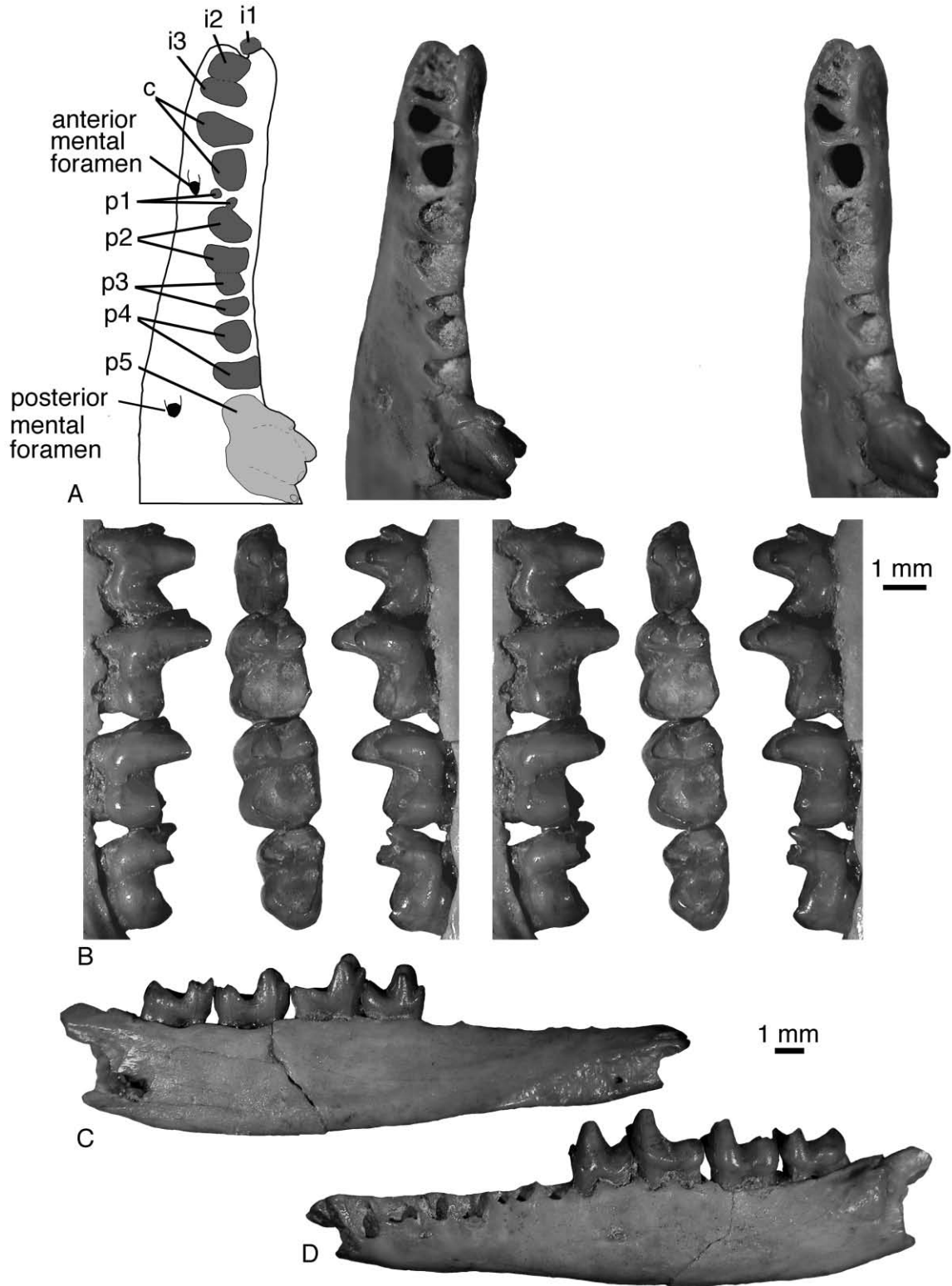


**Figure 17.** *Parazhelestes mynbulakensis*, stereophotographs URBAC 98–13, left dentary with i1–3, c, p1–4 alveoli, and p5, m1–3. A, stereophotograph and line drawing of anterior end. Light grey indicates teeth and dark grey indicates alveoli. B, stereophotograph of teeth in labial, occlusal, and lingual views. Photographs showing entire dentary, C, lingual view and D, labial view.

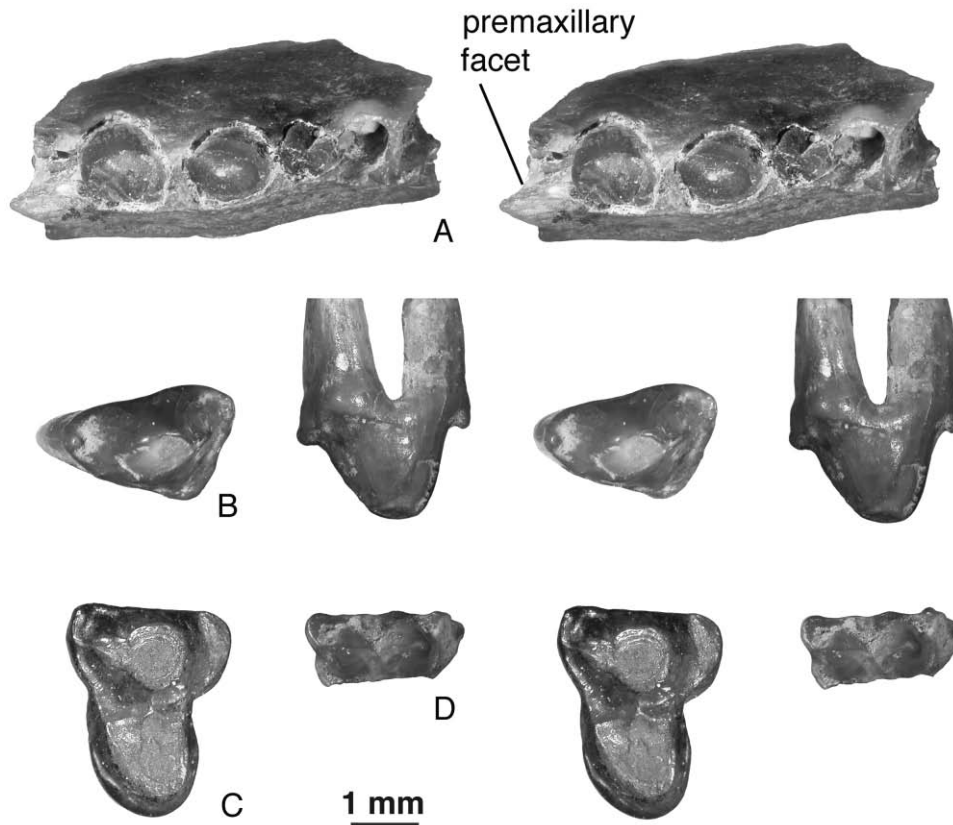


**Figure 18.** *Parazhelestes robustus*, stereophotographs of URBAC 02–24, left maxillary fragment with C and P1 roots, and P2 alveoli, A, occlusal view; URBAC 98–23, left P4, B, occlusal and labial views; CCMGE 35/12176, right P5, C, occlusal view; URBAC 04–270, labial half of right DP5, D, occlusal view.

*Holotype*: CCMGE 70/12455, left maxilla with heavily worn and eroded P4–5, M1–3.

*Type locality and horizon*: CBI-14, Dzharakuduk, Kyzylkum Desert, Uzbekistan. Bissekty Formation, Upper Cretaceous (middle–upper Turonian). Found in 1987.

*Revised diagnosis*: Differs from *P. mynbulakensis* in lower teeth averaging 13% larger (range equals 4 to 21%) and upper teeth averaging 10% larger (range equals 7 to 13%) and M3 narrower than M2 [37(1)].

*Description*: Maxilla. The jugal facet on the holotype of *P. robustus* is higher than in *P. mynbulakensis* and *Aspanlestes*: it comes close to the alveolar border only above M3. The infraorbital foramen is slightly more posterior than in *P. mynbulakensis*, approximately at the level between P4 and P5. The maxilla has a distinct facet for the maxilloturbinals (holotype), as in *Aspanlestes*. The palatal process on URBAC 02–24 has a small premaxillary facet on the anterior end (Fig. 18).

Upper dentition. No upper incisors, canines, or anterior premolars are known for *P. robustus*. The only anterior maxillary fragment referable to *P. robustus* is URBAC 02–24 (Fig. 18A). It has two approximately equal and labiolingually compressed canine roots, two roots for a small P1 set somewhat obliquely, and alveoli for a double-rooted P2 (the P2 was more than twice as long as P1). There are no diastemata between the teeth. There is some space on the maxilla anterior to the canine, but the alveolar border is broken here and it is not clear if this space contained the alveolus of the last incisor.

The P4 is known from the holotype maxilla and an isolated specimen, URBAC 98–23 (Fig. 18B). In the holotype the enamel of this tooth is eroded so description is based on the isolated specimen. This is a double-rooted tooth with a robust main cusp, very small mesial and distal accessory cusps, and a well-developed protocone swelling supported by the transversely widened distal root. There is a prominent distal ridge extending from the main cusp apex towards the posterior accessory cusp but it does not reach the latter. There is a short distolabial cingulum

at the distal accessory cusp and a longer distolingual cingulum extending around the whole protocone swelling.

The P5 is known from the holotype maxilla, where the enamel of this tooth is somewhat eroded, and from isolated CCMGE 35/12176 (Nesov, 1985a: pl. 3, fig. 1; 1997: pl. 53, fig. 5; Nesov *et al.*, 1998: fig. 14P, Q) (Fig. 18C). For description of CCMGE 35/12176 see Nesov *et al.* (1998: 59).

The DP5 labial fragment URBAC 04–270 (Fig. 18D) is referred to *P. robustus* because it is larger than the DP5s of *P. mynbulakensis* and coincides in size with the P5 of *P. robustus*. The styler shelf is of equal width (very narrow) labial to the paracone and metacone. There is a minute stylocone but no other styler cusps.

The upper molars are known from the holotype maxilla, where they are heavily worn, and from isolated specimens. The upper molars of *P. robustus* are larger and more robust than the upper molars of *P. mynbulakensis* but have basically the same structure. The main structural difference between the two species is a somewhat more labially placed protocone in *P. robustus*. The known sample of M1s shows almost no variation. The styler cusp E is present in CCMGE 20/12953 (Fig. 19A). Except for the holotype, M2 of *P. robustus* is known only from an isolated specimen, URBAC 99–13 (Fig. 19B). This tooth has a relatively small parastylar lobe and the ectocingulum is expanded in the region of cusp C. The metastylar lobe was certainly small but some of the labial margin has been eroded away. The M3 is somewhat less worn in the maxilla fragment URBAC 98–22 (Fig. 19C) compared to the holotype. Both maxillary fragments show that the lingual border of M3 is placed somewhat labial to the lingual margin of M1–2. The M3 in URBAC 98–22 differs from M3 URBAC 03–179, referred to *P. mynbulakensis*, in having a relatively shorter parastylar lobe.

Dentary. The posterior mental foramen is usually under the distal root of p5 (ZIN 88465). In URBAC 03–120 the posterior mental foramen is very large, extending beneath the distal root of p4 and both roots of p5. The Meckelian groove is absent (URBAC 97–5, 03–120). The masseteric crest is high. There are two (URBAC 03–120, ZIN 88466) or three (ZIN 88455) labial mandibular foramina. In some specimens there is a marked tuberosity in the area of the coronoid facet of more primitive mammals, which is on the medial side of the dentary between the m3 and base of the coronoid process (ZIN 88466). In ZIN 88463 on the medial side of the coronoid process there is a robust subhorizontal crest delimiting the ventral border for the temporalis muscle. The base of the angular process and the mandibular foramen are present only in ZIN 88969; these structures do not differ from those in other zhelestids.

Lower dentition. The lower incisors, canines, and premolars (except a tentatively attributed isolated p2) are not known for *P. robustus*. However, in IZANUZ P2155-M-5 there is a minute alveolus for i4 at the mesiolabial corner of the canine anterior root, exactly as in URBAC 99–109 of *P. mynbulakensis* (Fig. 16). This suggests that at least some individuals of *P. robustus* had four lower incisors as well. The lower canine is double-rooted, as evident from alveoli in IZANUZ P2155-M-5. In this specimen there are no alveoli for p1 and p3, but judging from the closely spaced alveoli, it is likely to be an immature specimen and the postcanine dentition could have been dp2–4. The referral of IZANUZ P2155-M-5 to the larger *Eoungulatum* is unlikely because the latter has a single-rooted lower canine. The alveoli for p2 and p3 are similar in size. The p3 was much smaller and mesiodistally aligned (ZIN 88489, URBAC 03–120) or oblique (ZIN 88465) to the tooth row.

URBAC 04–324 is a lower premolar tentatively attributed to *P. robustus* (Fig. 20A, B). It has two long roots, a conical central cusp, which is inclined anteriorly, no mesial accessory cusp, and a small distal accessory cusp. It is likely to be p2 because p1 and p3 are reduced in zhelestids and p4 has a distinct anterior accessory cusp. It is larger than p2 in URBAC 97–3 and 02–13 attributed to *P. mynbulakensis*.

Amongst the lower molars, m1 is not known for *P. robustus*, m2 is known from three isolated specimens and one dentary fragment, URBAC 97–5 (Fig. 20C, D), and m3 is known from a single isolated specimen (URBAC 03–38; Fig. 20E). The lower molars have the same morphology as in *P. mynbulakensis*, but are slightly larger. The postcingulid is absent in URBAC 04–260, short in URBAC 98–14, and longer in URBAC 97–5. In the latter specimen there is a faint labial cingulid. The single m3 is wider than this tooth in *P. mynbulakensis*, but has a much shorter talonid. The hypoconulid projects only slightly distally. The m3 paraconid is reduced and in a more labial position as in m1, whereas it is little reduced and more lingual in m2 as in *P. mynbulakensis*.

*Measurements:* See Appendices 2 and 3.

#### PARAZHELESTES SP.

(See Appendix 4 for synonymies, referred illustrations, and referred specimens.)

*Locality and horizon:* CDZH-117, Dzharakuduk, Kyzylkum Desert, Uzbekistan. Aitym Formation, Upper Cretaceous (upper Turonian–Coniacian?).

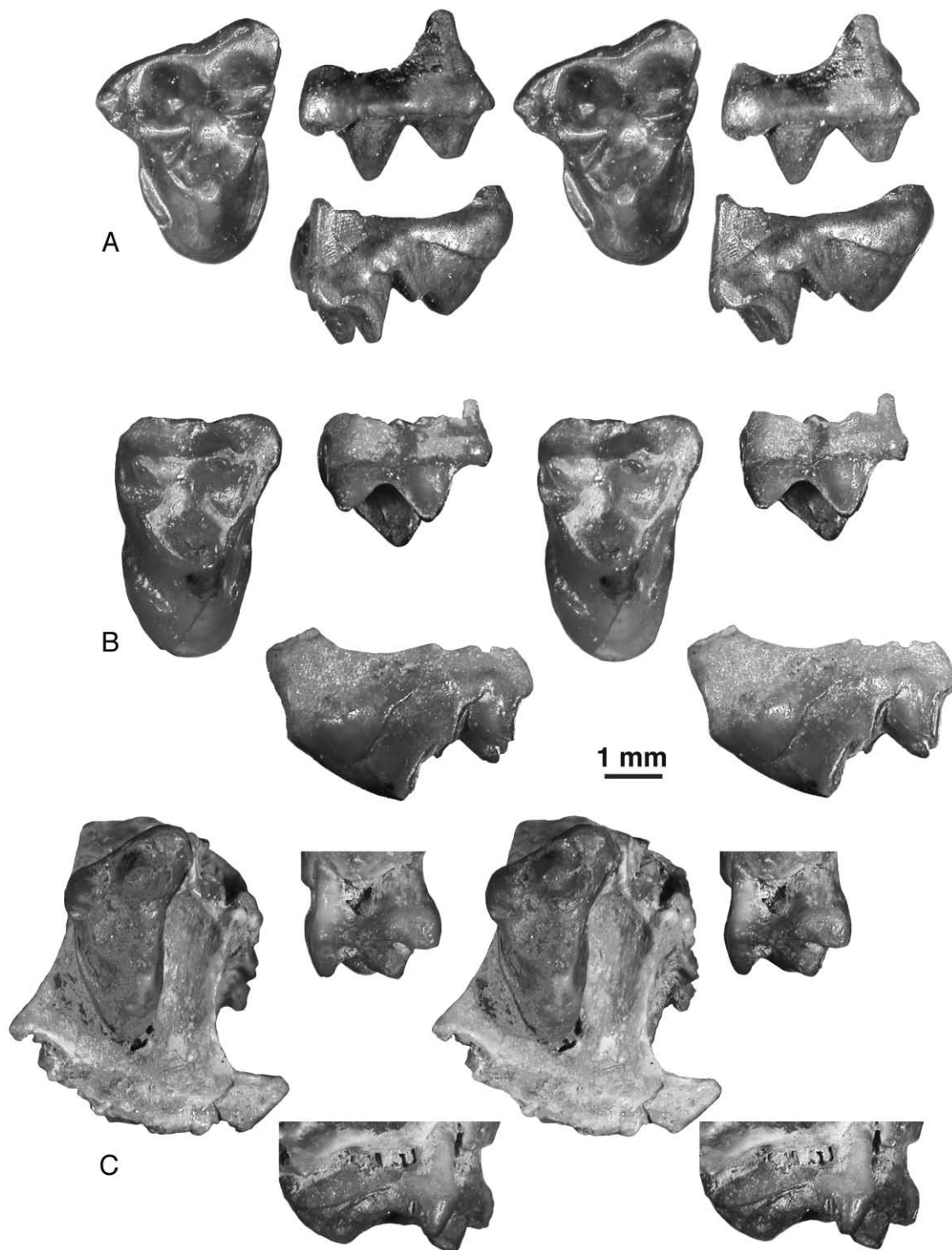


**Figure 19.** *Parazhelestes robustus*, stereophotographs of CCMGE 20/12953, left M1. A, occlusal, labial, and distal views; URBAC 99–13, right M2 with small part of metastylar lobe missing; B, occlusal, labial, and distal views; URBAC 98–22, right maxillary fragment with M2 partial alveoli and M3; C, occlusal, labial, and distal views.

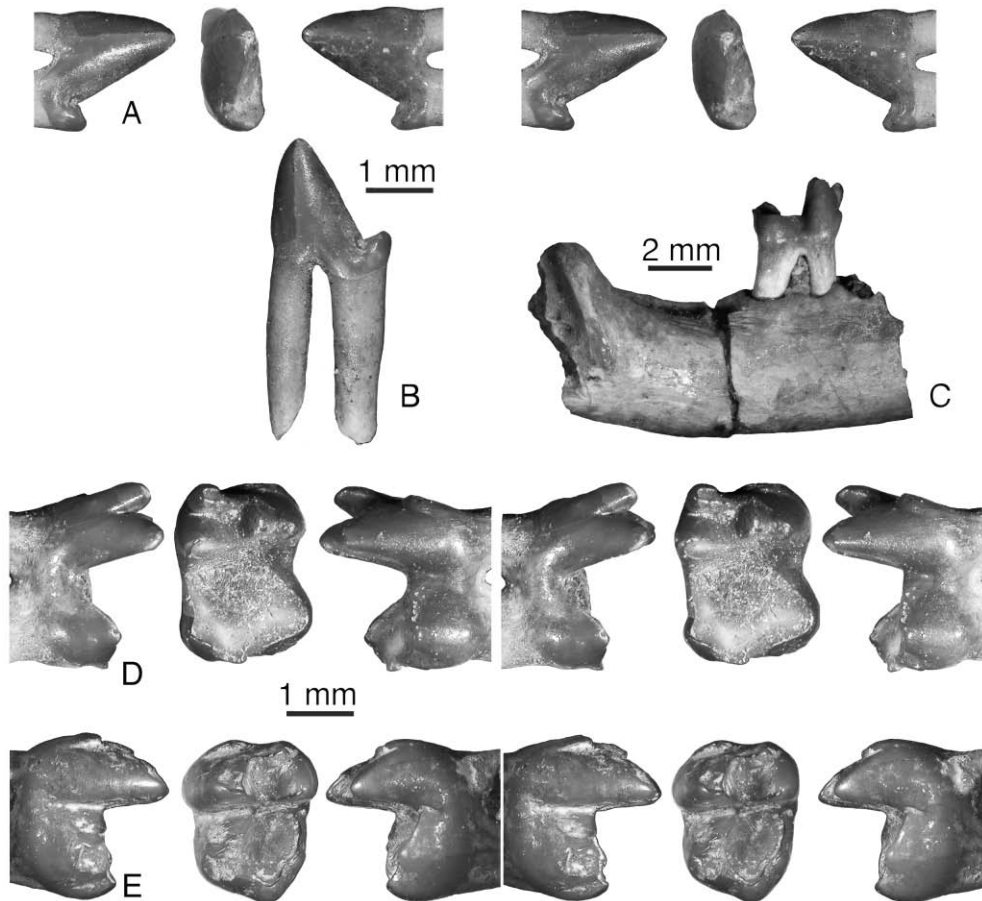


**Figure 20.** *Parazhelestes robustus*, URBAC 04–324, left p2, A, stereophotographs of labial, occlusal, and lingual views, and B, photograph in labial view showing roots; URBAC 97–05, right dentary fragment with m1 and 3 alveoli, and m2; C, photograph of dentary in labial view and D, m2 in lingual, occlusal, and labial views; URBAC 03–38, left m3, E, labial, occlusal, and lingual views.

*Description:* The morphology of DP5 is the same as in other zhelestids and in size it is most similar to DP5s of *P. mynbulakensis*. There are three crenulations on the ectocingulum, the smallest one in the position of cusp E, the middle one in the position of cusp C, and the largest one mesial to the latter. For a more detailed description of the tooth see Averianov & Archibald (2003: 179–180). The latter description is incorrect in regard to the preparacrista and stylocone: in ZIN 85293 the preparacrista is absent through wear and the stylocone was most probably absent (this area of the ectocingulum is chipped).

For description of M3 see Averianov & Archibald (2003: 181). This tooth is distinctly smaller than the isolated M3 URBAC 03–179 referred to *P. mynbulakensis* and approximates the size of this tooth in the holotype maxilla of *P. robustus*. The fragmented M3 ZIN 85295 differs from the previous specimen in having a small stylocone, and possibly in having a relatively longer parastylar lobe.

*Measurements:* See Appendix 2.

*Comments:* There are possibly two species of *Parazhelestes* in the Aitym local fauna, which differ in size, as in the Bissekty local fauna. Whether or not they are conspecific with the Bissekty species is not clear.

#### ZHELESTES NESOV, 1985A

*Cretahomunculus* [nomen nudum]: Nesov & Golovneva, 1983: 131.

*Kumsuperus* [nomen dubium]: Nesov, 1984: 62.

*Sorlestes*: Nesov, 1985a: 14.

*Zhelestes*: Nesov, 1985a: 16.

*Type species:* *Zhelestes temirkazyk* Nesov, 1985a.

*Included species:* Type species only.

*Diagnosis:* As for the type species.

*Distribution:* Uzbekistan; Late Cretaceous (Turonian).

*Comments:* *Sorlestes budan* and *Zhelestes temirkazyk* were described in the same paper by Nesov (1985a) where the former has a page priority. *Kumsuperus avus* was established a year earlier (Nesov, 1984), but it is based on an inadequate specimen (CCMGE 13/11758), a dentary fragment with extremely worn m1–3 that lack diagnostic features. We consider *Kumsuperus avus* Nesov, 1984 to be a nomen dubium. By the principle of the first reviser (ICZN Article 24.2) we choose the name *Zhelestes temirkazyk* Nesov, 1985a as a senior objective synonym for the name *Sorlestes budan* Nesov, 1985a, as it is based on a more diagnostic specimen (maxilla with dentition) rather than a dentary fragment with a not particularly diagnostic lower molar. Additionally, the loss of the nominal genus for Zhelestidae would create unnecessary confusion in the systematic literature.

#### ZHELESTES TEMIRKAZYK NESOV, 1985A

##### FIGURES 21–23

(See Appendix 4 for synonymies, referred illustrations, and referred specimens.)

*Holotype:* CCMGE 10/12176, left maxilla with heavily worn P2, P3 (now broken), P4–5, M1–3 and alveoli for C, P1. Found in 1980.

*Type locality and horizon:* CBI-17, Dzharakuduk, Kyzylkum Desert, Uzbekistan. Bissekty Formation, Upper Cretaceous (middle–upper Turonian).

*Revised diagnosis:* Differs from *Aspanlestes* and *Parazhelestes* by upper and lower canine single-rooted; mandibular condyle above alveolar level; p5 paraconid cingulid cusp or absent. Differs from *Aspanlestes*, *Parazhelestes*, and *Eoungulatum* by diastema between upper canine and premolars present; diastema posterior to P1 present; P3 single-rooted. Differs from *Parazhelestes* and *Eoungulatum* by protocone labial shift absent. Differs from *Parazhelestes* by mandibular symphysis at p3 or more posterior; trigonid angle between 36–49°. Differs from *Eoungulatum* by P5 protocone smaller than paracone; P5 metacone swelling; P5 para- and metastylar lobes subequal; upper molar preparastyle present; metacone slightly smaller than paracone; ‘coronoid’ facet absent; masseteric fossa bordered ventrally by well-defined crest connected to condyle; m3 subequal to larger than m2.

*Description:* Maxilla. The maxilla is almost completely preserved in the type specimen (Fig. 21). In structure it is quite similar to the maxilla URBAC

02–45 of *Aspanlestes* (Fig. 6, see description above), and preserves a more complete palatal process. The proportions are somewhat different, which may be related to size differences between the specimens. The facial process is relatively shorter and higher; it is highest above P4 (Fig. 21A). Its anterodorsal corner is inflated and has a large hole for the canine root. In *Aspanlestes* there is no such inflation. A thin anterior projection of the facial process, covering the canine laterally and present in URBAC 02–45, is not preserved in CCMGE 10/12176. Dorsal to the broken area an intact bone edge is preserved, suggesting that at least part of the lateral alveolus for the canine was formed by the premaxilla. The infraorbital foramen is placed higher and relatively further backward compared with URBAC 02–45, above the distal root of P4. The palatal process is quite narrow (widest at the level of P4) and slightly convex ventrally. The anterior end of the palatal process projects anteriorly beyond the canine alveolus, as in *Aspanlestes*. The intermaxillary suture is straight. The maxillo-palatine suture extends from a level between P4 and P5 to the posterior end of the bone. Here the medial border of the palatal process is convex and approximates the molar’s alveoli. The jugal facet is wide posteriorly and tapers anteriorly to the level between P4 and P5. Its widest part is between M2 and M3 (above M3 in *Aspanlestes*). The lacrimal facet is not discernible.

*Upper dentition.* The upper canine is not known, but judging from its alveolus in the holotype maxilla it was large, single-rooted, and quite curved throughout its length. The anterior premolars or their alveoli are known only from the type specimen, representing a quite old individual. The P1 was mesiodistally aligned with other premolars. The alveolus for its mesial root is more than twice as small as the alveolus for the distal root and confluent with the canine alveolus. In Nesov *et al.* (1998: fig. 10) P1 was reconstructed as single-rooted, but we think that it more likely had two roots. The P2 is a relatively large conical tooth with two roots and without distinct accessory basal cusps. P3 is small, peg-like, and single-rooted; the crown is now missing but can be seen in previous photos (e.g. Nesov *et al.*, 1998: fig. 9A). P3 is separated by a small diastema from P2 and by a twice longer diastema from P4. The posterior upper premolars and molars are heavily worn in all known specimens. The structure of P4–5 is essentially the same as in *Parazhelestes*. In an isolated P4 URBAC 98–117 there is a better-developed anterior accessory cusp. The upper molars are similar to those of *Parazhelestes* in morphology, but differ in proportions: they are relatively wider labiolingually and more mesiodistally constricted at the centre. In M2 URBAC 02–81 there are some crenulations on the

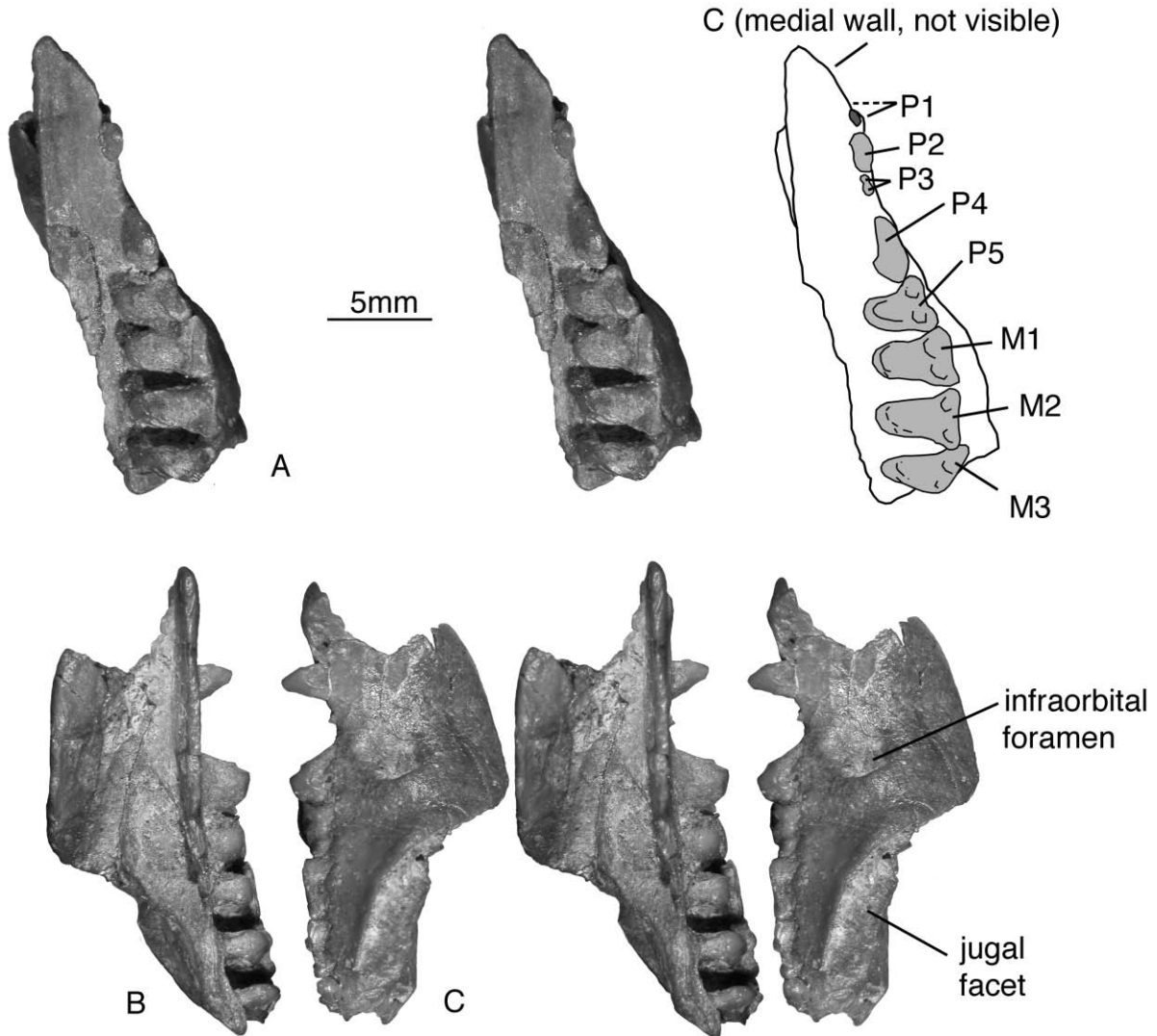


**Figure 21.** *Zhelestes temirkazyk*, CCMGE 10/12176 (holotype), left maxilla with heavily worn P2, P3 (now broken), P4–5, M1–3 and alveoli for C, P1, stereophotographs of A, occlusal; B, labial; and C, lingual views.

ectocingulum. The M3 is as wide labiolingually as M2 (narrower than M2 in *P. robustus*).

**Dentary.** There are two anterior mental foramina: one is at the anterior end of the canine alveolus, just beneath the i4 alveolus, another is under the mesial root of p1 (CCMGE 3/11658, ZIN 88480). The posterior mental foramen is under the distal root of p5 (ZIN 88480). The masseteric crest is strong and there are multiple labial mandibular foramina (ZIN 88453, 88461, and other specimens). The mandibular symphysis is quite long, with the posterior end at the level between the roots of p2 (juvenile specimen ZIN 88469), or between p2 and p3 (adult specimen ZIN 88480). The Meckelian groove is absent (ZIN 88461). In the juvenile specimen ZIN 88469 the angular and part of the condylar processes are preserved (Fig. 22A). The

condyle was probably not fully ossified and was placed significantly above the alveolar level. The angular process is constructed as in *Aspanlestes* and *P. mynbulakensis* with only a slight lingual inflection.

**Lower dentition.** In a young specimen, CCMGE 3/11658, with an erupting canine (Fig. 22B), there are alveoli for four incisors, with i3 largest and i4 smallest. In an older edentulous dentary ZIN 88480, the alveoli for i1–3 are similar in size and the alveolus for i4 is much smaller and confined within the canine alveolus. The lower canine was large and single-rooted (ZIN 88480). CCMGE 3/11658 preserves the crown of the erupting lower canine (Fig. 22B).

Judging from alveoli in edentulous dentaries (e.g. ZIN 88461 and 88480), p1 and p3 were double-rooted and smaller than p2, but not as reduced as in

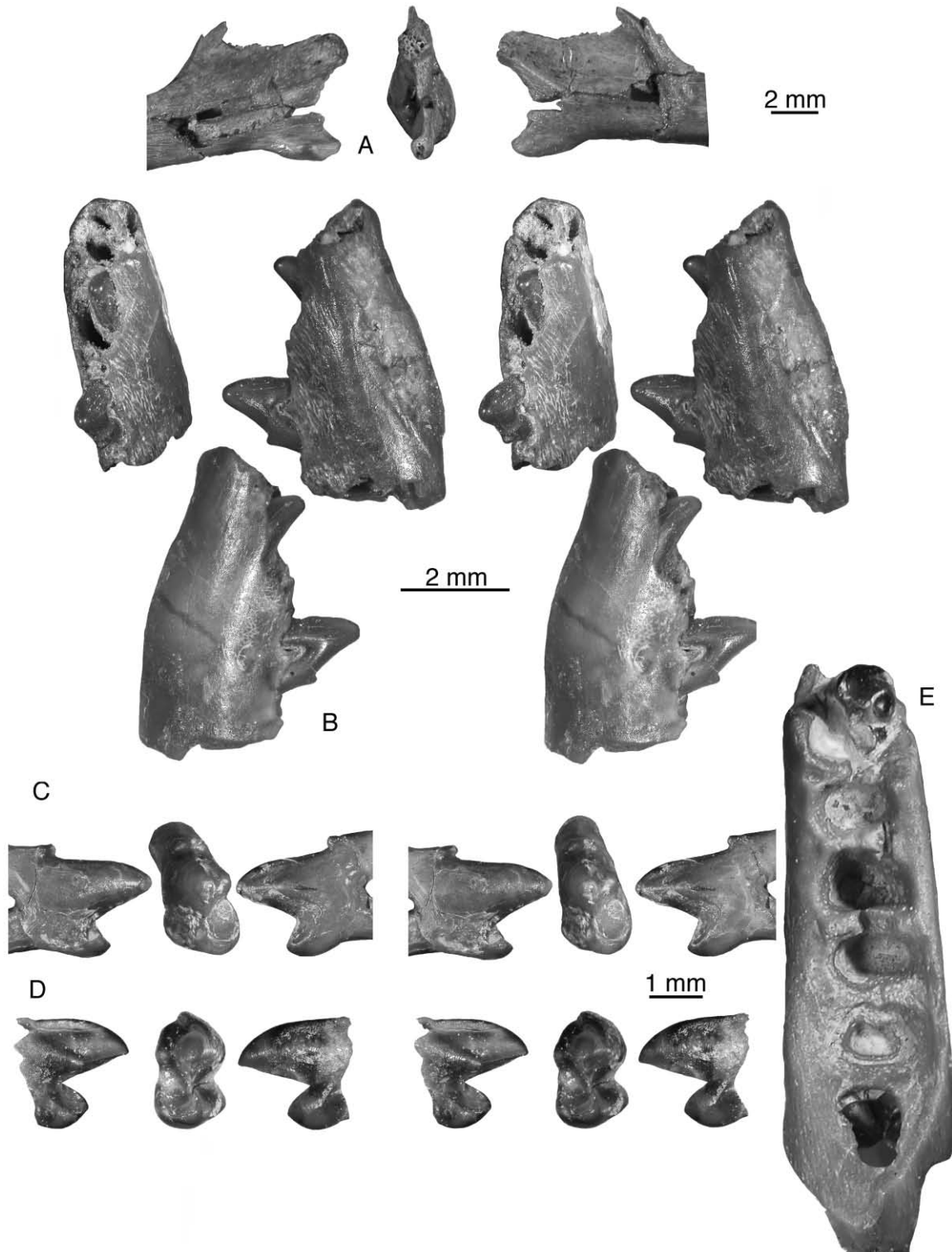


**Figure 22.** *Zhelestes temirkazyk*, ZIN 88469, photograph of posterior of damaged edentulous dentary preserving the angular and part of the condylar processes, A, lingual, posterior, and labial views; stereograph of CCMGE 3/11658, i1–4 alveoli, erupting canine, dc alveolus, p1 alveolus, p2, B, anterocclusal, lingual, and labial views (see also Fig. 28D); stereograph of CCMGE 2/12953, left p5, C, labial, occlusal, and lingual views; stereograph of URBAC 03–218, erupting right p5 with roots unformed, D, lingual, occlusal, and labial views (see also Fig. 28J); photograph of ZIN 88448, erupting p5, m1–2 alveoli, unerupted m3, E, occlusal view.

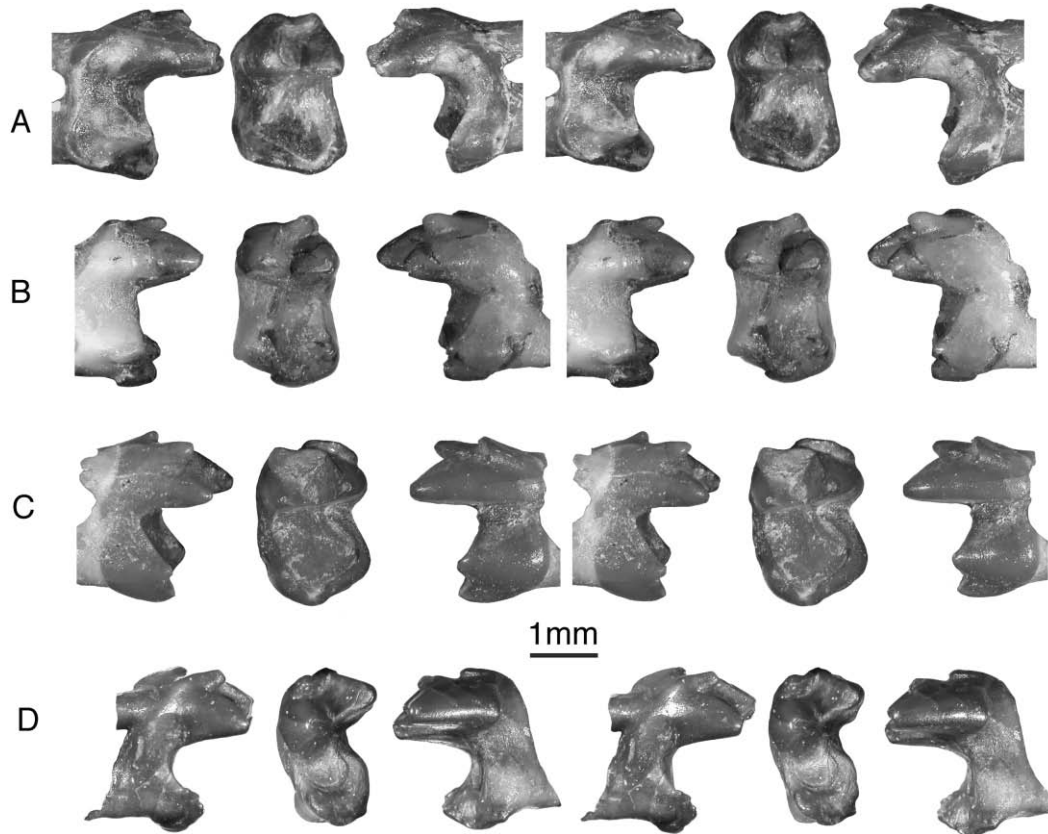


**Figure 23.** *Zhelestes temirkazyk*, stereophotographs of CCMGE 37/12000, left m1, A, labial, occlusal, and lingual views; URBAC 04-190, worn left m1?, B, labial, occlusal, and lingual views; URBAC 04-309, right m2, C, lingual, occlusal, and labial views; CCMGE 3/12953, worn right m3, D, lingual, occlusal, and labial views.

*Parazhelestes*. In ZIN 88461 there is a relatively large diastema between p2 and p3.

The p2 is known from a dentary fragment CCMGE 3/11658 (Fig. 22B). The central cusp is conical and slightly turned distally. There are no mesial accessory cusps and only a small distal accessory cusp. The roots are swollen and spread apart. It is possible that this tooth could be a dp2 because the canine in this dentary fragment is at the initial stage of erupting. An unerupted crown of p2 is also present in ZIN 82555.

The p5 is known from three specimens, the isolated tooth CCMGE 2/12953 and unerupted crowns in dentary fragments URBAC 03-218 and ZIN 88448 (Fig. 22C–E). CCMGE 2/12953 is unique amongst p5s of Dzharakuduk's zhelestids in having a very small, cingulid paraconid, which is placed very low on the crown. It is not preserved and may not have been present on the two other p5s, where this portion of the crown was not fully formed and is now missing. A cingulid-like paraconid on p5 may have been a consistent feature of *Zhelestes*, whereas in *P. mynbulakensis* it is a trigonid cusp. In this character *Zhelestes*

is very similar to *Borisodon*. The p5 of *Zhelestes* is clearly distinct from that tooth in *Borisodon* in having a metaconid, present in all three known specimens. The small talonid basin lingual to the talonid ridge is somewhat more expanded than in *Borisodon*. In URBAC 03-218 there is a small second talonid cusp, the entoconid (absent in CCMGE 2/12953; in ZIN 88448 this part of the crown is missing). In CCMGE 2/12953 there is a well-developed, distolabial cingulid.

The lower molars of *Zhelestes* are similar to those of other Dzharakuduk zhelestids, but differ from the lower molars of *Parazhelestes* in having a larger trigonid angle, which is presumably correlated to mesio-distally narrower upper molars in *Zhelestes* compared to *Parazhelestes*. The best-preserved m1 is CCMGE 37/12000 (Fig. 23A). The trigonid angle is slightly greater than that in m2 and m3. The paraconid is more labially shifted than in m2 or m3, and is smaller than this cusp in m2 but larger than in m3. The precingulid is ridge-like, as in *P. mynbulakensis*.

The m2 trigonid has a lesser angle than m1 or m3, whereas the paraconid is the larger and more lingually placed. The sample of m2s is more numerous

than for other lower molars and shows more variation. The most variable structures are the precingulid and postcingulid. The labial cingulid is complete, connecting the precingulid and the postcingulid in URBAC 98–15; very short, confined to the hypoflexid area in URBAC 06–26; or absent in other specimens. URBAC 04–309 has the best-developed precingulid amongst the sample, but the postcingulid is totally lacking in this specimen (Fig. 23B). The postcingulid is the strongest in URBAC 02–35 and 02–65.

There are two unerupted m3s represented by two unerupted crowns in dentary fragments (URBAC 03–218, ZIN 88448; Fig. 22E). The m3 is best known from an isolated and worn specimen CCMGE 3/12953 (Fig. 23D). The trigonid is constructed as in m1 except that the paraconid is even smaller. The precingulid is quite small. The talonid is longer and narrower than the trigonid. The talonid is quite damaged so was probably originally somewhat wider. All three talonid cusps are similar in size. The hypoconulid is about equidistant from the hypoconid and the entoconid.

*Measurements:* See Appendices 2 and 3.

*EOUNGULATUM* NESOV, ARCHIBALD &  
KIELAN-JAWOROWSKA, 1998

*Eoungulatum:* Nesov *et al.*, 1998: 58.

*Type species:* *Eoungulatum kudukensis* Nesov *et al.*, 1998.

*Included species:* Type species and *Eoungulatum* sp.

*Diagnosis:* As for the type species.

*Distribution:* Uzbekistan; Late Cretaceous (Turonian–?Coniacian).

*EOUNGULATUM KUDUKENSIS* NESOV, ARCHIBALD  
& KIELAN-JAWOROWSKA, 1998

FIGURES 24–25

(See Appendix 4 for synonymies, referred illustrations, and referred specimens.)

*Holotype:* CCMGE 2/12455, left M1. Found in 1989.

*Type locality and horizon:* CBI-14, Dzharakuduk, Kyzylkum Desert, Uzbekistan. Bissekty Formation, Upper Cretaceous (middle–upper Turonian).

*Revised diagnosis:* Differs from *Aspanlestes* and *Parazhelestes* by upper and lower canine single-rooted. Differs from *Aspanlestes* and *Zhelestes* by P1

double-rooted; protocone labial shift present. Differs from *Zhelestes* by diastema between upper canine and premolars absent; diastema posterior to P1 absent; P3 double-rooted. Differs from *Aspanlestes*, *Parazhelestes*, and *Zhelestes* by P5 protocone approaching paracone in height; P5 metacone large; P5 parastylar lobe larger than metastylar lobe; upper molar preparastyle absent; metacone subequal to larger than paracone; masseteric fossa extends to ventral margin of dentary; m3 smaller than m2. Differs from *Parazhelestes* by mandibular symphysis at p3 or more posterior.

*Referred specimens:* URBAC 02–60, left maxilla with alveoli for C, P1–3 (CBI-4e); URBAC 99–42, right maxilla with alveoli for P4–5, M1–3 (CBI-14); URBAC 03–60, right P5 (CBI-14); URBAC 03–185, left M1 (CBI-4e); ZIN 85055, left MX, very worn; URBAC 99–6, right dentary with alveoli for i1–4, single-rooted c, p1–5, m1–3 (CBI-14); CCMGE 15/12953, left dentary with single-rooted c, p4, and alveoli for two incisors and p1–3 (CBI-14, 1984); ZIN 88459, right dentary with alveoli for c, p1–2 (CBI-14, 1984); CCMGE 23/12953, right dentary with alveoli for c, p1–5, m1–3 (CBI-14, 1989); URBAC 00–12, left dentary with p4 and alveoli for c, p1–3, and p5 (CBI-4e); ZIN 88464, left dentary with alveoli for c, p1–4 (CBI-14, 1989); URBAC 04–80, left dentary with alveoli for c, p1–4 (CBI-14); ZIN 88460, right dentary with alveoli for c, p1–5 (CBI-4v, 1979); ZIN 88452, right dentary with m3 trigonid in crypt and alveoli for m1–2 (CBI-14, 1993); ZIN 88471, left dentary with roots of m2–3 (CBI-14, 1993); URBAC 02–25, left dentary with worn m2 and alveoli for m3 (CBI-4e); CCMGE 17/12953, right m1 (CBI-14); URBAC 00–46, left m2 (CBI-14); URBAC 00–49, right m2 (CBI-14); URBAC 04–88, left m2 trigonid (CBI-14); URBAC 06–42, left m2 (CBI-14); URBAC 04–135, right m1 or m2 heavily worn (CBI-14); CCMGE 16/12953, left m3 (CBI-14, 1984); CCMGE 18/12953, left m3 (CBI-14); URBAC 04–74, right m3 lacking lingual part of trigonid and heavily worn (CBI-14); URBAC 04–119, left m3, heavily worn (CBI-14).

*Description:* Maxilla. There are two maxillary fragments referable to *Eoungulatum*. URBAC 02–60 is an anterior maxillary fragment, with inflated facial process accommodating a large canine root. The root is subdivided on the labial side by a distinct vertical ridge. The lateral margin of the maxilla is concave. The alveoli for double-rooted p1–3 are closely spaced, with the alveoli for p1 set obliquely to the tooth row. The P2 is about twice as large as P1 and P3. Unfortunately, URBAC 02–60 was badly damaged before it could be photographed. URBAC 99–42 is a posterior

maxillary fragment with alveoli for P5, M1–2, and part of M3 (Fig. 24A). The shape of the zygomatic process and jugal facet are different from those in *Zhelestes* and other Dzharakuduk zhelestids in that they appear to extend only as far anteriorly as M2. The alveoli for M3 are as wide labiolingually as those for M2, a feature not found in other zhelestids.

Upper dentition. URBAC 03–60 is the largest and most molariform amongst the zhelestid P5s from Dzharakuduk (Fig. 24B). Compared to P5 of *P. robustus*, URBAC 03–60, the labial portion is relatively longer mesiodistally mostly because of a greatly expanded parastylar lobe. The ectocingulum is well defined, with a cuspule in D position. The metacone is about twice as small as the paracone and mostly separated from the latter. The preparacrista is straight and directed towards the parastyle. The area on the parastylar lobe lingual to the preprotocrista is heavily worn. The postmetacrista is curved. The protocone is placed mesially relative to the condition in *P. robustus*, slightly mesial to the level of the paracone. It is almost as high as the paracone. Both protocone cristae are considerably worn. The preprotocrista is the shorter of the two. The postprotocrista terminates below (dorsal to) the metacone base, some distance before the postmetacrista. There is a ridge connecting the protocone apex with the base of the paracone. The pre- and postcingulum are well developed and extend on the lingual side of the protocone but do not coalesce.

Only two M1s are known of the upper molars. For description of the holotype specimen CCMGE 2/12455 see Nesov *et al.* (1998: 58–59; misidentified there as M2). The newly collected specimen URBAC 03–185 (Fig. 24C) is quite similar in morphology to the holotype but differs in some details. The ectocingulum is more pronounced. The ectoflexus is concave at the paracone but convex at the metacone (more evenly concave on the holotype). The parastylar lobe is wider labiolingually than on the holotype, with a more developed wear facet. The protocone seems to be more lingual in position, which may be at least partially attributed to the greater dental wear of this specimen. The lingual cingulum is well developed and almost complete, interrupted for a short distance mesiolingual to the protocone apex. All these differences are interpreted as individual variation.

Dentary. The dentary is known from two quite complete horizontal rami (CCMGE 23/12953: Nesov *et al.*, 1998: fig. 19A,C; URBAC 99–6: Fig. 25A) and several fragments. There is no Meckelian groove. The posterior end of the mandibular symphysis is under p2 (CCMGE 23/12953), between p3 and p4 (URBAC 99–6), or under p4 (URBAC 04–80). In URBAC 99–6 the anterior mental foramen is quite large and placed between c and p1, close to the alveolar margin and

continuing anteriorly into a groove extending around the whole canine alveolus. In ZIN 88459 this foramen is even larger and placed under the mesial root of p2. In CCMGE 15/12953 and ZIN 88464 there are two anterior mental foramina, one under the canine and another under the p1 distal root (CCMGE 15/12953) or p2 mesial root (ZIN 88464). The posterior mental foramen is between p4 and p5 (URBAC 99–6) or under the anterior root of p5 (CCMGE 23/12953, URBAC 00–12). There is a deep pocket of the masseteric fossa under the coronoid crest. In both CCMGE 23/12953 and URBAC 99–6 there appears to be a single large labial mandibular foramen. In contrast with other zhelestids, the ventral border of the masseteric fossa is represented by a faint ridge approximating the ventral border of the dentary (CCMGE 23/12953). In both CCMGE 23/12953 and URBAC 99–6 there is a slight tuberosity at the position of the ‘coronoid facet’. In ZIN 88452 there is a horizontally placed trigonid of an unerupted m3 in the crypt.

Lower dentition. The anterior end of dentary is preserved in URBAC 99–6 (Fig. 25A). There are multiple but indeterminable numbers of incisor alveoli, a single canine alveolus, and double alveoli for p1–5, m1–3. In CCMGE 15/12953 there are alveoli for only two incisors preserved. CCMGE 15/12953, having a considerably worn p4, represents an individual distinctly older than URBAC 99–6, suggesting that some incisors might be lost during ontogeny.

The lower canine is preserved in CCMGE 15/12953 (Nesov *et al.*, 1998: fig. 19D–F). The canine is single-rooted and quite large. It is wide at the base, with a strongly convex anterior side and slightly concave posterior side. The crown is laterally compressed.

The alveoli for a double-rooted p1 are placed somewhat obliquely and crowded with alveoli of other teeth in the immature specimens URBAC 99–6 and CCMGE 23/12953 (in Nesov *et al.*, 1998: fig. 19A they are incorrectly shown within the canine alveolus). In an older specimen, ZIN 88459, the alveoli for p1 are aligned with the tooth row and separated by diastemata from c and p2. In ZIN 88464, p1 seems to be single-rooted.

The p3 is double-rooted and distinctly smaller than p2. In ZIN 88459, representing an old individual, p3 may be missing as there is a long diastema posterior to the p2 alveoli.

The p4 is known from two specimens (CCMGE 15/12953: Nesov *et al.*, 1998: fig. 19D–F; and URBAC 00–12: Fig. 25B); it is distinctly larger in CCMGE 15/12953. There is no mesial accessory cusp and the conical central cusp is mesially placed, mostly above the mesial root. There is a distinct distal heel surrounded by a distal cingulid, but no distal accessory cusp. In URBAC 00–12 there is a distal crest connecting the central cusp with the distal cingulid.

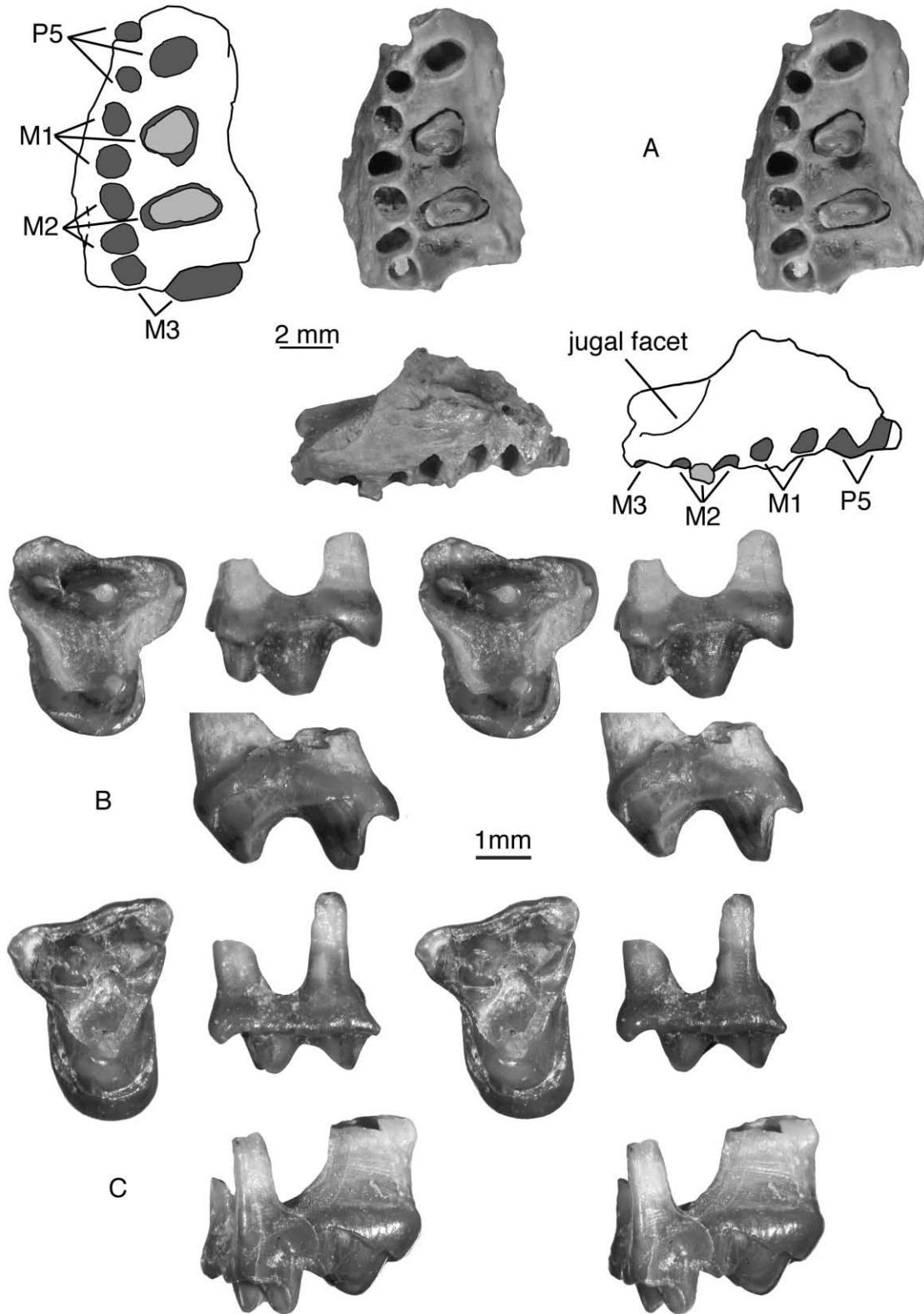


**Figure 24.** *Eoungulatum kudukensis*, URBAC 99–42, right maxillary fragment with alveoli for P5, M1–3, A, stereophotograph and line drawing in occlusal view, and photograph and line drawing in labial view; URBAC 03–60, right P5, B, stereophotographs of occlusal, labial, and distal views; URBAC 03–185, left M1, C, stereophotographs of occlusal, labial, and distal views.

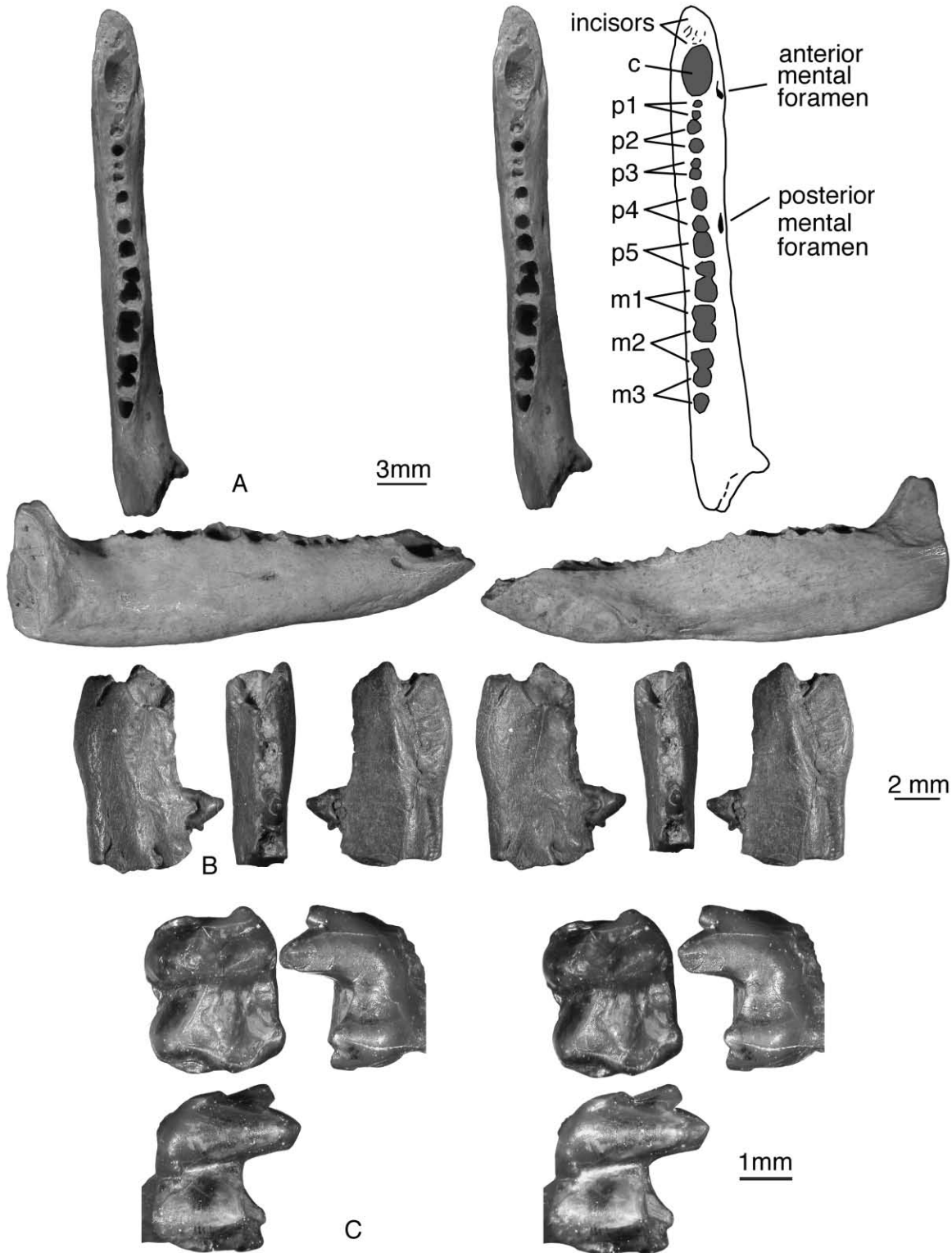


**Figure 25.** *Eoungulatum kudukensis*, URBAC 99-6, right edentulous right dentary with multiple but undetermined number of incisor alveoli, single canine alveolus, and double alveoli for p1-5, m1-3, A, stereophotograph and line drawing of occlusal view, and photographs of labial and lingual views; stereophotographs and line drawing, URBAC 00-12, dentary with c, p1-3, p5 alveoli, and p4, B, labial, occlusal, and lingual views; stereophotographs, URBAC 06-42, left m2, C, occlusal, lingual, and labial views.

Unfortunately, p5 is not known for *Eoungulatum*.

The only known m1 of *Eoungulatum* is CCMGE 17/12953 (Nesov *et al.*, 1998: fig. 14 K–O; identified there as m2). The paraconid is more reduced and more labially placed compared with m2. The metaconid and the protoconid are of similar height, although the protoconid is more worn. There is a strong precingulid. The talonid is wider than the trigonid. There is heavy wear on the hypoconid, cristid oblique, and the postcristid. The cristid obliqua is directed towards the protocristid notch. The hypoconulid closely approximates the entoconid. The postcingulid is faint.

There are five m2s of *Eoungulatum*. On less worn teeth the protoconid is somewhat higher than the metaconid. The postcingulid is more variable than the precingulid, being strongest in URBAC 06–42 (Fig. 25C) and weakest in URBAC 00–49. In URBAC 06–42 there is a short labial cingulid within the hypoflexid (Fig. 25C).

The m3 is known from four isolated teeth, two of which were described by Nesov *et al.* (1998: 59, fig. 14F–J), and two other specimens that are quite worn. The trigonid is as in m2. In the unworn CCMGE 16/12953 the protoconid and the metaconid are of the same height. The talonid is as wide as or narrower than the trigonid. The hypoconulid is larger than the entoconid and equidistant from other talonid cusps. The postcingulid is variably developed.

*Measurements:* See Appendices 2 and 3.

*Comments:* *Eoungulatum* is the largest recognized zhelestid in the Bissekty local fauna but appears not to be the largest mammal there. ZIN 88458 represents an edentulous dentary fragment with alveoli for p5 and m1 (a small posterior mental foramen is below the distal root of p5), which is markedly larger than *Eoungulatum*. It is not certain if this specimen belongs to a larger, as yet unknown zhelestid or to another mammal.

In a previous publication (Archibald & Averianov, 2005), we suggested that *Eoungulatum* was synonymous with *Parazhelestes robustus*. On further analysis and with the recovery of more specimens, this now appears less likely; thus *Eoungulatum* is retained.

#### *EOUNGULATUM* SP.

(See Appendix 4 for synonymies, referred illustrations, and referred specimens.)

*Locality and horizon:* CDZH-117, Dzharakuduk, Kyzylkum Desert, Uzbekistan. Aitym Formation, Upper Cretaceous (upper Turonian–Coniacian?).

*Description:* See Averianov & Archibald (2003: 183).

*Measurements:* See Appendix 3.

*Comments:* The specimen is distinctly larger than m3 of *P. robustus* from the Bissekty local fauna at Dzharakuduk and agrees well in size and morphology, especially in the swollen crown, with m3s of *E. kudukensis* from that fauna, documenting the presence of an *Eoungulatum*-like zhelestid in the younger Aitym local fauna.

#### ZHELESTIDAE INCERTAE SEDIS

*SHEIKHDZHEILIA* AVERIANOV & ARCHIBALD, 2005

*Sheikhdzheilia:* Averianov & Archibald, 2005: 599.

*Type species:* *Sheikhdzheilia rezvyii* Averianov & Archibald, 2005.

*Included species:* Type species only.

*Diagnosis:* As for the type species.

*Distribution:* Uzbekistan; Late Cretaceous (Cenomanian).

#### *SHEIKHDZHEILIA REZVYII* AVERIANOV & ARCHIBALD, 2005

(See Appendix 4 for synonymies, referred illustrations, and referred specimens.)

*Holotype:* ZIN 88438, right dentary fragment with p5, m1, talonid of m2, and alveoli for p4 and m3. Found in 2003 from concentrate obtained in 1998.

*Type locality and horizon:* SSHD-8, Sheikhdzheili, Kyzylkum Desert, Uzbekistan. Upper part of Khodzhakul Formation, Upper Cretaceous (early Cenomanian).

*Revised diagnosis:* Differs from other zhelestids by having a deep ectoflexus; styler cusp B (stylocone) small but distinct; lingual cingula on upper molars absent. Differs from other zhelestids except *Lainodon* by protoconid tallest cusp on trigonid; labial postcingulid absent. Differs from other zhelestids except *Eoungulatum* by preparastyle absent. Differs from other zhelestids except *Lainodon* and *Avitotherium* by protocristid oblique. Differs from *Avitotherium*, *Lainodon*, and *Gallolestes* by paraconid not on lingual margin. Differs from *Avitotherium*, *Gallolestes*, and *Parazhelestes* by trigonid angle between 36–49°. Differs from *Aspanlestes*, *Parazhelestes*, and *Zhelestes* by p5 metaconid absent; p5 lingual cingulid complete.

Differs from *Aspanlestes* and *Parazhelestes* by p5 paraconid cingulid cusp absent. Differs from *Parazhelestes* and *Eoungulatum* by protocone not labially shifted.

*Description:* See Averianov & Archibald (2005: 600–601).

*Measurements:* See Averianov & Archibald (2005: 600–601).

#### **BORISODON GEN. NOV.**

*Etymology:* Named after our irascible colleague and very good friend, the late Boris Gregorievich Veretenikov of Tashkent, Uzbekistan.

*Type species:* *Sorlestes kara* Nesov, 1993.

*Included species:* Type species only.

*Diagnosis:* As for the type species.

*Distribution:* Kazakhstan; Late Cretaceous (Turonian).

#### *BORISODON KARA* (NESOV, 1993)

##### FIGURE 26

(See Appendix 4 for synonymies, referred illustrations, and referred specimens.)

*Holotype:* CCMGE 106/12455, right dentary with p5, m1–3, alveoli for p2–4, and coronoid, angular, and condyloid processes. In the original description the collection number was incorrectly indicated as CCMGE 101/12455 (Nesov, 1995: 123). Found in 1988.

*Type locality and horizon:* Near Ashchikol' Lake, Kyzylorda Province, Kazakhstan. Drilling core from about 500 m depth. Grey siltstone of lower Turonian age (Nesov, 1993).

*Diagnosis:* Differs from *Aspanlestes*, *Zhelestes*, *Parazhelestes*, and *Eoungulatum* by tilting of coronoid process 95–105°. Differs from *Aspanlestes*, *Zhelestes*, and *Eoungulatum* by mandibular symphysis at p2 or more anterior. Differs from *Aspanlestes*, *Zhelestes*, and *Parazhelestes* by 'coronoid' facet present; p5 metaconid absent; p5 lingual cingulid complete. Differs from *Zhelestes*, *Parazhelestes*, and *Eoungulatum* by Meckelian groove present. Differs from *Aspanlestes* and *Parazhelestes* by mandibular condyle slightly above alveolar level; p5 paraconid cingulid cusp absent. Differs from *Eoungulatum* by masseteric fossa

bordered ventrally by well-defined crest connected to condyle; m3 subequal or larger than m2.

*Description:* The posterior portion of the dentary horizontal ramus is about 1.5 times higher than the tooth crowns. On the labial side at the mid-height of the horizontal ramus under the p5 distal root there is a large posterior mental foramen, connected to a short groove that becomes shallower posteriorly. On the medial side of the horizontal ramus the posterior end of the mandibular symphysis is at the level between the roots of p2. There is a rather faint Meckelian groove extending between the level of the distal end of m3 and towards the point anteroventrally of the mandibular foramen.

The horizontal ramus gradually continues into the ascending ramus without constriction. The ascending ramus is about three times higher than the horizontal ramus, with a steep anterior border of the coronoid process, sloping at an angle of 75° toward the alveolar margin. The coronoid process, or its impression, was complete before its removal from the encasing matrix; thus, the outline in Figure 26 is quite accurate. It is trapezoidal in shape, with an almost straight anterior margin and a slightly concave posterior margin. The masseteric fossa is very large and deep, extending posteriorly to the condylar process, and bordered anteriorly by a very prominent coronoid crest. It is deepest at the anteroventral corner, where there is a large, slit-like labial mandibular foramen concealed laterally by the coronoid crest. Ventrally the masseteric fossa is bordered by an extensive posterior shelf continuing to the mandibular condyle. The medial side of the coronoid process is flat and slightly depressed along the anterior margin. The mandibular foramen is relatively large, oval-shaped, and faces posteroventrally. It opens above the anterior portion of the angular process, in the posterior half of the ascending ramus.

The mandibular condyle is distinctly above the alveolar level. The condyle is convex and oval-shaped in posterior and dorsal views, with the lateral end more pointed and placed more dorsally compared with the medial end (Fig. 26B–D).

The mandibular angle is a thin triangulate plate somewhat deflected medially. Its anteroventral margin is convex and the posterior margin is concave, forming part of the round incisura between the mandibular angle and condyle.

There are alveoli for double-rooted p2–4 preserved in the anterior portion of the dentary fragment and partially visible laterally because of the broken dentary wall. The alveoli for p4 are approximately the same size as for p5. The anterior alveolus for p2 is incomplete but it seems that this tooth was only slightly shorter than p5. The alveoli for p3 are twice as small as those of p4.

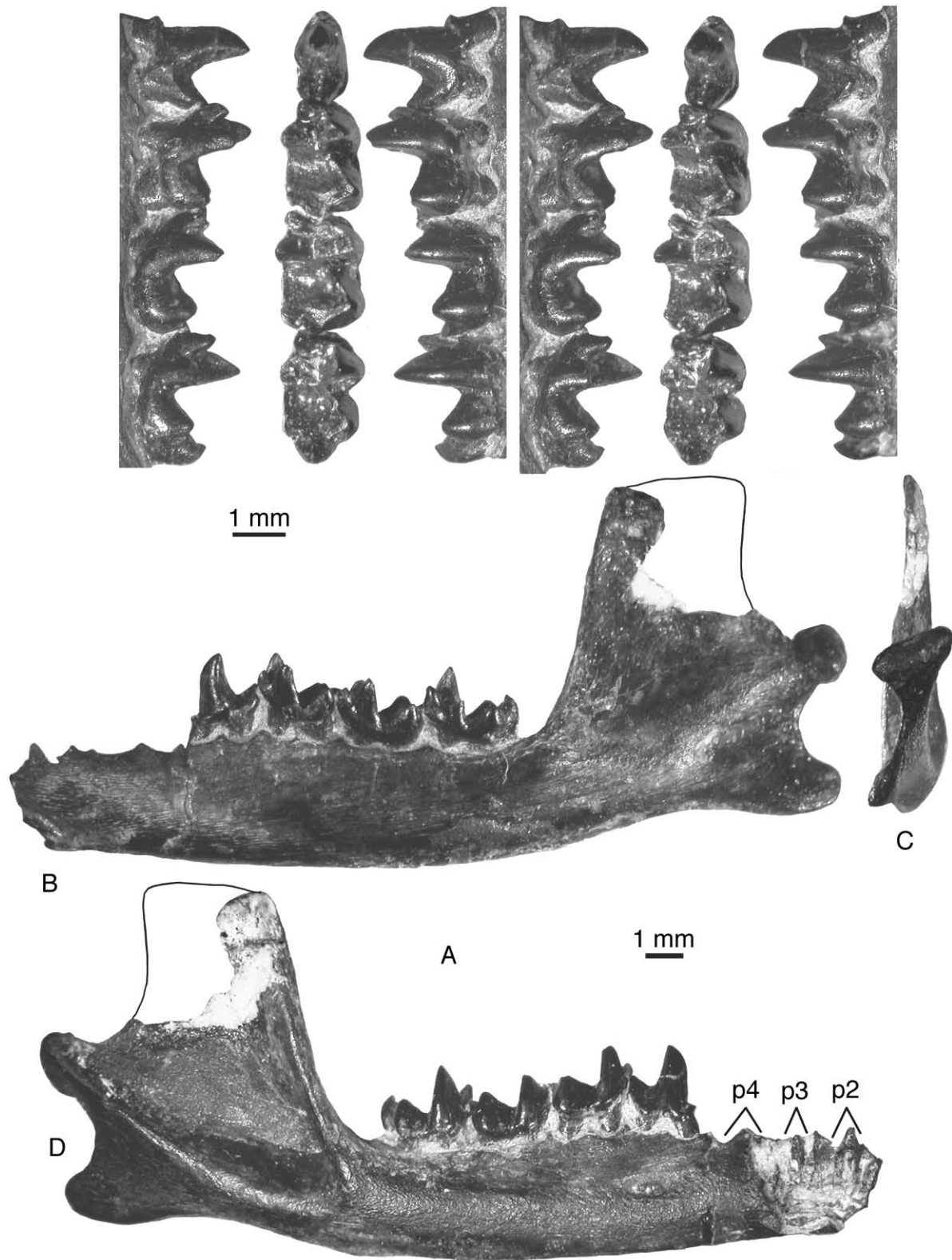


**Figure 26.** *Borisodon kara*, CCMGE 106/12455, right dentary with p2–4 alveoli, p5, m1–3. A, stereophotographs of p5, m1–3 in labial, occlusal, and lingual views. Photographs of dentary, B, lingual; C, posterior; D, lingual views. Line shows reconstruction of ascending ramus based on impression in surrounding matrix.

The p5 is a semimolariform tooth without a metaconid, and with a unicusped talonid with an incipient 'basin'. It is as tall as the molars. The main cusp (protoconid) is distinctly curved, hook-like, with its apex pointed distally. Its mesial margin is a sharp vertical crest. The distal side of the cusp is wide, concave, facing linguodistally, and sloping into the talonid basin. Mesial to the base of the protoconid there is a small triangular platform at the junction of the lingual and labial cingulids and the protoconid mesial crest. This structure could be a cingulid mesial accessory cusp (paraconid). The talonid is formed by a large cusp, reaching half the height of the protoconid, and is pointed dorsodistally. Its mesiolingual side is distinctly concave, forming the incipient talonid basin. The lingual cingulid is continuous, extending from between the mesial end towards the distal point of the talonid cusp. It is elevated above the space between the roots and forms the lingual border of the talonid basin. The labial cingulid is interrupted at the space between the roots and vanishes at the posterior portion of the talonid cusp.

The lower molars are of rather similar morphology. The m2 is the largest and the m1 the smallest. The trigonid is about twice as tall as the talonid on m3 (on m1–2 the protoconid is not complete and could be taller). The metaconid seems to be only slightly lower than the protoconid. The metaconid apex is bent somewhat distally. The paraconid is smaller than the metaconid but still relatively unreduced. It is largest on m3 and smallest on m1. On m3 the paraconid is distinctly taller than the talonid of m2 whereas as in m1–2 the paraconid is confluent with the talonid surface of the preceding tooth. The mesiolingual vertical side of the paraconid forms a keel on all molars. The protocristid is almost straight and transverse. The paracristid is not straight but angled at the paracristid notch. The bases of the paraconid and metaconid are connate lingually, leaving only a slit-like opening into the trigonid basin. The trigonid basin is a small triangular area between the bases of the trigonid cusps. The talonid is distinctly wider than the trigonid on m1, slightly wider on m2, and narrower on m3. The cristid obliqua contacts the trigonid wall at the protocristid notch. The hypoconid is the largest talonid cusp and the entoconid the smallest. The hypoconulid projects distally and is closer to the entoconid but is not twinned with the latter. In m3 the hypoconulid is hook-like and separated by a greater distance from the entoconid than in m1–2. The talonid basin slopes mesiolingually towards its deepest point at the mesial end of the entocristid. The development of the precingulid increases from m1 to m2. It is a short subvertical crest whose

lingual end is abutted against the hypoconulid (or talonid cusp) of the preceding tooth. A very faint postcingulid is present only in m2.

*Measurements:* See Appendix 3.

*LAINODON GHEERBRANT & ASTIBIA, 1994*

*Lainodon:* Gheerbrant & Astibia, 1994: 1126.

*Type species:* *Lainodon orueetxebarriai* Gheerbrant & Astibia, 1994.

*Included species:* Type species only.

*Diagnosis:* As for the type species.

*Distribution:* Spain; Late Cretaceous (Campanian or Maastrichtian).

*LAINODON ORUEETXEBARRIAI GHEERBRANT & ASTIBIA, 1994*

(See Appendix 4 for synonymies, referred illustrations, and referred specimens.)

*Holotype:* L1AT 14, left m2. Identified by Gheerbrant & Astibia (1994, 1999) as m1(?).

*Type locality and horizon:* Laño, Álava Province, Basque Autonomous Community, Spain; unnamed stratigraphical unit, Late Cretaceous (late Campanian or early Maastrichtian).

*Revised diagnosis:* Differs from all zhelestids except *Sheikhdzheilia* with protoconid tallest cusp on trigonid; labial postcingulid absent. Differs from all zhelestids except *Sheikhdzheilia* and *Avitotherium* by protocristid oblique. Differs from all zhelestids except *Avitotherium* and *Gallolestes* by paraconid on lingual margin present. Differs from all zhelestids except *Avitotherium*, *Gallolestes*, and *Parazhelestes* by trigonid angle between 36–49°.

*Description:* See Gheerbrant & Astibia (1999: 297–301, 310–314).

*Measurements:* See Gheerbrant & Astibia (1999: tabs 1–4).

*Comments:* *Lainodon orueetxebarriai* was based on permanent lower molars whereas milk lower premolars from the same site were referred by Gheerbrant & Astibia (1999) to *Lainodon* sp. nov. We see no basis for this assignment. All differences between these 'taxa' noted by Gheerbrant & Astibia (1999) are

differences between permanent molars and deciduous premolars. We refer tentatively to *L. oruuetxebarriai* all therian teeth from the Laño locality, except possibly a tooth L1AT 11 identified as ?*Labes* sp. (Gheerbrant & Astibia, 1999: 314, fig. 5, pl. 2, figs 7–9). A right molar or dp5 trigonid from the Late Cretaceous of Taveiro, Portugal (Antunes, Sigogneau-Russell & Russell, 1986: fig. E; Gheerbrant & Astibia, 1999: fig. 3e) may belong to *Lainodon*.

A fragmentary lower molar from the Maastrichtian of Madagascar may belong to a zhelestid similar to *Lainodon* (Averianov, Archibald & Martin, 2003).

*LABES* SIGÉ IN POL ET AL., 1992

*Labes*: Pol et al., 1992: 296.

*Type species*: *Labes quintanillensis* Sigé in Pol et al., 1992.

*Included species*: Type species and *Labes garimondi* Sigé in Pol et al., 1992.

*Revised diagnosis*: Differs from *Sheikhdzheilia* and *Lainodon* by protoconid subequal to paraconid or metaconid in height. Differs from *Avitotherium*, *Lainodon*, and *Gallolestes* by paraconid not on lingual margin. Differs from *Parazhelestes*, *Avitotherium*, and *Gallolestes* by paracristid–protocristid angle between 36 and 49°. Differs from *Sheikhdzheilia*, *Avitotherium*, and *Lainodon* by protocristid transverse. Differs from all zhelestids except *Sheikhdzheilia* and *Lainodon* by absence of labial postcingulid. Differs from all zhelestids by cristid obliqua labial to protocristid notch; hypoconulid on m1–2 equidistant from hypoconid and entoconid.

*Distribution*: France and Spain; Late Cretaceous (Campanian and Maastrichtian).

*Comments*: The two species of *Labes* are known from noncomparable material: m3 for *L. quintanillensis* and m1–2 for *L. garimondi*. At least some of the differences between the two species listed by Sigé in Pol et al. (1992: 299) may pertain to the positional variation. The only reliable difference between the two species is the size; the Maastrichtian species is distinctly smaller.

Referral of *Labes* to the Zhelestidae is tentative until the discovery of more complete specimens. The most striking difference of this taxon compared to zhelestids is the hypoconulid on m1–2, which is equidistant from the hypoconid and entoconid.

Tabuce, Vianey-Liaud & Garcia (2004) described a poorly preserved dentary fragment with some remnants of dentition as '*Valentinella vitrollense*'.

This taxon is considered here as a nomen dubium because it lacks diagnostic features. It was said to be more derived than *Labes* and *Lainodon* in having fully compressed trigonids, but the trigonids are actually not preserved on the holotype specimen. The lower molars of this specimen seem to be somewhat larger than in *L. garimondi*.

*LABES QUINTANILLENSIS* SIGÉ IN POL ET AL., 1992  
(See Appendix 4 for synonymies, referred illustrations, and referred specimens.)

*Holotype*: QTC 2, right m3. Depository not indicated.

*Type locality and horizon*: El Molino, near Quintanilla del Coco, Burgos Province, Spain; Calizas de Lychnus Formation, Late Cretaceous (Maastrichtian).

*Revised diagnosis*: About 30% smaller than *L. garimondi*.

*Description*: See Pol et al. (1992: 296–298).

*Measurements*: See Pol et al. (1992: 298).

*LABES GARIMONDI* SIGÉ IN POL ET AL., 1992  
(See Appendix 4 for synonymies, referred illustrations, and referred specimens.)

*Holotype*: GAR 007, right m1–2. Depository not indicated.

*Type locality and horizon*: Champ-Garimond, Fons-outré-Gardon, Gard, France; unnamed stratigraphical unit, Late Cretaceous (Campanian).

*Revised diagnosis*: About 30% larger than *L. quintanillensis*.

*Description*: Not available.

*Measurements*: See Pol et al. (1992: 300).

*GALLOLESTES* LILLEGRAVEN, 1976  
*Gallolestes*: Lillegraven, 1976: 438.

*Type species*: *Gallolestes pachymandibularis* Lillegraven, 1976.

*Included species*: Type species and *Gallolestes agujaensis* Cifelli, 1994.

*Distribution*: Mexico and Texas, USA; Late Cretaceous (Campanian).

*GALLOLESTES PACHYMANDIBULARIS*

LILLEGRAVEN, 1976.

(See Appendix 4 for synonymies, referred illustrations, and referred specimens.)

*Holotype*: LACM 42633, right dentary with fragmented p4, dp5, and m1–3.

*Type locality and horizon*: LACM locality 3302, Baja California del Norte, Mexico. 'El Gallo Formation', Late Cretaceous (late Campanian).

*Revised diagnosis*: About 40% larger than *G. agujaensis* in dental measurements.

*Description*: See Lillegraven (1976: 438–440) and Clemens (1980: 2–3).

*Measurements*: See Lillegraven (1976: tab. 1).

*Comments*: We follow Butler (1977, 1990) in the interpretation of the last premolar on the holotype of *G. pachymandibularis* as a milk tooth, dp5, contra our previous claim that this tooth is a molariform p5 (Archibald & Averianov, 2001; see also discussion in Lillegraven, 1976; Clemens, 1980; Nesov *et al.*, 1998; Kielan-Jaworowska, Cifelli & Luo, 2004). The deciduous nature of this tooth was rejected on the ground that 'the roots are well formed, very unusual for a deciduous tooth that was soon destined to be shed' (Archibald & Averianov, 2001: 543). The roots of this tooth, however, actually are formed as well as in some dp5s of zhelestids from Dzharakuduk having the same state of wear. The smaller size relative to m1 and the much heavier wear strongly argue that this is a milk tooth. As was pointed out by Clemens (1980), retention of the last deciduous premolar until the m3 has erupted is quite unusual. In the Asiatic Zhelestinae dp5 is replaced when m3 is not fully erupted (see the next section). A similar delay in replacement of dp5 was noted for the zalambdalestid *Barunlestes* by Butler (1990).

*GALLOLESTES AGUJAENSIS* CIFELLI, 1994

(See Appendix 4 for synonymies, referred illustrations, and referred specimens.)

*Holotype*: OMNH 22788, left dentary fragment with m1 or 2.

*Type locality and horizon*: OMNH V58, 8 km north-north-east of Study Butte, Brewster County, Texas, USA. Upper shale member, Aguja Formation, Late Cretaceous (late Campanian).

*Revised diagnosis*: About 40% smaller than *G. pachymandibularis* in dental measurements.

*Description*: See Cifelli (1994: 132).

*Measurements*: See Cifelli (1994: tab. 7).

*AVITOTHERIUM* CIFELLI, 1990

*Avitotherium*: Cifelli, 1990: 353.

*Type species*: *Avitotherium utahensis* Cifelli, 1990.

*Included species*: Type species only.

*Distribution*: Utah and Montana, USA; Late Cretaceous (Campanian).

*AVITOTHERIUM UTAHENSIS* CIFELLI, 1990

(See Appendix 4 for synonymies, referred illustrations, and referred specimens.)

*Holotype*: MNA V4650, right M1.

*Type locality and horizon*: OMNH locality V9, upper Wahweap Creek area, Kane County, Utah, USA. Lower Kaiparowits Formation, Late Cretaceous (late Campanian).

*Description*: See Cifelli (1990: 353–355).

*Measurements*: See Cifelli (1990: tab. 3).

*Comments*: An isolated upper molar UCMP 131240 from the Judith River Formation of Montana, USA, identified as 'tribotherian' (Montellano, 1992: fig. 32) is possibly a DP5 of *Avitotherium*.

## ?ZHELESTIDAE NESOV, 1985A

*EOZHELESTES* NESOV, 1997

*Eozhelestes*: Nesov, 1997: 169.

*Type species*: *Eozhelestes mangit* Nesov, 1997.

*Included species*: Type species only.

*Diagnosis*: As for the type species.

*Distribution:* Western Uzbekistan; Late Cretaceous (Cenomanian).

#### ?ZHELESTIDAE

##### *EOZHELESTES MANGIT* NESOV, 1997

(See Appendix 4 for synonymies, referred illustrations, and referred specimens.)

*Holotype:* CCMGE 26/12176, left m1. Found in 2003 from concentrate obtained in 1998.

*Type locality and horizon:* SSHD-8, Sheikhdzheili, Kyzylkum Desert, Uzbekistan. Upper part of Khodzhakul Formation, Upper Cretaceous (early Cenomanian).

*Revised diagnosis:* Differs from *Eomaia*, *Prokennalestes*, *Murtoilestes*, and *Bobolestes* by anteroposterior compression of trigonid; entoconid subequal to or larger than hypoconid or hypoconulid; labial postcingulid present. Differs from *Eomaia*, *Prokennalestes*, and *Bobolestes* by 'coronoid' facet absent; i4 greatly reduced; hypoconulid on m1–2 about twice as close to entoconid than to hypoconid. Differs from *Eomaia* and *Prokennalestes* by mandibular symphysis posterior margin reaching p3 or more posteriorly; posterior-most mental foramen below p5 or more posterior; p3 shorter than p2. Differs from *Prokennalestes* and *Bobolestes* by lower canine enlargement. Differs from *Eomaia* by p1–p2 diastema absent. Differs from *Prokennalestes* by lower canine single-rooted. Differs from *Bobolestes* by oblique protocristid; cristid obliqua lingual to protocristid notch. Differs from the clade Zhelestidae + *Paranyctoides* by trigonid height twice or more the height of talonid; oblique protocristid; talonid narrower than trigonid; cristid obliqua lingual to protocristid notch.

*Description:* See Averianov & Archibald (2005: 602–603).

*Measurements:* See Averianov & Archibald (2005: 603).

*Comments:* *Eozhelestes mangit* was originally established on a single lower molar and though to be the most ancient and primitive member of Zhelestidae (Nesov, 1997), extending the fossil record of the group by about five million years earlier than Dzharakuduk. Kielan-Jaworowska *et al.* (2004) excluded this taxon from Zhelestidae and considered it to be order and family *incertae sedis* following a conclusion expressed in 'note added in proof' to Nesov *et al.* (1998: 87). Averianov & Archibald (2005) referred to *E. mangit* eight additional specimens and

provided a revised diagnosis for this taxon citing a unique combination of primitive and derived characters. They noted that this taxon differs from the Turonian zhelestids by a number of ancestral retentions, which is consistent with its older geological age, and classified it within Zhelestidae. According to the phylogenetic analysis by Wible *et al.* (2004: fig. 3) *Eozhelestes* forms a clade with *Paranyctoides* that is less basal than Zhelestidae on the phylogenetic tree, forming a sister relationship to all other eutherians. This result is somewhat surprising because in most characters *Eozhelestes* is clearly plesiomorphic relative to Zhelestidae. According to the phylogenetic analyses in the last section of the present paper, *Eozhelestes* is either a sister taxon to a Zhelestidae + *Paranyctoides* clade or is in a polytomy with other zhelestids. For now we place *Eozhelestes* as ?Zhelestidae. *Paranyctoides* will be treated in a separate publication.

#### DENTARY TOOTH REPLACEMENT IN DZHARAKUDUK ZHELESTIDS

There are a number of dentary fragments of zhelestids from Dzharakuduk exemplifying different stages of dental replacement. This permits us to reconstruct the pattern of dental replacement for the dentary from the canine posteriorly. For this reconstruction, specimens from all zhelestine taxa were used, assuming that these closely related species do not show variation in the replacement pattern. We have no evidence for such variation in replacement although the number of roots for the lower canine and p1 may vary between one and two both intra- and interspecifically. We do not have any specimens showing replacement of incisors but this region is poorly known for zhelestids. We can, however, surmise that for almost all of the specimens for which there is evidence based on alveoli, there were either three or four lower incisors. The fourth incisor position may be absent, but when present, it was definitely much smaller than the other incisors and it was positioned just anteriorly and slightly lower than the canine. The third incisor may have been larger than the first and second, but this cannot be ascertained with any certainty. Figure 27 shows the eruption sequence for teeth from the canine posteriorly. For convenience seven stages (I–VII) are recognized in this figure. Specimens representing these stages are illustrated in Figure 28. All incisor alveoli in Figure 28 are labelled as permanent but some may well have been deciduous.

The vast majority of specimens in this replacement analysis have at least one dental remain. Of the 12 specimens shown in Figure 28, all but that in Figure 28F have a least one partial tooth. Dental remains are not, however, the only criteria by which

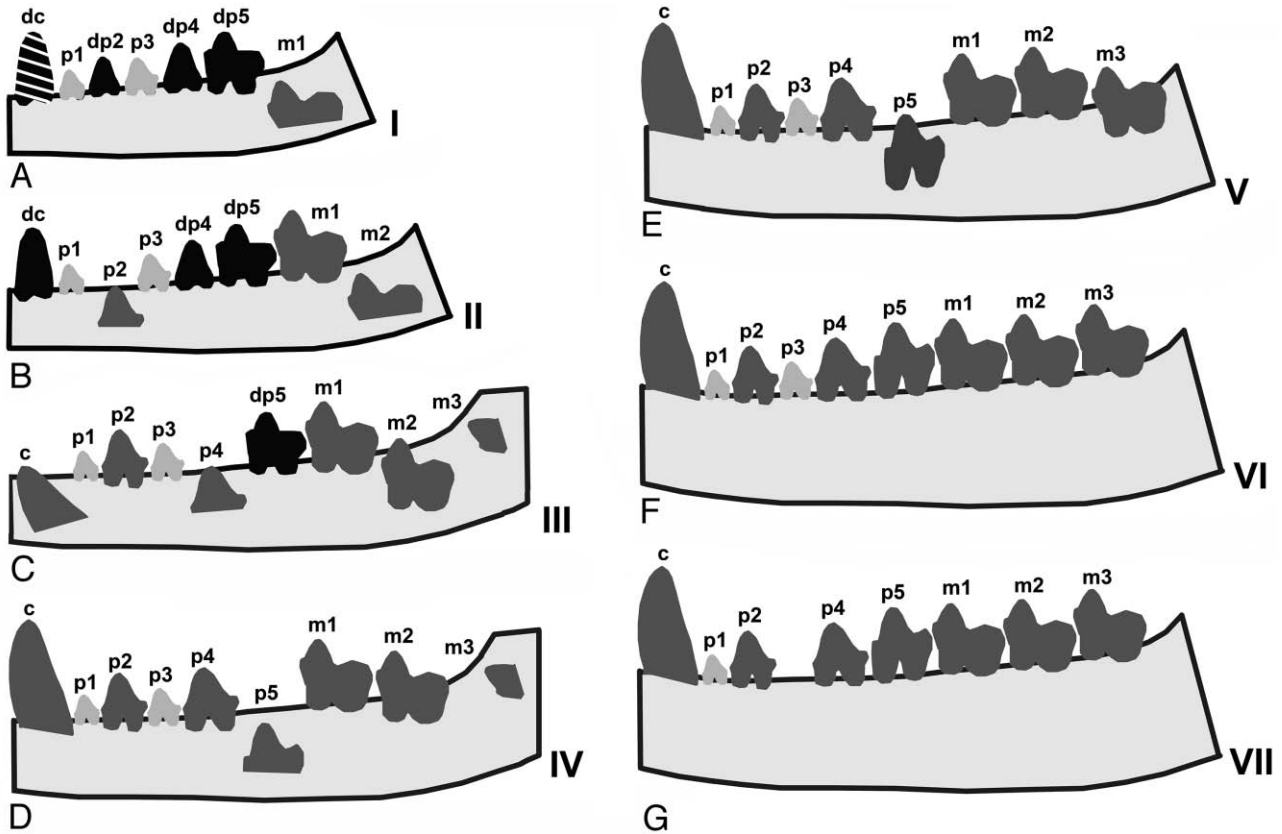


**Figure 27.** Seven stages of dental replacement in the lower dentition of zhelestids from the canine posteriorly. See text and Figure 28 for specimens upon which the first five stages are based. Shading is as follows: deciduous teeth, black; permanent teeth, dark grey; premolars for which only one generation is known, light grey. Cross hatching indicates the condition is speculative for that stage.

Dzharakuduk zhelestid dentary (or maxillary) remains can be identified. The only eutherian from Dzharakuduk approaching the size of zhelestids is *Kulbeckia* (a zalambdalestid). *Kulbeckia* does not have p3, which is present in all but the oldest zhelestid individuals. Further, the p3 or its alveoli are noticeably reduced. In *Kulbeckia* on the labial side of the dentary, a small mental foramen occurs below p2 and a larger one occurs below p4. This is not the pattern in zhelestids, which may have two foramina, a smaller one under i1, i2, or the canine and one between p4 and p5. A third can be present under p1.

#### STAGE I

The erupted teeth are dc, p1, dp2, p3, dp4, and dp5. The crown of m1 is formed but not erupted, hidden in its crypt. The crowns of m2–3 are not yet formed. This stage is exemplified by a single specimen, URBAC 02–68 (Fig. 28A), which has a partially broken dp4, a slightly worn complete dp5, and an inflated thin walled chamber for the unerupted m1 crown (the tooth itself

is not preserved). The presence of more anterior teeth is hypothetically reconstructed, based on what we see in the next stages. In the next stages we see no replacement in the first and third dental loci; this may have two explanations. In the first explanation, p1 and p3 of zhelestids are deciduous teeth retained into the adult because the permanent teeth, which should replace them, were suppressed and did not erupt. This explanation is in line with the fact that p3 is sometimes lost in adult specimens of zhelestids, where its alveoli are plugged and there is a diastema between p2 and p4 (stage VII). Furthermore, p1 does not replace dp1 in many groups of eutherian mammals (Luckett, 1994, in reference to dP1). The second, alternative, explanation is that dp1 and dp3 were the first premolars to be replaced and we simply do not have specimens documenting this earlier ontogenetic stage. This explanation is in line with the mode of tooth replacement in Jurassic dryolestids, which had alternate replacement of premolars in two waves and in which dp1 and dp3 were replaced in the first wave (Martin, 1997). This condition is probably ancestral for

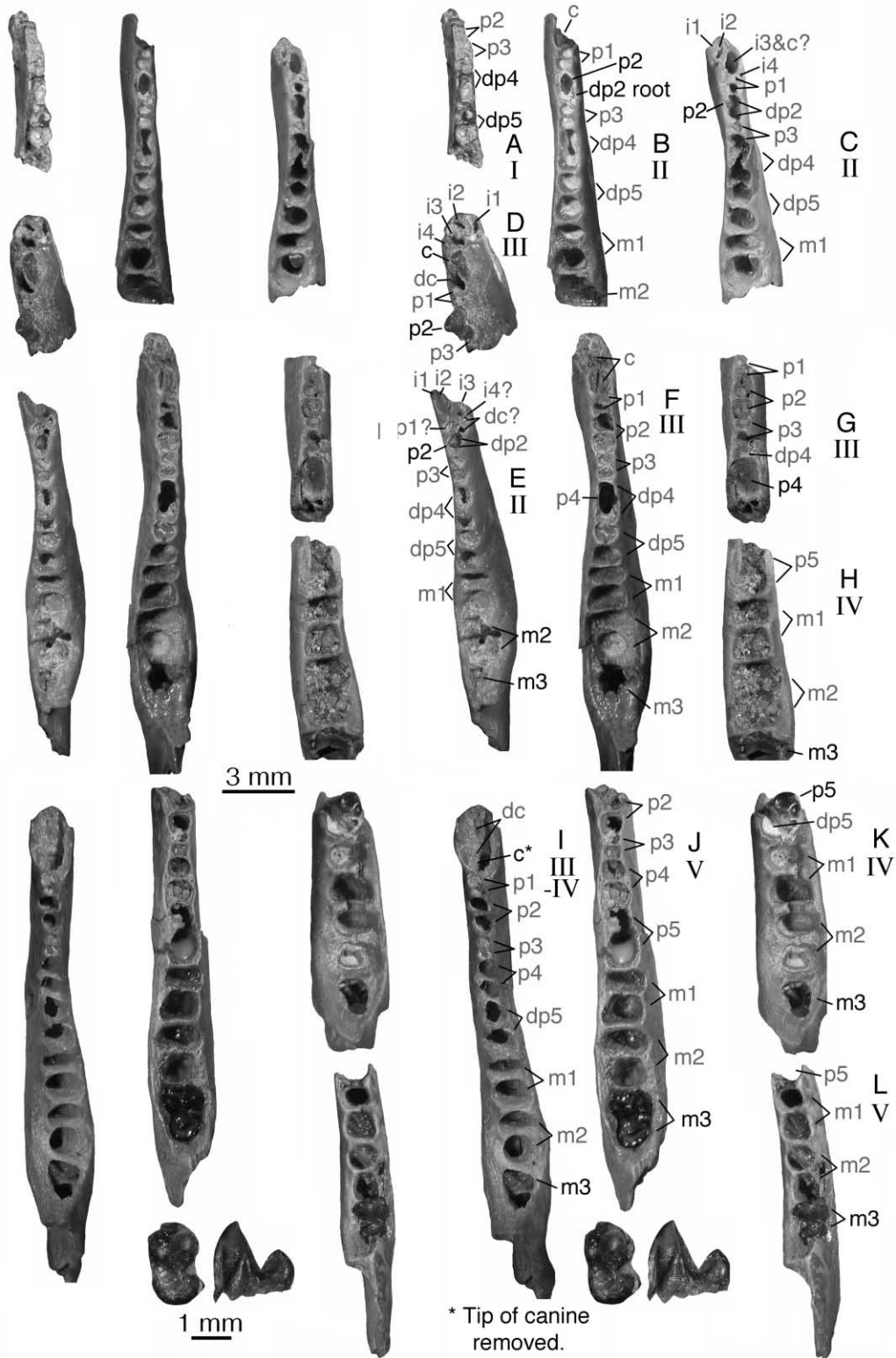


**Figure 28.** Stereophotographs of zhelestids showing dental replacement. Roman numerals are stages described in the text and shown in Figure 27. The ‘d’ designation refers to deciduous teeth or alveoli for such teeth. Light grey letters indicate alveoli and black letters indicate at least partial crowns or roots. A, URBAC 02–68; B, URBAC 00–68; C, ZIN 88491; D, CCMGE 3/11658; E, ZIN 82555; F, ZIN 88469; G, ZIN 88485; H, URBAC06-110; I, ZIN 88470; J, URBAC 03–218, with removed p5 crown in occlusal and lingual views; K, ZIN 88448; L, URBAC 00–29.

therians. In the symmetrodont *Zhangheotherium*, which is not as close to therian ancestry as is *Dryolestes*, and which has only three lower premolars, dp3 is replaced much later in ontogeny, simultaneously with the eruption of m5 (Luo, Kielan-Jaworowska & Cifelli, 2004). However, this tooth may be homologous with a more posterior dental locus of therians such as p4 or p5. In zhelestids these teeth have been designated p1 and p3, favouring the first explanation and following the previous conventional interpretation of these teeth in zhelestids (e.g. in Nesov *et al.*, 1998). We cannot exclude the possibility that these teeth are in reality dp1 and dp3.

#### STAGE II

The erupted teeth are dc, p1, p3, dp4, dp5, and m1. The dp2 is already shed and p2 is just erupting, with most of the crown hidden in a crypt and the roots undeveloped. The crown of m2 is in a crypt. The crown of m3 appears not to have been formed. There are three specimens exhibiting this stage, URBAC 00–68 (Fig. 28B), ZIN 88491 (Fig. 28C), and ZIN 82555 (Fig. 28F). This stage documents replacement in the second premolar locus.

#### STAGE III

The erupted teeth are p1, p2, p3, dp5, and m1. The dc has been shed, but the permanent canine is not yet fully erupted as in CCMGE 3/11658 (Fig. 28D) and ZIN 88470; Fig. 28I). The dp4 is also being shed in this stage, with the crown of p4 just emerging above the alveolar border as in ZIN 88485 (Fig. 28G). The roots of p4 are not fully developed and possibly not ossified at this stage. ZIN 88469 (Fig. 28F) still preserves the alveoli for dp4 with a larger hole for the erupting crown tip of p4 between them. The crown of m2 appears to be fully developed but not erupted (there is not a transverse septum separating the roots in the m2 alveolus in ZIN 88469, Fig. 28F). The m3 is possibly represented in this stage in some specimens by a trigonid not yet formed in enamel, judging from the alveolus in ZIN 88469 (Fig. 28F).

#### STAGE IV

The erupted teeth are c, p1, p2, p3, p4, and m1. The dp5 is being shed at this stage and p5 is starting to erupt as in ZIN 88448 (Fig. 28K). The m2 is not fully erupted because the septum between the roots is not formed in its alveolus as in URBAC 06–110 (Fig. 28H). The m3 is represented by a trigonid in the crypt at the base of the coronoid process; the trigonid is horizontally placed with the trigonid cusps facing

mesially as in URBAC 06–110 (Fig. 28H), ZIN 88470 (Fig. 28I), and ZIN 88448 (Fig. 28K).

#### STAGE V

The erupted teeth are c, p1, p2, p3, p4, m1, and m2. The p5 is still erupting. The m2 is fully erupted, with a bony septum between the roots in the alveoli as in URBAC 03–218 (Fig. 28J). The m3 is fully formed, is beginning to erupt, and is still in part on the anterior slope of the coronoid process as in URBAC 03–218 (Fig. 28J) and URBAC 00–29 (Fig. 28L). The m3 rotates vertically during the erupting in connection with the posterior shift of the coronoid process.

#### STAGE VI

All postcanine permanent teeth are fully erupted, as is the case in URBAC 99–109 (Fig. 16) and URBAC 98–13 (Fig. 17).

#### STAGE VII

At stage VII p3 is lost, its alveoli plugged by bone, and there is a diastema between p2 and p4. This is present in some older individuals. Other individuals presumably retained p3 for their whole life. URBAC 99–109 (Fig. 16A) may have one p3 alveolus or it may have been lost in this individual.

The pattern of dental replacement as reconstructed above suggests that zhelestids had an alternate replacement of premolars, as in dryolestids (Martin, 1997): [p1, p3, if replaced] -> p2 -> p4 -> p5. The p1 and p3, if replaced, were replaced in the first wave, and p2, p4, and p5 in the second wave. The replacement pattern would still be alternating even if p1 and p3 were not replaced and these tooth positions were represented by deciduous teeth. Luo *et al.* (2004) postulated that in crown group placental mammals there was a reversal from the ancestral alternate replacement of premolars toward the sequential replacement, observed in some stem mammals. This 'reversal' is, however, an artefact of counting the premolars differently than the method used by us. In placental taxa, which lose p3, the p4 and p5 are counted as p3 and p4. Thus in *Canis*, the pattern of premolar replacement, usually depicted as sequential (p2 -> p3 -> p4; e.g. Luo *et al.*, 2004), is in fact the alternative sequence (p2 -> p4 -> p5), as in zhelestids, if the correct homology of premolars is applied. The pattern of tooth eruption for all the postcanine teeth in zhelestids can be described as: [dc, p1, dp2, p3, dp4, dp5] -> m1 -> p2 -> c, p4, m2 -> p5 -> m3.

The oldest therian specimen showing dental replacement is the holotype of *Slaughteria eruptens* Butler 1978, a dentary fragment with four teeth from the Early

Cretaceous Trinity fauna of Texas. Kobayashi, Winkler & Jacobs (2002) examined this specimen using computed tomography scanning and established its dental formula as p2, p3, dp4 (under replacement), m1 and the premolar replacement sequence as p3 -> p2 -> p4. Luo *et al.* (2004: fig. 4C; see also Kielan-Jaworowska *et al.*, 2004: fig. 3.24C) reported without explanation a different dental formula of p2, dp3, dp4, m1 and a premolar replacement sequence of p2 -> p4 -> p3 for this specimen. The problem with both interpretations is the premolar count. The complete set of premolars or premolar alveoli are not known for *Slaughteria* or any other therian taxon in the Trinity fauna. However, there are five premolars in *Peramus* and stem eutherians, implying by phylogenetic bracketing that *Slaughteria* also should have had five premolars. Thus the three last premolars in the holotype of *S. eruptens* should represent the third, fourth, and fifth premolar loci. In the third locus there is a not fully erupted p3 and in the last locus there is a replacement of a molariform dp5 by a premolariform p5. The question is what tooth is represented in the fourth locus? Is it a permanent tooth (Butler, 1978; Kobayashi *et al.*, 2002) or a milk tooth (Luo *et al.*, 2004)? If it is dp4, the replacement sequence would be p3 -> p5 -> p4, but if p4, then the sequence is p4 -> p3 -> p5. In both cases the pattern is different from that in zhelestids. We need more specimens of *Slaughteria* or similar mammals in order to understand better the replacement pattern in this taxon.

In the asioryctitherian *Daulestes* from the Bissekty local fauna the pattern of dental eruption can be reconstructed as [c, p1, p2, m1] -> p4, m2 -> p5, m3 and the replacement pattern is [p1, p2] -> p4 -> p5 (Archibald & Averianov, 2006 for alternative interpretations see McKenna, Kielan-Jaworowska & Meng, 2000 and Luo *et al.*, 2004). If the p3 position was lost in *Daulestes*, these patterns are identical to those in zhelestids. Luo *et al.* (2004: fig. 4D) published reconstructions of the dental replacement for the Mongolian asioryctitherian *Kennalestes*, which are incorrect in some points. The juvenile stage in this reconstruction is based on ZPAL MgM-I/1 (Kielan-Jaworowska, 1981: pls 14, 15). First, this specimen has in the last premolar position a milk tooth, not a permanent tooth as depicted by Luo *et al.* (2004). Second, the tooth designated as DP2 is in fact P3. It is present on the right side of the specimen, but is lacking from the left side. The premolars in this specimen would be P1, P2, P3, P4 (erupting), and DP5, not P1, P2, DP2, P3, and P4, as determined by Luo *et al.* (2004). According to our interpretation, the replacement sequence for *Kennalestes* would be [P1, P2, P3] -> P4 -> P5 and the eruption sequence is [DC, P1, P2, P3, DP5, M1, M2] -> C, P4, M3 -> P5. This replacement sequence for the uppers of *Kennalestes* is thus similar to that for

the lowers of zhelestids. In the eruption sequence *Kennalestes* shows a faster eruption of molars: M3 erupts together with C and P4 and prior to the eruption of P5. In zhelestids m2 erupts together with c and p4, and m3 erupts fully after p5.

## PHYLOGENETIC ANALYSIS

The two major analyses and conclusions discussed in this section are: (1) although only weakly supported by bootstrap analyses, Zhelestidae consistently forms a clade in all four treatments that we performed in the first analysis, and (2) the best supported hypothesis is that Zhelestidae is a stem eutherian clade (Wible *et al.*, 2007) rather than belonging within the crown clade Placentalia as shown in the second analysis.

Appendix S1 lists all better known Cretaceous eutherians used in the first analysis examining the monophyly of Zhelestidae and this clade's relationship to other Cretaceous eutherians. *Cimolestes* was treated as a single terminal taxon, although recent work suggests that it may be paraphyletic (Strauss, 2008). Three taxa excluded from this analysis that have been identified as zhelestids are *Labes*, '*Sorlestes*' *mifunensis*, and *Alostera*. In the case of the first two taxa we believe them to be zhelestids but because they are rather poorly known, we did not include them in the phylogenetic analysis. As discussed earlier, *Labes* may be sister to *Lainodon* and '*Sorlestes*' *mifunensis* is reminiscent of clades within and near Zhelestinae, but we cannot determine where this taxon might belong based on current published evidence. In the case of *Alostera*, although rather poorly known, it is best treated as an archaic ungulate because like these taxa it lacks a parastylar groove, has a metacingulum formed by the postmetaconular crista continuing onto the metastylar lobe, and has no ectoflexus (the latter is also the case in *Eoungulatum*) and accordingly is not included in this analysis.

In the analysis of Cretaceous eutherians, we performed four different PAUP\* 4.0b10 runs. In all four runs the default settings were used and a heuristic search was performed using 1000 stepwise-addition random replicates. Tree measures and statistics are given in Figure 29. In the first run all 85 characters were unordered and in the second run 22 of the 85 characters were ordered. The topology for both runs was the same (Fig. 29A). Following each of these runs the characters were reweighted using the rescaled consistency index (RC). Figure 29B shows the results for the ordered reweighted run, whereas Figure 29C shows the results for the unordered reweighted run. For each of the four runs, a bootstrap analysis was performed using 10 000 replicates of the 'fast' stepwise-addition option. Bootstrap values greater than 50 are shown on each of the cladograms in Figure 29.

Although most bootstrap values are low, several patterns of relationship remain consistent across all four runs. First, in all four runs all taxa that we regard as Zhelestidae form a clade. Second, in all four the following three sister group relationships were found: *Sheikhdzheilia* + *Lainodon*, *Avitotherium* + *Gallolestes*, and *Parazhelestes mynbulakensis* + *P. robustus*.

In both reweighted runs shown in Figure 29B and C, *Paranyctoides* and *Eozhelestes* are sister taxa to what we recognize as Zhelestidae, but these two genera are united with Zhelestidae by only two state changes: 82, the entoconid is subequal to or larger than the hypoconid or hypoconulid, and 84, a labial postcingulid is present. We are accordingly hesitant to propose formally a higher-level clade including all these taxa. Work currently underway on *Paranyctoides* by us may provide some clarity, but unfortunately no additional specimens of *Eozhelestes* have been recovered.

Zhelestidae is recognized by six character state changes in Figure 29B and seven in Figure 29C. The six character state changes in Figure 29B are: 15, upper molar stylar shelf width is less than 25% of the molar length; 23, conular region width is more than 51% of the total molar width; 24, the paraconule is prominent and is midway or closer to paracone; 29, the molar protocone is similar in height to the paracone and metacone; 71, the p5 has an incipient basin lingual to the talonid ridge; and 76, the protoconid is subequal in height to the paraconid and or metaconid. Unfortunately, none of these state changes is unique to Zhelestidae; however, no other clade or taxon shares this suite of changes. The closest in this analysis is Zalambdalestidae + *Gypsonictops*, which shares four of these six state changes.

Five of the character state changes in Figure 29C (15, 23, 24, 26, and 71) are the same as in Figure 29B, whereas one character (76) is absent and two others (35 and 36) are included. For these two different state changes in zhelestids, in character 35 the M1 parastylar lobe is anterior rather than anterolabial to the paracone and for character 36 the M2 metastylar lobe is more labial than the parastylar lobe. As for Figure 29B, none of these state changes is unique to Zhelestidae, but again, no other clade or taxon shares this suite of changes.

Of the two trees we favour that in Figure 29B over 29C, even though there is less resolution within Zhelestidae in the former. In Figure 29B, however, all Turonian-aged zhelestids from Uzbekistan form a clade to the exclusion of other zhelestids whereas in Figure 29C, the two North America taxa *Avitotherium* and *Gallolestes* form a clade nested within the Turonian-aged zhelestids from Uzbekistan. Given the differences in both age and biogeography this relationship seems unlikely, plus Figure 29B makes fewer

assumptions of bifurcating relationships based on the same data.

Because of the ambiguity of relationships within Zhelestidae as seen in Figure 29B, we recognize only one subfamilial taxon, Zhelestinae, for the four Turonian-aged zhelestids from Uzbekistan, *Zhelestes*, *Aspanlestes*, *Parazhelestes* (*P. mynbulakensis* and *P. robustus*), and *Eoungulatum*. Based on Figure 29B, Zhelestinae is united by character state changes in 38, mandibular symphysis extends posteriorly to at least p3 or further; 39, the Meckelian groove is absent; 69, p5 metaconid is a separate cusp; and 70, p5 lingual cingulid is absent. Further work may show that other taxa belong within Zhelestinae.

As noted above, at lower taxonomic levels, in all four analyses shown in Figure 29A–C, the following three sister group relationships were found: *Sheikhdzheilia* + *Lainodon*, *Avitotherium* + *Gallolestes*, and *P. mynbulakensis* + *P. robustus*. The first two relationships have interesting biogeographical implications.

The Campanian–Maastrichtian *Lainodon* (and *Labes*) from Europe retain some character states thought to be ancestral for Zhelestidae, suggesting an earlier biogeographical tie with Middle Asia at least in the early Cenomanian when the similar *Sheikhdzheilia* was extant (Averianov & Archibald, 2005). *Lainodon* and *Labes* have not been previously included in a phylogenetic analysis with zhelestids, but the current analysis that includes *Lainodon* supports the earlier assessment of zhelestid affinities. In all analyses *Sheikhdzheilia* and *Lainodon* are grouped, but only on the basis of what we interpret as reversals. For the tree that we favour (Fig. 29B), the three reversals uniting these two taxa are, for character 76, the protoconid becomes the tallest trigonid cusp; for character 78, the protocristid becomes oblique rather than transverse; and, for character 84, the loss of a labial postcingulid. It is of course possible and even likely that these three states are ancestral retentions in these two taxa. Thus, their resemblances may be a result of ancestral retentions rather than any synapomorphies.

The next pair of sister taxa that occur in all analyses are *Avitotherium* and *Gallolestes*. It is biogeographically interesting that both are Campanian in age and are the only North American representatives of Zhelestidae that we recognize. As noted above we no longer include *Alostera* in Zhelestidae. For the tree that we favour (Fig. 29B), two character state changes unite *Avitotherium* and *Gallolestes*. These two state changes are the anteroposterior compression of the trigonid with the paracristid and protocristid forming an angle of less than 35° (character 75) and the shift of the lower molar paraconid away from the lingual margin (character 77). These seem to be

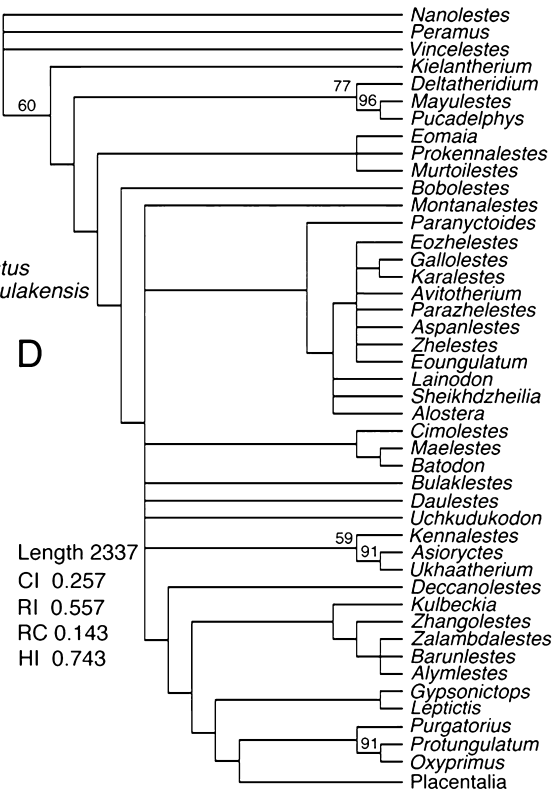
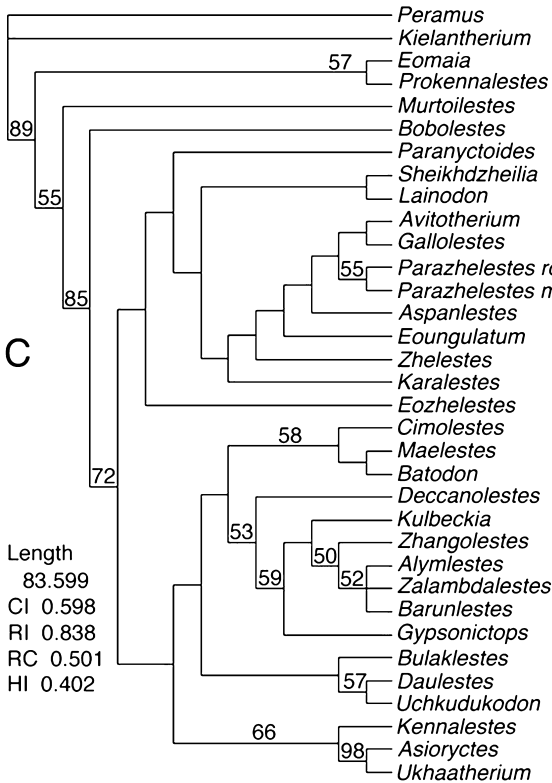
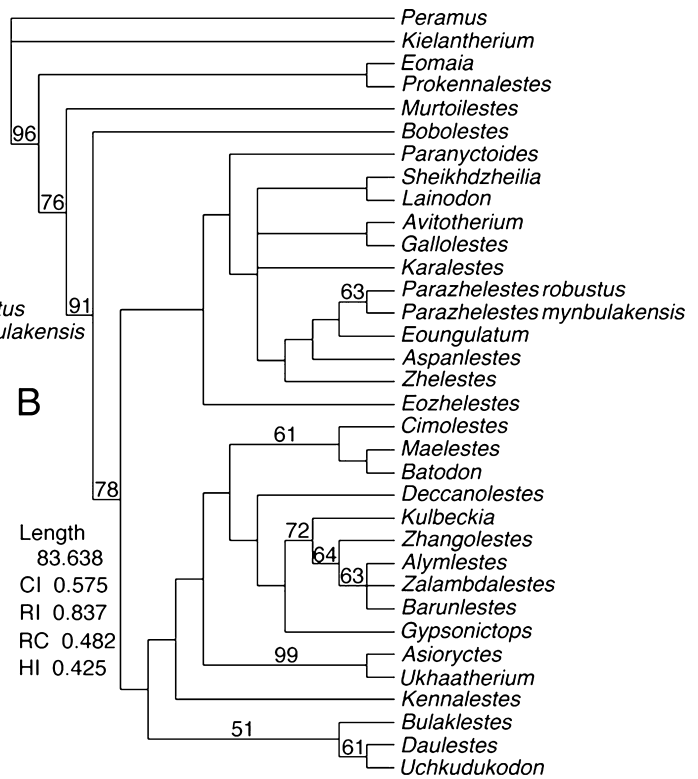
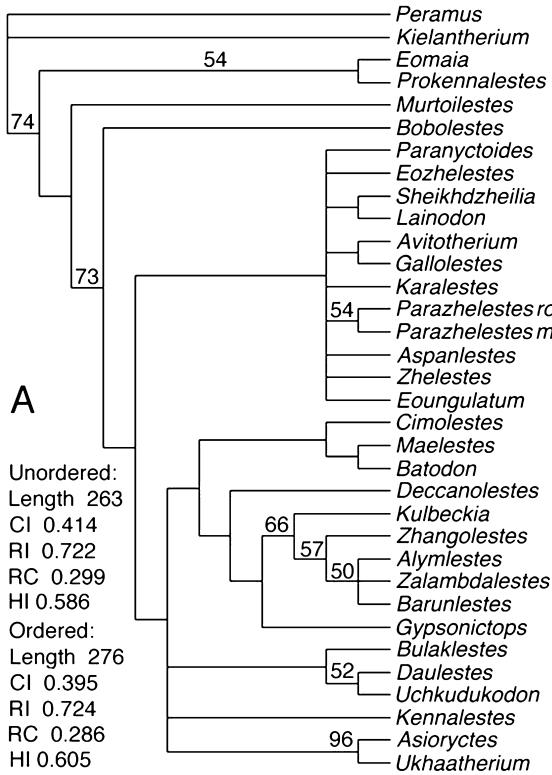


**Figure 29.** Phylogenetic analyses (A–C) of Cretaceous eutherians (Appendix S1) using PAUP\* 4.0b10. Default settings were used and a heuristic search was performed using 1000 stepwise-addition random replicates. Tree measures for each analysis are provided next to each analysis. A, strict consensus tree, which was the same topology whether all 85 characters were unordered (108 trees) or the 22 of the 85 characters were ordered (99 trees). Following each of these two runs, characters were reweighted using the rescaled consistency index (RC). B, strict consensus tree for 15 trees for the ordered reweighted run. C, strict consensus tree for three trees for the unordered reweighted run. For each of the four runs, a bootstrap analysis was carried out using 10 000 replicates of the ‘fast’ stepwise-addition option. Bootstrap values of greater than 50 are shown. We favour the results shown in B, as discussed in the text. D, strict consensus of 722 trees based on a reanalysis of Wible *et al.* (2007, 2009) using PAUP\* 4.0b10 following their indicated protocols, with the addition of more Cretaceous eutherians, most notably all the zhelestids used in the above analyses but also including *Alostera*. All placentals used by Wible *et al.* (2007, 2009) were also used in our analysis. They were found to be monophyletic and for purposes of space only Placentalia is listed, but all placental taxa are listed in Appendix S2. Modifications and additions to the Wible *et al.* (2007, 2009) character matrix are given in Appendix S3.

clear synapomorphies, with only the former being shared convergently with *Parazhelestes*.

The final pair of sister taxa that occur in all analyses are *P. mynbulakensis* and *P. robustus*, which are both from the Turonian–Coniacian of Uzbekistan. In the tree that we favour (Fig. 29B), these species are united by two character state changes, the mandibular symphysis extends posteriorly to at least p3 or further (character 38) and the anteroposterior compression of the trigonid with the paracristid and protocristid forms an angle of less than 35° (character 75). The former is interpreted as a reversal within Zhelestinae and the latter is an apomorphy shared convergently with *Avitotherium* and *Gallolestes*. These seem to be reasonable characters states for recognizing *Parazhelestes*.

Although the central phylogenetic goal was to investigate the monophyly of Zhelestidae and relations within Zhelestidae, and its relations to other Cretaceous eutherians, we should also comment on the relations found for other taxa in our analyses in Figure 29A–C. In all analyses, a (Zalambdalestidae + *Gypsonictops*) + *Deccanolestes* clade, a (*Maelestes* + *Batodon*) + *Cimolestes* clade, an *Ukhaatherium* + *Asioryctes* clade, and an (*Uchkudukodon* + *Daulestes*) + *Bulaklestes* clade were recovered. In addition, in all analyses zhelestids and their allies form a clade with all the above taxa.

Interestingly, what was not recovered was an Asioryctitheria clade as recognized by Archibald & Averianov (2006). The tree in Figure 29B has 284 steps in MacClade. If branches are swapped in MacClade with the following results: a (Zhelestidae + *Paranyctoides*) + *Eozhelestes* clade, and an (Asioryctitheria + Cimolestidae) ((Zalambdalestidae + *Gypsonictops*) + *Deccanolestes*) clade the resulting tree length is 293 steps. We did not investigate the higher-level relationships further, but the nine-step difference in the two analyses suggests that we have not yet reached a truly stable understanding of all Late Cretaceous eutherian groups.

The second major analysis that we performed was to re-examine Wible *et al.* 2007, 2009) with the addition of more Cretaceous eutherians, most notably all the zhelestids used in the above analysis but also including *Alostera* (Appendix S2). These additions as well as some corrections to the Wible *et al.* (2009) character and state matrix are given in Appendix S3. We used PAUP\* 4.0b10 and followed their indicated protocols (Wible *et al.*, 2009). The results are shown in Figure 29D.

Our analysis showed less resolution than that of Wible *et al.* (2007, 2009) for most Late Cretaceous eutherians, but we did recover Placentalia excluding known Cretaceous eutherians. The only difference in topology relevant to our discussion of zhelestids, other than less resolution in our analysis, was that in our analysis, *Eozhelestes* clustered with zhelestids whereas in Wible *et al.* (2007) *Eozhelestes* and *Paranyctoides* formed a clade separate of Zhelestidae. Our second analysis supports the contention of Wible *et al.* (2007) that Placentalia does not include any known Cretaceous eutherians, notably with Zhelestidae placed as a stem eutherian clade rather than belonging within Placentalia.

#### ACKNOWLEDGEMENTS

We thank John Wible and Eric Ekdale for providing very helpful comments on the skull structure of *Aspanlestes*. An anonymous reviewer provided very constructive criticisms. The continued cooperation of the Zoological Institute, National Academy of Sciences of Uzbekistan, notably D. A. Azimov and Y. A. Chikin is much appreciated. We thank the URBAC expedition members A. V. Abramov, G. O. Cherepanov, I. G. Danilov, S. Dominguez, C. King, N. Morris, C. Redman, A. S. Resvyi, C. Skrabec, P. P. Skutschas, H.-D. Sues, E. V. Syromyatnikova, and D. W. Ward for their myriad field help and scientific expertise. The financial support of the National Geographic Society (5901–97 and 6281–98), the National Science Foundation (EAR-9804771 and 0207004), the

Navoi Mining and Metallurgy Combinat, the Civilian Research and Development Foundation (RU-G1-2571-ST-04 and RUB1-2860-ST-07), and the Russian Fund of Basic Research (07-04-91110-AFGIRa) is gratefully acknowledged. The work of A. A. was also supported by the President of Russia's grant MD 255.2003.04, by the Russian Fund of Basic Research grants 04-04-49113, 04-04-49637, 07-04-00393, and 10-04-01350.

## REFERENCES

- Antunes MT, Sigogneau-Russell D, Russell DE. 1986.** Sur quelques dents de Mammifères du Crétacé supérieur de Taveiro, Portugal (Note préliminaire). *Comptes Rendus de l'Académie des Sciences Paris, Séries II* **303**: 1247–1250.
- Archibald JD. 1982.** A study of Mammalia and geology across the Cretaceous-Tertiary boundary in Garfield County, Montana. *University of California Publications in Geological Sciences* **122**: 1–286.
- Archibald JD. 1996.** Fossil evidence for a Late Cretaceous origin of 'hoofed' mammals. *Science* **272**: 1150–1153.
- Archibald JD. 1998.** Archaic ungulates ('Condylarthra'). In: Janis CM, Scott KM, Jacobs LL, eds. *Evolution of tertiary mammals of North America. Volume 1: terrestrial carnivores, ungulates, and ungulatelike mammals*. New York: Cambridge University Press, 292–331.
- Archibald JD, Averianov AO. 2001.** *Paranyctoides* and allies from the Late Cretaceous of North America and Asia. *Acta Palaeontologica Polonica* **46**: 533–551.
- Archibald JD, Averianov AO. 2005.** Mammalian faunal succession in the Cretaceous of the Kyzylkum Desert. *Journal of Mammalian Evolution* **12**: 9–22.
- Archibald JD, Averianov AO. 2006.** Late Cretaceous asioryctitherian eutherian mammals from Uzbekistan and phylogenetic analysis of Asioryctitheria. *Acta Palaeontologica Polonica* **51**: 351–376.
- Archibald JD, Averianov AO, Ekdale EG. 2001.** Late Cretaceous relatives of rabbits, rodents, and other extant eutherian mammals. *Nature* **414**: 62–65.
- Astibia H, Buffetaut E, Buscalioni AD, Cappetta H, Corral JC, Estes RD, Garcia-Garmilla F, Jaeger J-J, Jimenez-Fuentes E, Le Loeuff J, Mazin J-M, Orue-Etxebarria X, Pereda Suberbiola X, Powell JE, Rage J-C, Rodriguez-Lazaro J, Sanz JL, Tong H. 1991.** The fossil vertebrates from Laño (Basque Country, Spain); new evidence on the composition and affinities of the Late Cretaceous of continental Europe. *Terra Nova. Official Journal of the European Union of Geosciences* **2**: 460–466.
- Averianov AO. 1997.** New Late Cretaceous mammals of southern Kazakhstan. *Acta Palaeontologica Polonica* **42**: 243–256.
- Averianov AO. 2000.** Mammals from the Mesozoic of Kirgizstan, Uzbekistan, Kazakhstan and Tadzhikistan. In: Benton MJ, Shishkin MA, Unwin DM, Kurochkin EN, eds. *The age of dinosaurs in Russia and Mongolia*. Cambridge: Cambridge University Press, 627–652.
- Averianov AO, Archibald JD. 2003.** Mammals from the Upper Cretaceous Aitym Formation, Kyzylkum Desert, Uzbekistan. *Cretaceous Research* **24**: 171–191.
- Averianov AO, Archibald JD. 2005.** Mammals from the mid-Cretaceous Khodzhaikul Formation, Kyzylkum Desert, Uzbekistan. *Cretaceous Research* **26**: 593–608.
- Averianov AO, Archibald JD, Martin T. 2003.** Placental nature of the alleged marsupial from the Cretaceous of Madagascar. *Acta Palaeontologica Polonica* **48**: 149–151.
- Butler PM. 1977.** Evolutionary radiation of the cheek teeth of Cretaceous placentals. *Acta Palaeontologica Polonica* **22**: 241–269.
- Butler PM. 1978.** A new interpretation of the mammalian teeth of tribosphenic pattern from the Albian of Texas. *Breviora* **446**: 1–27.
- Butler PM. 1990.** Early trends in the evolution of tribosphenic molars. *Biological Reviews* **65**: 529–552.
- Chester SGB, Sargis EJ, Szalay FS, Archibald JD, Averianov AO. 2010.** Mammalian distal humeri from the Late Cretaceous of Uzbekistan. *Acta Palaeontologica Polonica* **55**: 199–211.
- Cifelli RL. 1990.** Cretaceous mammals of southern Utah. IV. Eutherian mammals from the Wahweap (Aquilan) and Kaiparowits (Judithian) formations. *Journal of Vertebrate Paleontology* **10**: 346–360.
- Cifelli RL. 1994.** Therian mammals of the Terlingua local fauna (Judithian), Aguja Formation, Big Bend of the Rio Grande, Texas. *Contributions to Geology, University of Wyoming* **30**: 117–136.
- Cifelli RL. 2000.** Counting premolars in early eutherian mammals. *Acta Palaeontologica Polonica* **45**: 195–198.
- Clemens WA. 1980.** *Gallolestes pachymandibularis* (Mammalia: Theria, incertae sedis) from Late Cretaceous deposits in Baja California del Norte, Mexico. *PaleoBios* **33**: 1–10.
- Crouch JE. 1969.** *Text-atlas of cat anatomy*. Philadelphia: Lea & Febiger.
- Ekdale EG, Archibald JD, Averianov AO. 2004.** Petrosal bones of placental mammals from the Late Cretaceous Uzbekistan. *Acta Palaeontologica Polonica* **49**: 161–176.
- Gheerbrant E, Astibia H. 1994.** Un nouveau mammifère du Maastrichtien de Laño (Pays Basque espagnol). *Comptes Rendus de l'Académie des Sciences Paris* **318**: 1125–1131.
- Gheerbrant E, Astibia H. 1999.** The Upper Cretaceous mammals from Laño (Spanish Basque country). *Estudios del Museo de Ciencias Naturales de Alava* **14** (Num. espec. 1): 295–323.
- Gill TN. 1872.** Arrangement of the families of mammals. With analytical tables. *Smithsonian Miscellaneous Collections* **11**: 1–98.
- Gradstein FM, Ogg JG, Smith A. 2004.** *A geologic time scale 2004*. Cambridge, New York, Melbourne: Cambridge University Press.
- ICZN. 1999.** *International code of zoological nomenclature, fourth edition*. London: International Trust for Zoological Nomenclature, c/o The Natural History Museum.
- Kielan-Jaworowska Z. 1981.** Evolution of the therian mammals in the Late Cretaceous of Asia. Part IV. Skull structure in *Kennalestes* and *Asioryctes*. *Palaeontologica Polonica* **42**: 25–78.

- Kielan-Jaworowska Z, Cifelli RL, Luo Z-X. 2004.** *Mammals from the age of dinosaurs: origins, evolution, and structure*. New York: Columbia University Press.
- Kobayashi Y, Winkler DA, Jacobs LL. 2002.** Origin of the tooth-replacement pattern in therian mammals: evidence from a 110 Myr old fossil. *Proceedings of the Royal Society of London, Series B: Biological Sciences* **269**: 369–373.
- Kusuhashi N, Ikegami N, Matsuoka H. 2008.** Additional mammalian fossils from the Upper Cretaceous Mifune Group, Kumamoto, western Japan. *Paleontological Research* **12**: 199–203.
- Ledoux J-L, Hartenberger J-L, Michaux J, Sudre J, Thaler L. 1966.** Découverte d'un Mammifère dans le Crétacé supérieur ? Dinosaures de Champ-Garimond près de Fons (Gard). *Comptes Rendus de l'Académie des Sciences Paris* **262**: 1925–1928.
- Lillegraven JA. 1972.** Preliminary report on Late Cretaceous mammals from the El Gallo Formation, Baja California del Norte, Mexico. *Natural History Museum Los Angeles County, Contributions to Science* **232**: 1–11.
- Lillegraven JA. 1976.** A new genus of therian mammal from the Late Cretaceous 'El Gallo Formation,' Baja California, Mexico. *Journal of Paleontology* **50**: 437–443.
- Linnaeus C. 1758.** *Systema naturae per regna tria naturae, secundum classes, ordines, genera, species, cum characteribus, differentiis, synonymis, locis. Vol. 1: Regnum animale. Editio decima, reformata*. Stockholm: Laurentii Salvii.
- Luckett WP. 1994.** Suprafamilial relationships within Marsupialia: resolution and discordance from multidisciplinary data. *Journal of Mammalian Evolution* **2**: 255–283.
- Luo Z-X, Kielan-Jaworowska Z, Cifelli RL. 2004.** Evolution of dental replacement in mammals. *Bulletin of the Carnegie Museum of Natural History* **36**: 159–175.
- Martin T. 1997.** Tooth replacement in Late Jurassic Dryolestidae (Eupantotheria, Mammalia). *Journal of Mammalian Evolution* **4**: 1–18.
- McKenna MC, Kielan-Jaworowska Z, Meng J. 2000.** Earliest eutherian mammal skull, from the Late Cretaceous (Coniacian) of Uzbekistan. *Acta Palaeontologica Polonica* **45**: 1–54.
- Mead JG, Fordyce RE. 2009.** The therian skull a lexicon with emphasis on the odontocetes. *Smithsonian Contributions to Zoology* **627**: 1–248.
- Montellano M. 1992.** Mammalian fauna of the Judith River Formation (Late Cretaceous, Judithian), northcentral Montana. *University of California Publications in Geological Sciences* **136**: 1–115.
- Nesov LA. 1982.** [The most ancient mammals of the USSR]. *Ezhegodnik Vsesoyuznogo Paleontologicheskogo Obshchestva* **25**: 228–242. [in Russian].
- Nesov LA. 1984.** [On some remains of mammals in the Cretaceous deposits of the Middle Asia]. *Vestnik Zoologii* **2**: 60–65. [in Russian].
- Nesov LA. 1985a.** [New mammals from the Cretaceous of Kyzylkum]. *Vestnik Leningradskogo Universiteta, Seriya 7*: 8–18. [in Russian].
- Nesov LA. 1985b.** [Rare bony fishes, terrestrial lizards and mammals from the zone of estuaries and coastal plains of the Cretaceous of Kyzylkum]. *Ezhegodnik Vsesoyuznogo Paleontologicheskogo Obshchestva* **28**: 199–219. [in Russian].
- Nesov LA. 1987.** [Results of search and study of Cretaceous and early Paleogene mammals on the territory of the USSR]. *Ezhegodnik Vsesoyuznogo Paleontologicheskogo Obshchestva* **30**: 199–218. [in Russian].
- Nesov LA. 1990.** [Deltatheroids, early placental and multi-tuberculate mammals of the coastal plains of Late Cretaceous of the western Middle Asia]. *V S'ezd Vsesoyuznogo Teriologicheskogo Obshchestva, Tezisy Dokladov*. 22–23. [in Russian].
- Nesov LA. 1993.** [New Mesozoic mammals of Middle Asia and Kazakhstan and comments about evolution of theriofaunas of Cretaceous coastal plains of Asia]. *Trudy Zoologicheskogo Instituta RAN* **249**: 105–133. [in Russian].
- Nesov LA. 1995.** [Dinosaurs of Northern Eurasia: new data about assemblages, ecology and paleobiogeography]. Saint Petersburg: Izdatelstvo Sankt-Peterburgskogo Universiteta. [in Russian].
- Nesov LA. 1997.** [Cretaceous nonmarine vertebrates of Northern Eurasia] (Posthumous edition by L.B. Golovneva and A.O. Averianov). Saint Petersburg: Izdatel'stvo Sankt-Peterburgskogo Universiteta. [in Russian].
- Nesov LA, Archibald JD, Kielan-Jaworowska Z. 1998.** Ungulate-like mammals from the Late Cretaceous of Uzbekistan and a phylogenetic analysis of Ungulatomorpha. In: Beard KC, Dawson MR, eds. *Dawn of the Age of Mammals in Asia. Bulletin of the Carnegie Museum of Natural History* **34**: 40–88.
- Nesov LA, Golovneva LB. 1983.** [Changes of vertebrate complexes of Cenomanian – Santonian (Late Cretaceous) of Kyzylkums]. In: Oleinikov AN, ed. [Paleontology and evolution of Biosphera. Transactions of XXV session of the all-union paleontological society]. Leningrad: Nauka, 126–134. [in Russian].
- Nesov LA, Kielan-Jaworowska Z. 1991.** Evolution of the Cretaceous Asian therian mammals. In: Kielan-Jaworowska Z, Heintz N, Nakrem H-A, eds. *Fifth symposium on Mesozoic terrestrial ecosystems and biota. Extended abstracts*. Contributions from the Paleontological Museum, University of Oslo, **364**: 51–52.
- Nesov LA, Sigogneau-Russell D, Russell DE. 1994.** A survey of Cretaceous tribosphenic mammals from Middle Asia (Uzbekistan, Kazakhstan and Tajikistan), of their geological setting, age and faunal environment. *Palaeovertebrata* **23**: 51–92.
- Novacek MJ. 1986.** The primitive eutherian dental formula. *Journal of Vertebrate Paleontology* **6**: 191–196.
- Parker TJ, Haswell WA. 1897.** *A text-book of zoology, volume 2*. London: MacMillan and Company.
- Pol C, Buscalioni AD, Carballeira J, Frances V, Lopez-Martinez N, Marandat B, Moratalla JJ, Sanz JL, Sigé B, Villate J. 1992.** Reptiles and mammals from the Late Cretaceous new locality Quintanilla del Coco (Burgos Province, Spain). *Neues Jahrbuch für Geologie und Paläontologie Abhandlungen* **184**: 279–314.

- Setoguchi T, Tsubamoto T, Hanamura H, Hachiya K. 1999.** An early Late Cretaceous mammal from Japan, with reconsideration of the evolution of tribosphenic molars. *Paleontological Research* **3**: 18–28.
- Sigogneau-Russell D, Dashzeveg D, Russell DE. 1992.** Further data on *Prokennalestes* (Mammalia, Eutheria, inc. sed.) from the Early Cretaceous of Mongolia. *Zoologica Scripta* **21**: 205–209.
- Strauss, J. 2008.** A systematic review of Late Cretaceous and Early Paleocene cimolestids (Mammalia, Eutheria). San Diego State University MSc Thesis.
- Szalay FS, Sargis EJ. 2006.** Cretaceous therian tarsals and the metatherian-eutherian dichotomy. *Journal of Mammalian Evolution* **13**: 171–210.
- Tabuce R, Vianey-Liaud M, Garcia G. 2004.** A eutherian mammal in the latest Cretaceous of Vitrolles, southern France. *Acta Palaeontologica Polonica* **49**: 347–356.
- Wible JR. 1990.** Late Cretaceous marsupial petrosal bones from North America and a cladistic analysis of the petrosal in therian mammals. *Journal of Vertebrate Paleontology* **10**: 183–205.
- Wible JR. 2003.** On the cranial osteology of the short-tailed opossum *Monodelphis breviceaudata* (Didelphidae, Marsupialia). *Annals of Carnegie Museum* **72**: 137–202.
- Wible JR. 2008.** On the cranial osteology of the Hispaniolan solenodon, *Solenodon paradoxus* Brandt, 1833 (Mammalia, Lipotyphla, Solenodontidae). *Annals of Carnegie Museum* **77**: 321–402.
- Wible JR, Novacek MJ, Rougier GW. 2004.** New data on the skull and dentition in the Mongolian Late Cretaceous eutherian mammal *Zalambdalestes*. *Bulletin of the American Museum of Natural History* **281**: 1–144.
- Wible JR, Novacek MJ, Rougier GW, Asher RJ. 2009.** The eutherian mammal *Maelestes gobiensis* from the Late Cretaceous of Mongolia and the phylogeny of Cretaceous Eutheria. *Bulletin of the American Museum of Natural History* **327**: 1–123.
- Wible JR, Rougier GW, Novacek MJ, Asher RJ. 2007.** Cretaceous eutherians and Laurasian origin for placental mammals near the K/T boundary. *Nature* **447**: 1003–1006.
- Wible JR, Rougier GW, Novacek MJ, McKenna MC. 2001.** Earliest Eutherian ear region: a petrosal referred to *Prokennalestes* from the Early Cretaceous of Mongolia. *American Museum Novitates* **3322**: 1–44.

## APPENDIX 1

## SKULL TERM ABBREVIATIONS

ac?, possibly ascending canal of the superior ramus of the stapedial artery; acf, anterior cranial fossa; al, alisphenoidal wing of basisphenoid; ar, annular ridge; 'asof', 'anterior small optic foramen'; bs, body of basisphenoid; bsc, midline crest of the basisphenoid; caf, carotid foramen; cf, cerebral fossa; cpc? fossa for craniopharyngeal canal?; cg, chiasmatic groove; ds, dorsum sellae; df, frontal diploic vein foramen; enpt, broken base of entopterygoid process; et, articulation with ethmoturbinals; ex, exoccipital; fc, fenestra cochleae; fm, foramen magnum; foo, foramen ovale (anteromedial edge); for?, foramen rotundum?; fr, frontal; fr/la?, possible frontal/lacrimal articulation; fr/na, frontal/nasal articulation; fr/pa, frontal/parietal articulation; fs, fossa for stapedius muscle; fse, fenestra semilunaris; fv, fenestra vestibuli; hf, hypoglossal foramen; hfa, hiatus Fallopii; hyf, hypophyseal fossa; iam, internal auditory meatus; iof, infraorbital foramen; ips, sulcus for inferior petrosal sinus; jf, jugular foramen; mpj, maxillary process of the jugal; mtc, maxilloturbinal cristae; oc, occipital condyle; of, optic foramen; olf, olfactory fossa; orb, orbitosphenoidal wing of presphenoid; orf, orbital fissure (half each on pre- and basisphenoid); pa?, parietal, presence uncertain; paf, palatine facet; pca, pars canicularis; pc, prootic canal; pco, pars cochlearis; pet, petrosal; pf, piriform fenestra (anteromedial edge); pmf, premaxillary facet; pm/mx, premaxilla/maxilla articulation; ppr, paroccipital process; pr, presphenoid exposed ventrally; pr/bs, presphenoid/basisphenoid articulation; prm, promontorium; pr/et, presphenoid/ethmoid lamina articulation; pr/pl, presphenoid/palatine articulation; pr/vo, presphenoid/vomer articulation; pscp, posterior semicircular canal prominence; 'psof', 'posterior small optic foramen'; ptc, post-temporal canal; ptf, post-temporal foramen (medial side); sf, subarcuate fossa; sica, sulcus for the internal carotid artery; 'smf', 'small foramen'; sof, suborbital foramen; ss, sphenoidal sinus; sss, sulcus for sigmoid sinus; ta, tympanic aperture facial canal; tr, transverse ridge separating cerebral and olfactory fossae; ts, tuberculum sellae; tt, tegum tympani.

## APPENDIX 2

Upper tooth measurements. Abbreviations: L, length; W, width; AW, anterior width; PW, posterior width; H, height. Five-digit numbers are ZIN specimens, those with a hyphen are URBAC specimens, and with forward slash are CCMGE numbers.

Specimen no.	P4		DP5			P5			M1			M2			M3		
	L	AW	L	AW	PW	L	AW	PW									
<i>Aspanlestes aptap</i>																	
04-100	2.13	1.39															
4/12455			1.78	1.92	2.11												
19/12953								2.50									
04-307						1.73	2.23	2.38									
02-45	1.57	1.12				1.80	3.34	2.61	2.00	2.87	2.93	1.85	3.16	2.99			
1/12455						1.94	2.09	2.73	2.33	2.66	3.06	2.36	2.90	3.08			
04-165									2.37	2.97	3.12						
99-65									2.22	2.68	2.92						
04-152														3.03			
06-84									2.25	2.88	3.17						
03-10									2.43	2.85	3.16						
3/12455									2.14	2.51	2.70						
04-271									2.42	2.83	3.06						
06-116									2.39	2.70	3.07						
97883									2.28	2.76	3.18						
04-209									2.36	2.99	3.30						
04-126									2.39	2.93	3.17						
98-009									2.17	2.70	2.94						
04-392														3.10			
68/12455												2.29	3.11	3.18			
02-101																	3.07
06-117												2.34	3.18	3.17			
06-67														3.20			
04-252												2.10	2.93	3.07			
03-188												2.39	3.40	3.29			
03-21												2.17	3.30	3.31			
Average	1.85	1.26				1.82	2.55	2.56	2.29	2.79	3.06	2.11	3.03	3.04			
<i>Aspanlestes</i> sp.																	
85299	2.14	1.13															
<i>Parazhelestes mynbulakensis</i>																	
04-168			2.29	2.55	2.59												
04-206			2.14	2.08	2.36												
85293			2.06	2.09	2.33												
04-151			2.23	2.43	2.65												
02-59						2.10	2.25	2.71									
02-1						2.14	2.66	2.93									
02-83						2.43	2.71	2.92									
02-2						2.39	2.80	3.13									
04-109						2.45	2.70	2.97									
02-8									2.80	3.27	3.61						
98-18									2.43	3.24	3.50						
03-177									2.34	3.44	3.57						
97884									2.55	3.17	3.39						
00-27									2.50	3.22							
11/12176						2.23	2.79	3.34	2.68	3.36	3.72	2.36	3.81	3.92			
22/12953									2.84	3.44	3.85						
98-19									2.61	3.32	3.63						
02-34									2.59	3.15	3.39						
04-137									2.61	3.08	3.53						
11/12953									2.57	3.13	3.53						

APPENDIX 2 *Continued*

Specimen no.	P4		DP5			P5			M1			M2			M3		
	L	AW	L	AW	PW	L	AW	PW									
02-28												2.52	3.73	3.92			
06-60												2.46	3.40				
04-162												2.50	3.72	3.72			
06-93												2.45	3.53	3.53			
04-192												2.47	3.41	3.57			
06-39												2.47	3.38	3.50			
03-179															2.283.91	3.38	
Average			2.18	2.29	2.48	2.29	2.65	3.00	2.59	3.26	3.57	2.46	3.57	3.69			
<i>Parazhelestes robustus</i>																	
70/12455	2.33	1.50				2.57	3.04	3.53	3.01	3.61	3.99	3.11	3.92	4.01	2.413.20	2.54	
98-23	2.55	1.75															
99-13												2.73	4.00	4.04			
04-200												3.55					
10/12953												3.78					
02-108															2.694.29	3.91	
35/12176						2.39	3.02	3.25									
98-22															2.233.58	3.06	
00-8									2.83	3.57	3.96						
20/12953									3.15	3.59	4.05						
04-270				2.28													
Average	2.44	1.63				2.48	3.03	3.39	3.00	3.59	3.87	2.92	3.96	4.03	2.443.69	3.17	
<i>Parazhelestes sp.</i>																	
85301															1.913.38	2.78	
<i>Zhelestes temirkazyk</i>																	
06-17						2.56	2.73	2.99									
10/12176	2.24	1.67				2.57	2.94	3.55	2.88	3.94	4.15	2.90	4.22	4.22	2.134.03	3.20	
02-81												2.66	3.63	3.76			
99-24												2.84	4.39	4.68			
Average						2.57	2.94	3.55				2.80	4.08	4.22			
<i>Eoungulatum kudukensis</i>																	
03-60						3.24	3.31	3.72									
2/12455									3.10	3.97	4.19						
03-185									3.07	3.72	4.01						
Average									3.10	3.97	4.19						

## APPENDIX 3

Lower tooth measurements. Abbreviations: L, length; W, width; TRW, trigonid width; TAW, talonid width; TRL, trigonid length; TAL, talonid length. Five-digit numbers are ZIN specimens, those with a dash are URBAC specimens, and with forward slash are CCMGE numbers.

Specimen no.	p2		p4		p5					dp5				
	L	W	L	W	L	TRW	TAW	TRL	TAL	L	TRW	TAW	TRL	TAL
<i>Aspanlestes aptap</i>														
4/12176			1.59	0.92	1.99	1.16	1.11	1.22	0.81					
04-288					2.17	1.12	1.07	1.34	0.80					
98-7					1.97	1.11	0.94	1.27	0.87					
82583										2.04	1.16	1.34	0.94	1.08
98-118										2.01	1.30	1.32	0.94	1.02
97-8										2.11	1.02	1.31	1.11	1.17
Average					2.04	1.13	1.04	1.28	0.83	2.05	1.16	1.32	1.00	1.09
<i>Parazhelestes mynbulakensis</i>														
02-13	1.32	0.71												

APPENDIX 3 *Continued*

Specimen no.	p2		p4		p5					dp5				
	L	W	L	W	L	TRW	TAW	TRL	TAL	L	TRW	TAW	TRL	TAL
97-3	1.35	0.73	2.19	0.91										
88477			1.71	0.76										
99-109			2.03	0.99	2.41	1.31	1.40	1.44	0.97					
98-13					1.99	1.20	1.20	1.12	0.90					
82580					2.09	1.21	1.30	1.21	0.88					
98-16					2.32	1.20	1.24	1.38	0.93					
1/12953					2.22	1.21	1.25	1.38	0.83					
04-226					2.41	1.34	1.35	1.35	1.01					
04-326										2.14	1.21	1.32	1.10	1.03
7/12953										2.17	1.32	1.57	1.15	1.17
Average	1.34	0.72	1.98	0.89	2.24	1.25	1.29	1.31	0.92	2.16	1.27	1.45	1.13	1.10
<i>Parazhelestes robustus</i>														
04-324		0.90												
<i>Zhelestes temirkazyk</i>														
2/12953					2.19	1.25	1.32	1.35	0.98					
<i>Eoungulatum kudukensis</i>														
00-12			1.82	0.94										
15/12953			2.00	1.25										
Average			1.91	1.10										
<i>Borisodon kara</i>														
106/12455					1.61	0.93	1.01	0.83	0.76					

Specimen no.	m1					m2					m3				
	L	TRW	TAW	TRL	TAL	L	TRW	TAW	TRL	TAL	L	TRW	TAW	TRL	TAL
<i>Aspanlestes aptap</i>															
4/12176	2.06	1.62	1.63	0.87	1.18	2.12	1.69	1.69	0.92	1.20					
04-134	2.36	1.50	1.59	1.03	1.34										
13/12953	2.27	1.58	1.61	1.01	1.29										
06-100	2.19	1.49	1.57	1.04	1.15										
98-148	1.92	1.41	1.24	0.92	0.99										
04-197	2.27	1.54	1.62	1.16	1.12										
99-032	2.22	1.52	1.59	1.07	1.16										
98-147	2.28	1.46	1.64	1.13	1.18										
97-004						2.22	1.64	1.58	0.99	1.22					
82584						2.19	1.54	1.45	1.13	1.21					
82852						2.28	1.68	1.71	0.99	1.26					
03-086						2.17	1.62	1.57	1.02	1.17					
00-063						2.17	1.59	1.59	0.92	1.25					
04-389						1.87	1.68	1.44	0.84	1.01					
04-185						2.27	1.75	1.64	1.02	1.27					
04-302						2.19	1.62	1.50	0.93	1.27					
96612						2.25	1.62	1.62	1.04	1.25					
6/12176								1.57		1.08	1.96	1.39	1.12	0.90	1.13
69/12455						2.03	1.49	1.55	0.83	1.20	2.01	1.38	1.21	0.78	1.22
98-152											2.31	1.48	1.29	1.03	1.29
82581											2.00	1.48	1.15	0.88	1.11
Average	2.20	1.52	1.56	1.03	1.18	2.16	1.63	1.58	0.97	1.20	1.99	1.39	1.17	0.84	1.18
<i>Parazhelestes mynbulakensis</i>															
04-402	2.45	1.72	1.68	1.03	1.34										
04-399	2.46	1.95	1.86	1.08	1.32										
04-398	2.34	1.66	1.77	0.94	1.36										
04-227	2.39	1.63	1.63	1.01	1.34										
03-211	2.39	1.57	1.61	1.04	1.32										
00-080	2.25	1.68	1.69	0.94	1.13										
99-109	2.37	1.86	2.00	1.09	1.29	2.54	2.01	2.09	1.11	1.39	2.53	1.93	1.63	0.92	1.61
98-13	2.41	1.87	1.86	1.11	1.30	2.48	1.90	1.83	1.11	1.38	2.28	1.57	1.38	0.94	1.34
03-192						2.28	1.66	1.67	0.99	1.26					
03-216						2.32	1.61	1.57	0.98	1.35					
04-141						2.31	1.75	1.69	1.04	1.32					
03-058						2.42	1.90	1.92	1.03	1.43					
04-096						2.48	1.89	2.01	1.06	1.43					
06-055						2.49	1.91	1.95	1.13	1.39					
03-170						2.42	1.81	1.83	1.11	1.35					
06-065						2.48	1.89	1.76	1.11	1.35					
04-312						2.37	1.73	1.77	0.93	1.36					
36/12000						2.31	1.76	1.82	1.01	1.31					
04-123						2.51	1.69	1.66	1.11	1.40					
04-006						2.50	1.81	1.86	1.04	1.46					
98-112						2.36	1.67	1.69	1.02	1.32					
99-003								1.72		1.29	2.15	1.48	1.36	0.89	1.22

APPENDIX 3 *Continued*

Specimen no.	m1					m2					m3				
	L	TRW	TAW	TRL	TAL	L	TRW	TAW	TRL	TAL	L	TRW	TAW	TRL	TAL
06-083											2.46	1.59	1.40	1.08	1.36
98-107											2.45	1.57	1.35	0.97	1.45
04-304											2.33	1.50	1.30	0.99	1.34
Average	2.38	1.74	1.76	1.03	1.30	2.42	1.80	1.80	1.05	1.36	2.37	1.61	1.40	0.97	1.39
<i>Parazhelestes robustus</i>															
04-324															
04-260						2.52	2.19	2.04	1.20	1.32					
98-14						2.54	2.00	2.17	1.07	1.45					
97-5						2.74	2.03	2.03	1.18	1.54					
04-176							2.17	1.97	1.08						
03-038											2.41	1.83	1.61	1.07	1.36
18/12953											2.76	2.24	1.96	1.20	1.54
Average						2.60	2.10	2.05	1.13	1.44	2.59	2.04	1.79	1.14	1.45
<i>Zhelestes temirkazyk</i>															
03-189	2.60	1.85	1.94	1.07	1.50										
14/12953	2.60	1.89	1.92	1.10	1.50										
06-031	2.28	1.50	1.58	0.97	1.24										
04-190	2.41	1.57	1.61	1.04	1.43										
04-310	2.41	1.59	1.73	0.99	1.40										
37/12000	2.33	1.45	1.57	1.07	1.41										
99-071			1.90		1.57	2.42	1.75	1.68	1.12	1.30					
3/12176						2.65	1.91	1.87	1.17	1.49					
6/12953						2.64	1.75	1.75	1.17	1.45					
02-035						2.55	1.80	1.78	1.12	1.44					
04-316							1.86		1.16						
06-073						2.42	1.75	1.68	1.12	1.30					
06-026						2.50	1.82	1.76	1.17	1.32					
02-065						2.65	1.89	1.80	1.25	1.52					
04-309						2.42	1.73	1.63	1.04	1.38					
98-15						2.69	1.97	1.89	1.18	1.48					
3/12953											2.31	1.43	1.21	0.93	1.26
Average	2.44	1.64	1.75	1.04	1.44	2.55	1.82	1.76	1.15	1.41					
<i>Eoungulatum kudukensis</i>															
17/12953	2.73	2.18	2.04	1.13	1.58										
00-049						2.84	2.42	2.33	1.29	1.57					
00-046						3.02	2.51	2.45	1.35	1.66					
04-088							2.25		1.38						
02-025						2.75	1.92	2.09	1.08	1.71					
06-042						2.94	2.28	2.29	1.36	1.57					
04-119											2.99	2.19	1.75	1.31	1.73
16/12953											2.80	2.08	1.90	1.16	1.63
Average						2.89	2.28	2.29	1.29	1.63	2.90	2.14	1.83	1.24	1.68
<i>Eoungulatum</i> sp.															
35052											2.70	1.90	1.97	1.40	1.29
<i>Borisodon kara</i>															
106/12455	2.13	1.63	1.49	0.90	1.20	2.22	1.78	1.68	0.96	1.24	2.39	1.63	1.55	1.02	1.36

## APPENDIX 4

SYNONYMIES, REFERRED ILLUSTRATIONS, AND  
REFERRED SPECIMENS*ASPANLESTES APTAP* NESOV, 1985A

*Aspanlestes aptap*: Nesov 1985a: 14, pl. 2, fig. 11; Nesov *et al.*, 1994: 62, pl. 4, fig. 1; Archibald, 1996: figs 2E, F, 3C; Nesov, 1997: pl. 49, fig. 14, pl. 50, figs 2, 4, pl. 52, figs 2, 4, pl. 53, figs 1, 6, pl. 55, fig. 2, pl. 56, fig. 1; Nesov *et al.* 1998: 49, figs 7, 20, 22F; Averianov, 2000: figs 30.4C, D, 30.6G, H, K, L and 30.7B, C; Kielan-Jaworowska *et al.*, 2004: fig 13.26F.

*Aspanlestes* cf. *aptap*: Nesov, 1985a: pl. 2, fig. 7.

*Theria* [indet.]: Nesov, 1985b: pl. 2, fig. 5; Nesov, 1993: fig. 4(11).

*Zhelestes* [sp.], or *Theria* indet. Nesov, 1985b: 213, pl. 2, fig. 5.

*Zhelestes? bezelgen*: Nesov, 1987: 207, pl. 1, fig. 1; Nesov & Kielan-Jaworowska, 1991: fig. 1; Nesov *et al.*, 1994: 66, pl. 6, fig. 1.

*Zhelestinae* [indet.]: Nesov, 1987: pl. 1, fig. 3.

*Eutheria* indet. Nesov, 1987: pl. 1, fig. 4; Nesov, 1993: fig. 2(4); Nesov, 1997: pl. 51, fig. 2.

*Zhelestes?* sp. cf. *Z. bezelgen*: Nesov, 1993: 125, figs 2(3), 5(5).

Gen. indet. Nesov *et al.*, 1994: pl. 7, fig. 6.

*Parazhelestes minor* [partim, nomen nudum]: Nesov, 1997: pl. 52, fig. 5.

*Ortalestes tostak*: Nesov, 1997: 171, pl. 48, fig. 8.

Zhelestidae cf. *Zhelestes* sp. Nesov, 1997: pl. 49, fig. 8.

*Sorlestes budan* [partim]: Nesov *et al.*, 1998: fig. 15F–J.

Cf. *Zhelestes* sp. Averianov, 2000: fig. 30.4I.

*Referred specimens*: URBAC 03–93, associated skull fragments, associated with URBAC 03–188, right maxillary fragment with M2 and alveoli for M1 and M3 (CBI-14); URBAC 02–45, left maxilla and jugal fragment with heavily worn C, P4–5, M1–2, and alveoli for P1–3 (CBI-4e); URBAC 00–15, left maxillary fragment with alveoli for P3–5, M 1 (CBI-14); URBAC 00–22, right maxillary fragment with alveoli for P5, M1–3 (CBI-14); URBAC 03–116, right maxillary fragment with alveoli for P5, M1–2 (CBI-14); URBAC 99–30, left maxillary fragment with M2 and alveoli for P5, M1, and M3 (CBI-14); CCMGE 68/12455, left maxillary with M2 and alveoli for P5, M1, and M3 (CBI-4, 1989); URBAC 03–188, right maxillary fragment with M2 and alveoli for M1 and M3, associated with URBAC 03–93, associated with skull fragments 03–93 (CBI-14); CCMGE 1/12455, left maxilla with P5, M1–2 and alveoli for P4 (holotype of? *Zhelestes bezelgen* Nesov, 1987, CBI-14, 1984); ZIN 88983, upper canine (CBI-4v, 1980); URBAC 04–100, right P4 (CBI-14); CCMGE 4/12455, left DP5 (holotype of *Ortalestes tostak* Nesov, 1997, CBI-4b); CCMGE 19/12953, right P5 (CBI-14); URBAC 04–229, left P5 (CBI-4e); URBAC 04–274, right P5 (CBI-14); URBAC 04–307, right P5 (CBI-14); URBAC 04–313, left P5 (CBI-14); CCMGE 38/12000, right M1 lacking parastylar lobe (CDZH-17a); CCMGE 3/12455, left M1 (CBI-14, 1984); ZIN 97883, left M1 (CBI-14, published previously under incorrect number CCMGE 103/12455); URBAC 03–10, left M1 (CBI-14); URBAC 03–78, left M1 (CBI-14); URBAC 04–126, left M1 (CBI-14); URBAC 04–152, left M1 lacking parastylar lobe (CBI-14); URBAC 04–165, right M1 (CBI-14); URBAC 98–9, left M1 (CBI-14); URBAC 99–65, left M1 (CBI-14); URBAC 04–271, left M1 (CBI-14); URBAC 04–392, left M1 lacking parastylar lobe (CBI-17); URBAC 06–84, left M1 (CBI-4e); URBAC 06–116, left M1 (CBI-14); URBAC 02–102, left M2 heavily worn (CBI-4e); URBAC 03–21, right M2 (CBI-14); URBAC 04–209, right M2 (CBI-14); URBAC 04–252, left M2 (CBI-14); IZANUz P2155-M-2, left M2 (CBI-14, 1994); URBAC 06–67, right M2 lacking metastylar lobe (CBI-4e); URBAC 06–117, left M2 (CBI-17); URBAC 04–390, right M2 labial fragment (CBI-17); ZIN 88984, right M2 lingual fragment (CBI-14, 1989); ZIN 82585, right M1 or M2 lingual fragment (CBI-14); URBAC 98–6, left M1 or M2 lingual fragment (CBI-14); URBAC 04–395, right dentary fragment with alveoli or roots for i1–4, c, p2, and partial p1 (CBI-14); ZIN 88488, right dentary fragment with alveoli for p2, p4–5 [p3 not indicated] (CBI-14, 1984); ZIN 88475, right dentary with partial m3 talonid and alveoli for p1–5, m1–2

(CBI-14, 1987); URBAC 02–66, right dentary fragment with alveoli for p3–5, m1–3 (CDZH-17a); URBAC 02–68, right dentary fragment with dp5, fragment of dp4, and anterior alveolus for m1 (CBI-4e); URBAC 99–77, right dentary fragment with incomplete p5 and alveoli for p4 and m1–3 (CBI-14); URBAC 03–25, left dentary fragment with alveoli for p5, m1–3 (CBI-14); URBAC 97–4, left dentary fragment with m2 and alveoli for m1 and m3 (CBI-14); URBAC 02–64, left dentary fragment with m2 talonid and alveoli for m1 and m3 (CBI-4e); URBAC 00–29, left dentary fragment with erupting m3 and alveoli for m1–2 (CBI-14); URBAC 03–31, left dentary fragment with alveoli for m1–3 (CBI-14); URBAC 03–87, right dentary fragment with alveoli for m1–3 (CBI-14); URBAC 06–18, right dentary fragment with alveoli for m1–3 (CBI-14); URBAC 02–77, left dentary fragment with incomplete m3 in crypt, coronoid process, angular process, and mandibular condyle (CBI-4e); URBAC 04–196, right dentary fragment with alveoli for m2 and erupting m3 and angular process (CBI-14); CCMGE 69/12455, left dentary fragment with worn m2–3 (CBI-14, 1987); CCMGE 6/12176, left dentary fragment with m2 talonid and m3 (CBI-14); URBAC 02–27, right dentary fragment with m3 talonid unerupted and angular process (CBI-4e); CCMGE 78/12455, right p5 worn (CBI-7a); ZIN 88473, right p5 [CDZH-17a, 1978(1980)]; URBAC 98–7, left p5 (CBI-14); URBAC 04–288, left p5 (CBI-4e); URBAC 04–320, left p5 worn (CBI-14); ZIN 82583, left worn dp5 (CBI-?); URBAC 97–8, left dp5 (CBI-14); URBAC 98–118, right worn dp5 (CBI-14); URBAC 98–130, left dp5 trigonid (CBI-14); CCMGE 13/12953, right m1 (CBI-14); URBAC 98–147, right m1 heavily worn (CBI-14); URBAC 98–148, left m1 (CBI-14); URBAC 99–32, right m1 (CBI-14); URBAC 04–134, right m1 (CBI-14); URBAC 04–197, left m1 (CBI-14); URBAC 06–100, left m1 (CBI-4e); URBAC 98–26, left m1 trigonid (CBI-14); URBAC 98–119, right m1 trigonid (CBI-14); URBAC 98–120, left m1 trigonid (CBI-14); ZIN 96612, right m2 (CBI-14) [published in Nesov *et al.*, 1998: 49 under incorrect number CCMGE 8/12953]; ZIN 82582, left m2 (CBI-?); ZIN 82584, left m2 (CBI-?); URBAC 00–63, right m2 (CBI-14); URBAC 03–86, right m2 (CBI-14); URBAC 04–185, right m2 (CBI-14); URBAC 04–302, right m2 worn (CBI-14); URBAC 04–389, right m2 (CBI-14); URBAC 98–110, right m2 trigonid (CBI-14); URBAC 98–160, right m2 trigonid (CBI-14); URBAC 04–311, right m1 or m2 talonid (CBI-14); URBAC 04–333, left m1 or m2 talonid (CBI-14); ZIN 82581, left m3 (CBI-?); URBAC 98–152, left m3 (CBI-14).

#### ASPANLESTES SP.

*Paranycetoides* sp. Archibald & Averianov, 2001: 542, fig. 4.

cf. *Aspanlestes* sp. Averianov & Archibald, 2003: 180, fig. 10.

*Eutheria* indet. [partim]: Averianov & Archibald, 2003: 183.

*Paranyctoides* sp. cf. *P. aralensis*: Averianov & Archibald, 2003: 190.

*Referred specimens*: ZIN 85299, right P4 (CBI-117, 1999); ZIN 85298, right P5 heavily worn (CBI-117, 1999); ZIN 85044, left DP5 (CBI-117, 1998); ZIN 85297, fragmented right M1 (CBI-117, 1999); URBAC 02–101, right M2 lacking parastylar lobe (CBI-117); ZIN 85051, left m2 lacking most of the talonid (CBI-117, 1998).

*PARAZHELESTES MYNBULAKENSIS* (NESOV, 1985B)

**COMB. NOV.**

*Zhelestes* cf. *temirkazyk*: Nesov, 1985a: pl. 3, fig. 5.

*Zalambdalestes?* *mynbulakensis* [partim]: Nesov, 1985b: 212, pl. 2, fig. 2; Nesov *et al.*, 1994: 66, pl. 5, fig. 2; Gheerbrant & Astibia, 1999: fig. 3h.

Zhelestidae [indet.]: Nesov, 1993: fig. 5(6); Nesov, 1997: pl. 54, fig. 4.

gen. indet. Nesov *et al.*, 1994: pl. 7, fig. 8.

*Parazhelestes* sp. nov. Archibald, 1996: fig. 2G, H; Averianov, 2000: figs 30.6Q, 30.7G.

*Parazhelestes minor* [partim, nomen nudum]: Nesov, 1997: pl. 52, fig. 3, pl. 54, fig. 1.

*Sorlestes budan* [partim]: Nesov, 1997: pl. 49, fig. 12, pl. 56, fig. 4; Nesov *et al.*, 1998: fig. 17.

*Parazhelestes minor*: Nesov *et al.*, 1998: figs 12, 13, 20.

Possible *Sorlestes budan*: Averianov, 2000: fig. 30.5E, F.

*Referred specimens*: URBAC 04–162, right maxillary fragment with M2 and alveoli for P1–5 and M1 (CBI-14); CCMGE 11/12176, right maxillary fragment with P5, M1–2, roots of P4, and alveoli of P2–3, M3 (CBI-14, 1980); URBAC 02–59, right maxillary fragment with P5 and alveoli for P2–4, M1 (CBI-4e); ZIN 88499, left maxillary fragment with alveoli for P3–5, M1–2 (CBI-14, 1989); URBAC 02–38, left maxillary fragment with alveoli for P4–5, M1–3 (CBI-4e); URBAC 02–1, left maxillary fragment with P5 and alveoli for P4 and M1 (CBI-4e); URBAC 00–24, right maxillary fragment with alveoli for P5, M1 (CBI-4e); URBAC 98–20, left maxillary fragment with not erupted and incomplete P5 (CBI-14); URBAC 06–80, right maxillary fragment with M2 labial part and alveoli for M1 and M2 (CBI-4e); ZIN 88468, left maxillary fragment with M1–3 heavily worn and palatine fragment (CBI-4b, 1980); CCMGE 21/12953, right P5 (CBI-14); URBAC 00–42, left P5 (CBI-14); URBAC 02–83, right P5 (CBI-4e); URBAC 04–109, left P5 (CBI-14); URBAC 04–151, right DP5 (CBI-14); URBAC 04–168, right DP5 (CBI-14); URBAC 04–206,

left DP5 (CBI-14); URBAC 04–213, right DP5 (CBI-14); URBAC 04–397, left DP5 (CBI-17); ZIN 97884, left M1 (?CBI-14; published previously under incorrect number CCMGE 104/12455); CCMGE 11/12953, right M1 (holotype of *Parazhelestes minor* Nesov *et al.*, 1998, CBI-4); CCMGE 22/12953, left M1 (CBI-14); URBAC 98–18, right M1 (CBI-14); URBAC 98–19, right M1 (CBI-14); URBAC 98–108, left M1 parastylar lobe and paracone (CBI-14); URBAC 00–27, right M1 (CBI-14); URBAC 00–34, right M1 with eroded enamel (CBI-4e); URBAC 00–70, right M1 paracone and parastylar lobe (CBI-14); URBAC 02–8, left M1 (CBI-4e); URBAC 02–34, right M1 (CBI-4e); URBAC 03–177, right M1 with eroded enamel (CBI-14); URBAC 04–99, right M1 (CBI-14); URBAC 04–137, right M1 (CBI-14); URBAC 04–212, left M1 (CBI-14); URBAC 04–275, left M1 lingual fragment (CBI-14); URBAC 06–50, left M1 (CBI-17); CCMGE 12/12953, right M2 lacking parastylar lobe (CBI-14, 1993); URBAC 98–21, right M2 (CBI-14); URBAC 02–28, left M2 (CBI-4e); URBAC 04–34, right M2 lacking parastylar lobe (CBI-14); URBAC 04–73, left M2 with eroded enamel (CBI-14); URBAC 04–121, left M2 lacking parastylar lobe (CBI-14); URBAC 04–192, right M2 (CBI-14); URBAC 04–308, left M2 heavily worn (CBI-14); URBAC 06–13, right M2 heavily worn (CBI-14); URBAC 06–39, left M2 (CBI-17); URBAC 06–60, left M2 with damaged metastylar region (CBI-4e); URBAC 06–93, left M2 (CBI-4e); URBAC 97–2, left M1 or M2 lingual part, heavily worn (CBI-14); URBAC 02–51, left M1 or M2 lingual part, heavily worn (CBI-4e); URBAC 03–27, right M1 or M2 lacking labial part (CBI-14); URBAC 03–45, left M1 or M2 lingual part (CBI-14); URBAC 04–396, left M1 or M2 lingual part, heavily worn (CBI-14); URBAC 03–179, left M3 (CBI-14); ZIN 88481, left dentary fragment with alveoli for i1–4, double-rooted c, p1–4 (CBI-14, 1991); URBAC 04–193, right dentary fragment with alveoli for i1–4, double-rooted c, and p1–4 (CBI-14); ZIN 88482, left dentary fragment with alveoli for i1–3, double-rooted c, p1–2, p4–5 [p3 probably lost during ontogeny] (CBI-14, 1991); URBAC 03–40, left dentary fragment with alveoli for i1–4, double-rooted c, p1–5 (CBI-14); ZIN 88470, left dentary fragment with erupting c, m3 trigonid in crypt, and alveoli for i1–4, p1–4, dp5, m1–2 (CBI-14, 1984); URBAC 06–113, left dentary fragment with i2–3 with worn and broken crowns, mesial root of c, and alveoli for i1, i4, and c distal root (CBI-4e); URBAC 99–109, left dentary fragment with p4–5, m1–3, alveoli for i2–3, root of i4, and alveoli for double-rooted c, p1–2 [p3 probably lost during ontogeny] (CBI-14); URBAC 98–13, left dentary fragment with p4, m1–3 and alveoli for i2–3, double-rooted c, p1–4 (CBI-14); URBAC 03–5, left dentary fragment with alveoli of i3, double-rooted c,

p1–5 (CBI-14); URBAC 98–17, left dentary fragment with alveoli for double-rooted c, p1–4 (CBI-14); URBAC 99–81, left dentary fragment with alveoli for double-rooted c, p1–4 (CBI-14); URBAC 03–8, left dentary fragment with alveoli for double-rooted c, p1–4 (CBI-14); URBAC 06–92, right dentary fragment with alveoli for double-rooted c, p1–4 (CBI-4e); ZIN 88484, right dentary fragment with alveoli for double-rooted c, p1–5 (CBI-14, 1987); URBAC 00–11, right dentary fragment with alveoli for double-rooted c, p1–5 (CBI-14); URBAC 02–104, right dentary fragment with alveoli for double-rooted c, p1–5 (CBI-4e); URBAC 06–111, left dentary fragment with p2 in crypt and alveoli for dc?, p1, p3 (CBI-4e); URBAC 97–3, right dentary with p2, p4, roots of p5, and alveoli for p1, p3, and m1 (CBI-14); URBAC 06–61, left dentary fragment with alveoli for p1–5 (CBI-4e); URBAC 02–13, left dentary fragment with p2, incomplete p4, and alveoli for c, p1, p3, and p5 (CBI-4e); URBAC 98–24, right dentary fragment with alveoli for double-rooted c, p1–5, m1–3 (CBI-14); ZIN 88497, left dentary fragment with alveoli for p1–4 (CBI-14, 1989); URBAC 03–62, right dentary fragment with alveoli for p1–4 (CBI-14); ZIN 88483, left dentary fragment with alveoli for p1–5, m1 (CBI-14, 1987); ZIN 88479, left dentary fragment with alveoli for p1–5, m1–3 (CBI-14, 1989); ZIN 88490, right dentary fragment with alveoli for p2–5, m1 (CDZH-17a, 1978[1983]); URBAC 00–68, right dentary fragment with erupting p2, root of dp2, and alveoli for dc, p3, dp4–5, m1–2 (CBI-14); ZIN 88491, right dentary fragment with not erupted p2 and alveoli for double-rooted dc1(?), p1, p3, dp4, p4, dp5, m1, not erupted m2 (CBI-14, 1987); URBAC 04–171, right dentary fragment with alveoli for p2–5 and m1–3 (CBI-14); ZIN 88449, right dentary fragment with alveoli for p3–5, m1–2 (CBI-14, 1989); ZIN 88485, right dentary fragment with not erupted p4 and alveoli for p1–3, dp4 (CBI-14); ZIN 88477, left dentary fragment with p4, anterior root of p5, and alveoli for p3 (CBI-5a, 1989); URBAC 02–9, right dentary fragment with alveoli for p4–5, m1–3 (CBI-4e); CCMGE 7/12953, right dentary fragment with dp5 (CBI-5a); CCMGE 1/12953, left dentary fragment with p5 and alveoli or roots for m1–3 (CBI-14, 1987); URBAC 00–45, right dentary fragment with alveoli for p5, m1–3 (CBI-5); ZIN 88474, right dentary fragment with alveoli for p5, m1–3 (CBI-14, 1984); URBAC 06–110, right dentary fragment with m3 trigonid in crypt and alveoli for p5, m1–2 (CBI-14); ZIN 88478, left dentary fragment with alveoli for m1–3 (CBI-14, 1985); URBAC 99–3, left dentary fragment with incomplete m2 and m3 (CBI-14); IZANUz P2155-M-1, left dentary fragment with erupting m3 and alveoli for m2, part of coronoid process, and angular process (CBI-14, 1994); ZIN 89006, left dentary fragment

with alveoli for m2–3 (CBI-14, 1989); URBAC 00–21, right dentary fragment with alveoli for m2–3 (CBI-14); URBAC 06–32, right dentary fragment with alveoli for m1–3 (CBI-17); ZIN 82580, right p5 (CBI-?); URBAC 98–16, right p5 (CBI-14); URBAC 04–226, right p5 (CBI-14); ZIN 88476, left dp5 heavily worn (CBI-14, 1985); URBAC 04–326, left dp5 (CBI-4e); URBAC 00–80, right m1 (CBI-14); URBAC 03–211, right m1 (CBI-14); URBAC 04–227, right m1 (CBI-14); URBAC 04–398, right m1 (CBI-14); URBAC 04–399, right m1 (CBI-17); URBAC 04–402, right m1 (CBI-14); URBAC 98–112, right m2 (CBI-14); URBAC 98–139, left m2 heavily worn (CBI-14); URBAC 03–58, left m2 worn (CBI-14); URBAC 03–170, right m2 (CBI-14); URBAC 03–192, right m2 (CBI-4e); URBAC 03–216, left m2 (CBI-14); URBAC 04–6, left m2 (CBI-14); URBAC 04–96, right m2 (CBI-14); URBAC 04–123, left m2 (CBI-14); URBAC 04–141, left m2 (CBI-14); URBAC 04–312, right m2 (CBI-14); URBAC 04–400, left m2 fragment (CBI-17); URBAC 06–55, right m2 (CBI-17); URBAC 06–65, right m2 (CBI-4e); URBAC 98–111, left m1 or m2 talonid (CBI-14); URBAC 98–151, left m1 or 2 talonid (CBI-14); URBAC 98–156, right m1 or 2 talonid (CBI-14); URBAC 04–332, left m1 or m2 talonid (CBI-14); URBAC 04–401, right m1 or m2 talonid (CBI-14); URBAC 98–107, left m3 (CBI-14); URBAC 04–340, left m3? worn (CBI-14); URBAC 06–83, right m3 (CBI-4e); URBAC 04–304, right m3 (CBI-14); URBAC 03–210, right m2 or m3 trigonid (CBI-14); URBAC 04–323, right m2 or m3 trigonid (CBI-14).

*PARAZHELESTES ROBUSTUS* NESOV, 1993

Kennalestidae [indet.]: Nesov, 1985a: pl. 3, fig. 1.

*Parazhelestes robustus*: Nesov, 1993: 124, fig. 2(1); Nesov, 1997: pl. 53, figs 2, 3; Nesov *et al.*, 1998: 55, figs 11, 20; Averianov, 2000: figs 30.6R, 30.7A; Kielan-Jaworowska *et al.*, 2004: fig. 13.26D<sub>1, 2</sub>.

Condylarthra indet. Nesov, 1993: fig. 6(3).

cf. gen. et sp. nov. Archibald, 1996: fig. 2C.

cf. *Eoungulatum kudukensis* [nomen nudum, partim]: Nesov, 1997: pl. 53, fig. 5.

cf. *Eoungulatum kudukensis* [partim]: Nesov *et al.*, 1998: figs 14P, Q, 20.

*Referred specimens*: URBAC 02–24, left maxilla with alveoli for P2 and roots for C, P1 (CBI-4e); ZIN 88450, right maxillary fragment with alveoli for P5, M1–2 (CBI-14, 1984); URBAC 04–200, left maxillary fragment with M1 lacking parastylar lobe (CBI-14); URBAC 98–22, right maxillary fragment with M3 and alveoli for M2 (CBI-14); URBAC 98–23, left P4 (CBI-14); CCMGE 35/12176, right P5 (CBI-4v); URBAC 04–270, right DP5 labial fragment (CBI-14); CCMGE 10/12953, right M1 lacking parastylar lobe (CBI-14, 1993); CCMGE 20/12953, left M1 (CBI-14); URBAC

99–39, left M1 (CBI-14); URBAC 00–8, right M1 (CBI-14); URBAC 99–13, right M2 metastylar lobe somewhat damaged (CBI-14); URBAC 02–108, M1 or M2 heavily worn (CBI-4e); URBAC 04–11, right M1 or M2 lingual fragment (CBI-14); IZANUZ P2155-M-5, right dentary with alveoli for i4, double-rooted c and p2, 4, 5, or dp2–4 (CBI-14, 1994); ZIN 88465, right dentary with alveoli for p2–5, m1–3 (CBI-14, 1985); ZIN 88489, left dentary with alveoli for p2–5 (CBI-14, 1984); URBAC 03–120, right dentary with alveoli for p3–5, m1–3 (CBI-14); ZIN 88495, left dentary with alveoli for p3–5, m1–3 (CBI-14, 1985); URBAC 02–47, right dentary with alveoli for p4–5, m1–3 (CBI-4e); URBAC 02–10, right dentary with alveoli for p4–5, m1–2 (CBI-4e); ZIN 88462, right dentary with alveoli for m1–3, m3 was not erupted (CBI-14, 1980); ZIN 88454, left dentary with alveoli for m1–3 (CBI-56, 1989); URBAC 03–124, left dentary with alveoli for m1–3 (CBI-14); ZIN 88936, left dentary with roots or alveoli for m1–3 (CBI-14, 1989); URBAC 06–8, left dentary with alveoli or roots for m1–3 (CBI-14); URBAC 03–125, right dentary with alveoli or roots for m1–3, m3 was not erupted (CBI-14); ZIN 88451, right dentary with roots or alveoli for m2–3 (CBI-51, 1987); ZIN 88457, right dentary with alveoli for m2–3 (CBI-14, 1980); ZIN 88466, right dentary with alveoli for m2–3 (CBI-14, 1989); ZIN 88494, right dentary with alveoli for m2–3 (CBI-14, 1984); URBAC 00–17, left dentary with alveoli for m2–3 (CBI-14); ZIN 88455, left dentary with alveoli for m3 (CBI-14, 1984–1985); ZIN 88456, left dentary with alveoli for m3 (CBI-14, 1987); ZIN 88463, right dentary with alveoli for m3 (CBI-51, 1987); ZIN 88969, left dentary with posterior alveolus for m3 and angular process (CDZH-17a, 1978); URBAC 97–5, right dentary with m2 and alveoli for m1 and m3 (CBI-14); URBAC 04–324, left p2 (CBI-14); URBAC 98–14, right m2 (CBI-14); URBAC 04–176, right m2 lacking entoconid and hypoconulid (CBI-14); URBAC 04–260, right m2 (CBI-14); URBAC 03–38, right m3 (CBI-14).

#### PARAZHELESTES SP.

*Paranyctoides* sp. Averianov & Archibald, 2003: 179, fig. 8.

*Parazhelestes* sp. cf. *P. robustus* [partim]: Averianov & Archibald, 2003: 181, fig. 11a–c.

*Eutheria* indet. [partim]: Averianov & Archibald, 2003: 183.

*Referred specimens*: ZIN 85293, left DP5 (CBI-117, 1999); ZIN 85301, left M3 (CBI-117, 1999); ZIN 85295, left M3 paracone and parastylar lobe (CBI-117, 1999).

#### ZHELESTES TEMIRKAZYK NESOV, 1985A

Placentalia [indet.]: Nesov, 1982: pl. 2, fig. 2.

*Kumsuperus avus* [nomen dubium]: Nesov 1984: 63, fig. e-zh; Nesov & Kielan-Jaworowska, 1991: fig. 1; Nesov *et al.*, 1994: 59, pl. 2, fig. 1; Nesov, 1997: pl. 55, fig. 1; Nesov *et al.*, 1998: 65, fig. 18; Averianov, 2000: fig. 30.5C.

cf. *Cimolestes* sp. Nesov, 1984: fig. g, d.

*Zhelestes temirkazyk*: Nesov, 1985a: 16, pl. 3, fig. 14; Nesov *et al.*, 1994: 63, pl. 5, fig. 1; Archibald, 1996: fig. 4A; Nesov, 1997: pl. 52, fig. 1; Nesov *et al.*, 1998: 53, figs 9, 10, 20; Averianov, 2000: fig. 30.7D, E; Kielan-Jaworowska *et al.*, 2004: fig. 13.26A<sub>1, 2</sub>.

*Sorlestes budan* [partim]: Nesov, 1985a: 14, pl. 2, fig. 13; Nesov & Kielan-Jaworowska, 1991: fig. 1; Nesov *et al.*, 1994: 61, pl. 1, fig. 7; Nesov, 1997: pl. 50, fig. 3; Nesov *et al.*, 1998: figs 15A–D and 16; Gheerbrant & Astibia, 1999: fig. 3i; Averianov, 2000: fig. 30.7H, I; Kielan-Jaworowska *et al.*, 2004: fig. 13.26E<sub>1, 2</sub>.

*Zalambdalestes? mynbulakensis* [partim]: Nesov, 1985b: pl. 2, fig. 3; Nesov, 1997: pl. 49, fig. 15.

*Aspanlestes aptap* [partim]: Nesov, 1997: pl. 46, fig. 1; Averianov, 2000: fig. 30.4F.

*Referred specimens*: URBAC 98–117, right incomplete P4 (CBI-14); URBAC 06–17, right maxilla fragment with P5 and alveoli for P4 and M1 (CBI-14); URBAC 02–81, right maxilla with M2 and alveoli for M1 (CBI-4e); URBAC 99–24, left maxilla with worn M2 and alveoli for M1 and M3 (CBI-14); CCMGE 3/11658, left dentary with erupting c, p2, and alveoli for i1–4, p1 and p3 (CDZH-25); ZIN 88480, left dentary with alveoli for i1–4, single-rooted c, p1–5, m1 (CBI-56, 1989); ZIN 88469, right dentary with alveoli for single-rooted c, p1–3, dp4–5, m1–3, m2–3 were not erupted, part of coronoid process, and angular process (CBI-14, 1989); ZIN 82555, right dentary with not erupted p2 and m2, m3 in crypt, and alveoli for c, p1, p3–4, dp5, m1 (CBI-14, 1985); URBAC 00–51, left dentary with alveoli or roots for c, p1–5 (CBI-14); ZIN 88461, right dentary with alveoli for p2–5, m1–3 (CBI-14, 1987); ZIN 88448, left dentary with erupting p5, m3 trigonid in crypt, and alveoli for m1–2 (CBI-14, 1984); URBAC 03–218, right dentary with unerupted p5 and m3 and alveoli for p2–4 and m1–2 (CBI-14); URBAC 99–71, left dentary with m1 talonid and m2 (CBI-14); CCMGE 3/12176, right dentary with m2 and alveoli for m3 (holotype of *Sorlestes budan* Nesov, 1985a, CBI-14, 1980); CCMGE 13/11758, left dentary with heavily worn m1–3 (holotype of *Kumsuperus avus* Nesov, 1984, CBI-4v, 1979); ZIN 88453, left dentary with roots of m2–3 (CBI-14, 1985); CCMGE 2/12953, left p5 (CBI-14); CCMGE 37/12000, left m1 (CBI-4v, 1980); CCMGE 14/12953, left m1 (CBI-14); URBAC 03–189, right m1 (CBI-14); URBAC 04–310, right m1 (CBI-14); URBAC 06–31, right m1 (CBI-4e);

URBAC 04–190, left worn m1? (CBI-14); URBAC 02–35, right m2 (CBI-4e); CCMGE 6/12953, right m2 (CBI-14, 1993); URBAC 98–15, right m2 (CBI-14); URBAC 06–73, right m2 (CBI-4e); URBAC 04–309, right m2 (CBI-14); URBAC 02–65, left m2 (CBI-4e); URBAC 06–26, left m2 (CBI-14); URBAC 04–316, right m2 trigonid (CBI-14); CCMGE 3/12953, right worn m3 (CDZH-17a); ZIN 82586, right worn mx (CBI-14).

*EOUNGULATUM KUDUKENSIS* NESOV *ET AL.*, 1998

Advanced form of Proteutheria, intermediate to Condylarthra: Nesov, 1987: pl. 1, fig. 2.

Archaic ungulate mammals: Nesov & Kielan-Jaworowska, 1991: fig. 1.

Condylarthra of the family Periptychidae, new genus and species: Nesov, 1993: fig. 1(3).

Condylarthra cf. Periptychidae gen. et sp. nov. Nesov, 1995: pl. 11, fig. 6.

cf. gen. et sp. nov. Archibald, 1996: fig. 2A, B.

gen. et sp. nov. Archibald, 1996: figs 2D, 3D.

*Sorlestes budan* [partim]: Archibald, 1996: fig. 4B; Nesov, 1997: pl. 51, fig. 4; Averianov, 2000: fig. 30.6X; Kielan-Jaworowska *et al.*, 2004: fig. 13.26A<sub>2</sub>.

Zhelestidae indet. Nesov, 1997: pl. 51, fig. 5.

*Eoungulatum kudukensis* [nomen nudum]: Nesov, 1997: pl. 54, fig. 3.

cf. *Eoungulatum kudukensis* [nomen nudum, partim]: Nesov, 1997: pl. 54, figs 5, 6, 8.

*Eoungulatum kudukensis*: Nesov *et al.*, 1998: 59, figs 14A–E, 20, 22I; Kielan-Jaworowska *et al.*, 2004: fig. 13.26B<sub>1</sub>.

cf. *Eoungulatum kudukensis* [partim]: Nesov *et al.*, 1998: 59, fig. 14F–O; Kielan-Jaworowska *et al.*, 2004: fig. 13.26C<sub>1, 2</sub>.

'Zhelestidae' genus and species indeterminate: Nesov *et al.*, 1998: 65, fig. 19.

'Zhelestidae' gen. et sp. nov. Averianov, 2000: fig. 30.6S, T.

'Zhelestidae' indet. Averianov, 2000: fig. 30.7J.

*Referred specimens*: URBAC 02–60, left maxilla with alveoli for C, P1–3 (CBI-4e); URBAC 99–42, right maxilla with alveoli for P4–5, M1–3 (CBI-14); URBAC 03–60, right P5 (CBI-14); URBAC 03–185, left M1 (CBI-4e); ZIN 85055, left MX, very worn; URBAC 99–6, right dentary with alveoli for i1–4, single-rooted c, p1–5, m1–3 (CBI-14); CCMGE 15/12953, left dentary with single-rooted c, p4, and alveoli for two incisors and p1–3 (CBI-14, 1984); ZIN 88459, right dentary with alveoli for c, p1–2 (CBI-14, 1984); CCMGE 23/12953, right dentary with alveoli for c, p1–5, m1–3 (CBI-14, 1989); URBAC 00–12, left dentary with p4 and alveoli for c, p1–3, and p5 (CBI-4e); ZIN 88464, left dentary with alveoli for c, p1–4 (CBI-14, 1989); URBAC

04–80, left dentary with alveoli for c, p1–4 (CBI-14); ZIN 88460, right dentary with alveoli for c, p1–5 (CBI-4v, 1979); ZIN 88452, right dentary with m3 trigonid in crypt and alveoli for m1–2 (CBI-14, 1993); ZIN 88471, left dentary with roots of m2–3 (CBI-14, 1993); URBAC 02–25, left dentary with worn m2 and alveoli for m3 (CBI-4e); CCMGE 17/12953, right m1 (CBI-14); URBAC 00–46, left m2 (CBI-14); URBAC 00–49, right m2 (CBI-14); URBAC 04–88, left m2 trigonid (CBI-14); URBAC 06–42, left m2 (CBI-14); URBAC 04–135, right m1 or m2 heavily worn (CBI-14); CCMGE 16/12953, left m3 (CBI-14, 1984); CCMGE 18/12953, left m3 (CBI-14); URBAC 04–74, right m3 lacking lingual part of trigonid and heavily worn (CBI-14); URBAC 04–119, left m3, heavily worn (CBI-14).

*EOUNGULATUM* SP.

*Eoungulatum* sp. cf. *E. kudukensis*: Averianov & Archibald, 2003: 183, fig. 12.

*Referred specimen*: ZIN 35052, heavily worn left m3.

*SHEIKHDZHEILIA REZVYII* AVERIANOV & ARCHIBALD, 2005

*Otlestes meiman* [partim]: Nesov, 1985a: 15, pl. 1, fig. 4; Nesov & Kielan-Jaworowska, 1991: fig. 1; Nesov, 1993: fig. 5(3); Nesov, 1997: 166, pl. 44, fig. 3; Averianov, 2000: fig. 30.3C.

*Sheikhdzheilia rezvyii*: Averianov & Archibald, 2005: 600, fig. 4A–C.

cf. *Sheikhdzheilia rezvyii*: Averianov & Archibald, 2005: 600, fig. 4D.

*Referred specimens*: See Averianov & Archibald (2005: 600).

*BORISODON KARA* (NESOV, 1993)

Gen. indet. Nesov *et al.*, 1994: pl. 7, fig. 4.

*Sorlestes kara*: Nesov, 1993: 123, fig. 1(1); Nesov, 1997: pl. 47, fig. 10; Averianov, 2000: fig. 30.4L, M.

*Referred specimens*: The holotype only.

*LAINODON ORUEETXEBARRIAI* GHEERBRANT & ASTIBIA, 1994

Theria indet. A (Marsupialia?): Astibia *et al.*, 1991: 464, fig. 6.

Theria indet. B: Astibia *et al.*, 1991: 465.

*Lainodon orueetxebarriai*: Gheerbrant & Astibia, 1994: 1126, figs 1–9; Gheerbrant & Astibia, 1999: 296, figs 1, 3a–b, pl. 1; Kielan-Jaworowska *et al.*, 2004: 513, fig. 13.27D.

*Lainodon? orueetxebarriai*: Gheerbrant & Astibia, 1999: fig. 2a, pl. 2, figs 1–3.

*Lainodon oruetebarriai* or *Lainodon* n. sp. Gheerbrant & Astibia, 1999: 310, fig. 3c, pl. 2, figs 4–6.

*Lainodon* n. sp. Gheerbrant & Astibia, 1999: 312, figs 3d, 4, pl. 3, figs 3–6.

*Referred specimens*: L1AT 3, premolar [identified by Gheerbrant & Astibia (1994, 1999) as p2 or p3 but could also be an upper premolar]; L1AT 5, left dp5; L1AT 15, right dp5; L1AT 8, fragmented left dp5 [identified by Gheerbrant & Astibia (1999) as m1(?)]; L1AT 6, left m1; L1AT 1, right dentary fragment with damaged and worn m2; L1AT 7, left molar talonid; L1AT 13, left molar talonid. Gheerbrant & Astibia (1999: 320) mentioned five additional undescribed teeth that may belong to *L. oruetebarriai*.

*LABES QUINTANILLENSIS* SIGÉ IN POL *ET AL.*, 1992

*Labes quintanillensis*: Pol *et al.*, 1992: 296, fig. 8; Kielan-Jaworowska *et al.*, 2004: fig. 13.27E.

*Referred specimens*: QTC 8, fragment of right lower molar. Depository not indicated.

*LABES GARIMONDI* SIGÉ IN POL *ET AL.*, 1992

Theria indet. Ledoux *et al.*, 1966: fig. 2.

Champ-Garimond molar: Butler, 1977: fig. 5CG; Butler, 1990: fig. 10Ch.G.

*Labes garimondi*: Pol *et al.*, 1992: 300, fig. 9.

*Referred specimens*: GAR 008, right m1–2. Depository not indicated.

*GALLOLESTES PACHYMANDIBULARIS*

LILLEGRAVEN, 1976.

Insectivora family indefinite, new genus: Lillegraven, 1972: 7, figs 4A–C, 5A–C.

*Gallolestes pachymandibularis*: Lillegraven, 1976: 438, fig. 1, pl. 1; Butler, 1977: fig. 5Ga; Clemens, 1980: fig. 1; Butler, 1990: fig. 10Ga; Kielan-Jaworowska *et al.*, 2004: fig. 13.27C.

*Referred specimens*: LACM 27599, m1; LACM 27600, dentary with m1 talonid and heavily worn

m2–3; LACM 119327, right dentary with m3; LACM 42635, lower molar talonid.

*GALLOLESTES AGUJAENSIS* CIFELLI, 1994

*Gallolestes agujaensis*: Cifelli, 1994: 131, fig. 9.

*Referred specimens*: OMNH 25108, right upper molar lingual fragment; OMNH 25109, right upper molar lingual fragment; OMNH 25218, right M3 lacking protocone; OMNH 22792, right m1 or 2; OMNH 25268, right lower molar trigonid; OMNH 22793, left lower molar trigonid; OMNH 25111, left lower molar trigonid; OMNH 25269, right lower molar talonid.

*AVITOTHERIUM UTAHENSIS* CIFELLI, 1990

*Avitotherium utahensis*: Cifelli, 1990: 353, fig. 6; Nesov *et al.*, 1998: fig. 22G; Kielan-Jaworowska *et al.*, 2004: fig. 13.27B.

cf. *Paranyctoides* sp. Montellano, 1992: fig. 29.

*Referred specimens*: MNA V4515, left M1; UCMP 131245, left M1; OMNH 21980, broken upper molar; OMNH 20471, lingual fragment of left M1 or 2; OMNH 20532, left dentary fragment with p3, fragmented p2, and roots or alveoli of several teeth; OMNH 20424, right m1 or 2; OMNH 21981, broken right lower molar.

*EOZHELESTES MANGIT* NESOV, 1997

Mixotheridia [indet.]: Nesov, 1985a: pl. 1, fig. 3.

Theria [indet.]: Nesov, 1985a: pl. 1, fig. 11; Nesov, 1997: 139, pl. 43, fig. 5; Averianov, 2000: fig. 30.3F. gen. indet. Nesov *et al.*, 1994: pl. 7, fig. 2.

'Mixotheridia' cf. 'Zhelestidae': Nesov, 1997: 139.

*Eozhelestes mangit*: Nesov, 1997: 170, pl. 43, fig. 4; Kielan-Jaworowska *et al.*, 2004: 498, fig. 13.19E; Averianov & Archibald, 2005: 601, figs 5–6.

'Zhelestidae' gen. et sp. nov. Averianov, 2000: fig. 30.3D, E.

*Referred specimens*: See Averianov & Archibald (2005: 601).

## SUPPORTING INFORMATION

Additional Supporting Information may be found in the online version of this article:

**Appendix S1.** Nexus file of taxa, characters, character states, state distributions, character comments, and Attribute comments used in the analyses shown in Figure 29A–C.

**Appendix S2.** Nexus file of taxa, characters, character states, and state distributions modified after Wible *et al.* (2009) used in the analysis in Figure 29D. See Appendix S3 for list of these modifications.

**Appendix S3.** Modifications to the coding of the taxa present in the Wible *et al.* (2009) data matrix.

Please note: Wiley-Blackwell are not responsible for the content or functionality of any supporting materials supplied by the authors. Any queries (other than missing material) should be directed to the corresponding author for the article.